

MULTILEVEL SPACE-TIME TRELLIS CODES  
FOR  
RAYLEIGH FADING CHANNELS

By  
Marjan Baghaie Abchuyeh  
B.E. (Hons I)

SUBMITTED IN PARTIAL FULFILLMENT OF THE  
REQUIREMENTS FOR THE DEGREE OF  
MASTER OF ENGINEERING  
AT  
UNIVERSITY OF CANTERBURY  
CHRISTCHURCH, NEW ZEALAND

# Table of Contents

<b>Table of Contents</b>	<b>i</b>
<b>Abstract</b>	<b>vi</b>
<b>Acknowledgements</b>	<b>vii</b>
<b>1 Introduction</b>	<b>1</b>
1.1 Wireless Channels . . . . .	2
1.1.1 AWGN Channel Model . . . . .	3
1.1.2 Rayleigh Fading Channel Model . . . . .	4
1.2 Capacity . . . . .	7
1.3 MIMO Systems . . . . .	9
1.4 Space-Time Coding . . . . .	11
1.5 Thesis Focus . . . . .	12
1.5.1 Proposed System Structure . . . . .	12
1.5.2 Research Objectives . . . . .	13
1.6 Structure of the Thesis . . . . .	13
<b>2 Space-Time Trellis Codes</b>	<b>14</b>
2.1 Introduction . . . . .	14
2.2 System Model . . . . .	15
2.3 STC Design Criteria and Performance Bounds . . . . .	17
2.3.1 Pairwise Probability of Error (PEP) . . . . .	17
2.3.2 Rank and Determinant Criterion . . . . .	18
2.3.3 Trace Criterion . . . . .	21
2.4 CSTTC Encoder Structure . . . . .	22
2.5 CSTTC Decoder Structure . . . . .	25
2.6 An Example . . . . .	26
2.7 Summary . . . . .	28

<b>3</b>	<b>Multilevel Coded Modulation</b>	<b>29</b>
3.1	Introduction . . . . .	29
3.2	Multilevel Encoder . . . . .	32
3.3	Multistage Decoder . . . . .	34
3.4	MIMO Multilevel Codes . . . . .	35
3.5	Summary . . . . .	39
<b>4</b>	<b>Multilevel Space-Time Trellis Codes</b>	<b>40</b>
4.1	Introduction . . . . .	41
4.2	System Model . . . . .	42
4.3	Encoder Design . . . . .	44
4.3.1	Partitioning and constellation mapping . . . . .	45
4.3.2	Component Codes . . . . .	47
4.3.3	Mapping Symbols to Antennas . . . . .	49
4.4	Detection/Decoding . . . . .	49
4.4.1	Stage L . . . . .	50
4.4.2	Stage k . . . . .	52
4.4.3	Stage 1 . . . . .	53
4.5	Complexity Considerations . . . . .	54
4.5.1	Branch Metric Complexity Reduction . . . . .	57
4.6	Summary . . . . .	59
<b>5</b>	<b>System Performance</b>	<b>60</b>
5.1	Introduction . . . . .	60
5.2	An example MLSTTC system . . . . .	61
5.3	Unequal Error protection . . . . .	64
5.4	Imperfect Channel State Information . . . . .	65
5.5	Effect of Channel Correlation . . . . .	66
5.6	Receive Diversity . . . . .	66
5.7	Transmit Diversity . . . . .	68
5.8	Reduced Complexity Decoding . . . . .	70
5.9	Comparison with CSTTC's . . . . .	70
5.10	Higher Throughput MLSTTC's . . . . .	72
5.10.1	Error Performance . . . . .	76
5.10.2	Equal Error Performance . . . . .	77
5.10.3	Effect of Number of States . . . . .	78
5.10.4	Comparison with Layered STTC's . . . . .	79
5.10.5	Receive Diversity . . . . .	82
5.11	Summary . . . . .	83

<b>6 Conclusion</b>	<b>85</b>
6.1 Design considerations . . . . .	86
6.2 Coding implications . . . . .	87
6.3 Throughput Improvement . . . . .	87
6.4 Complexity Considerations . . . . .	88
6.5 Scalability and Flexibility . . . . .	88
6.6 Future Research Direction . . . . .	88
<b>Bibliography</b>	<b>90</b>

# List of Figures

1.1	AWGN channel model . . . . .	4
1.2	Demonstration of Rayleigh fading effects - slow fading, $f_D T = 0.01$ . . . . .	6
1.3	Demonstration of Rayleigh fading effects - fast fading, $f_D T = 0.1$ . . . . .	7
2.1	MIMO system model . . . . .	16
2.2	General STTC encoder structure for $N_t$ transmit antennas [18]. . . . .	23
2.3	An example trellis structure . . . . .	26
2.4	Simulated performance of CSTTCs . . . . .	27
3.1	General structure of a multilevel encoder . . . . .	32
3.2	General structure of a multistage decoder . . . . .	35
3.3	An example MIMO MLC structure . . . . .	36
3.4	An example hybrid coded modulation scheme . . . . .	37
3.5	An example STBC-MLC coded system . . . . .	38
	43	
4.2	Partitioning and labelling of the underlying constellation for 64-QAM. . . . .	46
5.1	An example MLSTTC system. . . . .	61
5.2	Partitioning and labelling of the 16-QAM constellation. . . . .	62
5.3	The labelling of the 16-QAM MRM constellation. . . . .	63
5.4	Unequal error performance . . . . .	64
5.5	Effect of imperfect CSI . . . . .	65
5.6	Effect of channel correlation . . . . .	66
5.7	Error performance of a 2 by 4 MLSTTC system . . . . .	67

5.8	Receive diversity effects (FER) . . . . .	67
5.9	Receive diversity effects (SER) . . . . .	68
5.10	Error performance of a 4 by 4 MLSTTC system . . . . .	69
5.11	Transmit diversity effects . . . . .	69
5.12	Trellis diagram for 4 transmit antenna component codes . . . . .	70
5.13	Reduced complexity metric . . . . .	71
5.14	Error performance of MLSTTC vs CSTTC . . . . .	72
5.15	Trellis diagram of a 16 state CSTTC . . . . .	73
5.16	Trellis diagram of the MLSTTC component codes . . . . .	73
5.17	MLSTTC system block diagram, 6 bits/sec/Hz . . . . .	74
5.18	Error performance of MLSTTC, 6 bits/sec/Hz . . . . .	76
5.19	Equal Error Performance . . . . .	77
5.20	Effect of number of states . . . . .	78
5.21	Block diagram of a layered STTC system . . . . .	80
5.22	Error performance of MLSTTC vs layered STTC's . . . . .	81
5.23	Receive diversity effect on higher throughput MLSTTC . . . . .	82

# Abstract

Demand for capacity in wireless communication systems has been rapidly growing worldwide. This has been driven by increasing data rate requirements of cellular mobile systems, and demand for wireless Internet and multimedia services. As the available radio spectrum is limited, higher data rates can only be achieved by designing more efficient signaling techniques.

In this thesis, we propose a new transmission scheme, which benefits from the advantages of conventional space-time trellis codes (CSTTCs) but does not have the disadvantages, especially for larger signal constellations. We achieve this by developing a new class of codes, called Multilevel Space-Time Trellis Codes (IMLSTTC). The new scheme provides a scalable and promising alternative to CSTTCs, by providing the system designer with the flexibility to choose any desired balance between code performance, complexity and throughput. The proposed scheme outperforms layered schemes at high SNRs, using a smaller number of antennas.

# Acknowledgements

I would like to thank my principal advisor, Prof. Desmond Taylor, for his thoughtful guidance, many insightful suggestions and generous support (academically, morally and financially) throughout this research. I am equally grateful to Dr. Philippa Martin for acting as my co-advisor, for her kind guidance and support and for sharing her insight on multilevel codes. It has been both a privilege and a pleasure to have been associated with them.

I am indebted to Assoc. Prof. Ian McLoughlin (now with Nanyang Technological University), for acting as my associate advisor and my mentor during my time in Tait Electronics. I am grateful to him for introducing me to the field and for his continued guidance and encouragement ever since. Working with him has been a very rewarding experience, both academically and otherwise.

The New Zealand Foundation of Research Science and Technology (FRST), University of Canterbury Communication Research Group (UCCRG), Tait Electronics Space-Time Research Array (STAR) Group and New Zealand Vice Chancellors' Committee (NZVCC) (Stratex Networks Fellowship) are gratefully acknowledged for awarding me funding and facilities to pursue this research. Thanks are also due to the NZFGW Trust for awarding me a grant to partially fund my travel expenses to present a paper in the IEEE VTC conference.

I would like to express my deepest gratitude to my parents, for their unbounded support and affection, for all they have given me throughout the years, all they have given up for me and above all for being such inspiring role models. I am also grateful to my siblings Nilufar, Nader (Amir) and Rezza for being who they are and for always being there for me.

Throughout this research, I had the privilege of working with two of New Zealand's best wireless research groups, namely the UCCRG and the Tait STAR group. I would like to acknowledge my gratitude to Adrian Busch, Dough McConnel and Michael Chick of Tait Electronics for being so kind and supportive during my time in Tait and for giving me the opportunity to be part of their team. Thanks also to all my other friends and colleagues (past and present) in both groups, most notably to Kishore, Howie (Shyh hao), James, Stefan, Siow Lim, Tom, Andrew, David, Parabath, Iain, Chris, Yan, Paul, Maureen, Peter, Rachel, Michael, Nick, Yau Hee, Sam, Rui, Gayathri, Milind, Yu, Alan, Craig and Magda for the pleasure of their company and for making the experience an enjoyable and memorable one.

Marjan Baghaie A.



# Chapter 1

## Introduction

Wireless communication is the communication industry's fastest growing segment [1, 2, 3]. Its wide applicability and relatively low cost infrastructure have helped it capture the attention of the media and the imagination of the public in recent years. The main driving force behind the rapid development of wireless communication is the promise of portability, mobility, and accessibility. In other words, wireless offers *freedom*, from being confined to a certain location or a bounded environment. While, this freedom is the main driving force for users, the penalty for this freedom is often lower quality, higher risk of disconnection, or lower throughput compared to the equivalent wired solution [5, 11]. The enormous number of challenges to achieve reliable wireless systems with high spectral efficiency, low complexity and good error performance results in the need for continued research in this field.

In this chapter, we summarize the history of wireless communication and highlight some of the recent advances in the area. A brief background is also presented followed by the motivation, main focus and the scope of this thesis. A summary of our main results and an overview of the thesis structure are also presented in this chapter. Key references are provided for further reading.

## 1.1 Wireless Channels

The pioneering work of James Clerk Maxwell, in 1864, who formulated a theory of electromagnetic propagation that predicted the existence of radio waves, can be considered to be the basis of the field of wireless communication. In 1873, Heinrich Hertz clarified and expanded the electromagnetic theory that had been developed by Maxwell and demonstrated the existence of radio waves. Through experimentation, he proved that transverse free space electromagnetic waves can travel over some distance. Hertz measured Maxwell's waves and demonstrated that the velocity of radio waves was equal to the velocity of light and that they possess many other properties of light. The electric field intensity and polarity was also measured by Hertz. In bulk, his work explained reflection, refraction, polarization, interference, and velocity of electric waves [10, 12, 13]. However, to him it was more a matter of theoretical curiosity, as he saw no practical use for radio waves. Speaking of his discovery, he once said [12]:

*It's of no use whatsoever ... this is just an experiment that proves Maestro Maxwell was right - we just have these mysterious electromagnetic waves that we cannot see with the naked eye. But they are there.*

He argued that since audio frequencies were low, where propagation was poor, radio waves could never carry voice; asked about the ramifications of his discoveries, Hertz replied, “*Nothing, I guess*”! Nonetheless, the work of Maxwell and Hertz ignited the era of wireless communication.

The first communication system based on these principles, was built in 1894 by Oliver Lodge. The transmission distance of this system was only 150 meters [14]. By 1901, electrical engineer and Nobel laureate Guglielmo Marconi [15] had managed to build arguably the first practical wireless system, that used telegraph signals to communicate the information over the Atlantic Ocean. In 1906, Reginald Fessenden used a form of amplitude modulation,

similar to what is used today, to translate signals to a higher frequency and thus circumvent the propagation limitations observed by Hertz at low frequencies. He managed to build the first system that could transmit voice and music [2].

Electromagnetic waves propagate through environments where they are reflected, scattered, and diffracted by walls, terrain, buildings, and other objects. The ultimate details of this propagation can be obtained by solving Maxwell's equations with boundary conditions that express the physical characteristics of these obstructions. Most often though, the difficulty of these calculations, the lack of knowledge of the necessary parameters and the complexity and variability of the radio channel make it difficult to obtain an accurate deterministic channel model. As a result, statistical models are often employed and used to characterize the signal propagation without resorting to Maxwell's equations. These channel models, in the context of developing transmission systems, allow for designs that work in the "average" environment.

Here we review two of the most commonly used channel models, namely the additive white Gaussian noise (AWGN) and Rayleigh fading channel models. A more comprehensive study of different channel and propagation models can be found in the literature [4, 6, 7].

### 1.1.1 AWGN Channel Model

The AWGN channel has only one impairment created by the linear addition of white noise with a constant spectral density and a Gaussian amplitude distribution. The model may be described mathematically by considering signal transmission as

$$r(t) = x(t) + n(t) \tag{1.1.1}$$

where, at time  $t$ ,  $r(t)$  and  $x(t)$  are the received and transmitted signals respectively and  $n(t)$  is the noise, represented as a sample function from a Gaussian random process with zero mean and variance  $N$ . The noise  $n(t)$  is assumed to be independent of the signal  $r(t)$ . The model is presented in Figure 1.1.

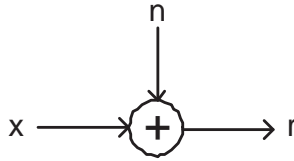


Figure 1.1: AWGN channel model.

The AWGN channel is a suitable model for many satellite and deep space communication links. However, the fact that it does not take into account the phenomena of fading, frequency selectivity, interference or non-linearity makes it a rather poor model for most terrestrial links. Nonetheless, due to the simplicity of the mathematical model, an AWGN channel is often used for gaining insight into the underlying behaviour of a system before other phenomena are considered [8].

### 1.1.2 Rayleigh Fading Channel Model

The Rayleigh fading channel is a channel in which the received signal is corrupted by multipath fading as well as AWGN. Multipath propagation results in more than one version of the transmitted signal being received; each version typically having a different delay, Doppler shift, attenuation and phase. This leads to constructive and destructive interference and phase shifting of the signal, commonly regarded as Rayleigh fading [60]. Generally, Rayleigh fading corresponds to the case, where there is no line of sight (LOS) path between transmitter and receiver. When there is a LOS path, then a Rician model [2] is more appropriate.

Rayleigh fading channels can be divided into two models based on the *coherence bandwidth* of the channel in comparison with the bandwidth of the transmitted signal. In narrowband systems, the transmitted signals usually occupy a bandwidth smaller than the channel's coherence bandwidth, which is defined as the frequency range over which the

channel fading process is correlated. This type of fading is referred to as *frequency flat* or *frequency nonselective* and all frequency components of a signal are faded equally.

In wideband systems, the transmitted signals usually undergo *frequency selective* fading. This occurs when the transmitted signal bandwidth is greater than the channel coherence bandwidth, and the spectral components of the transmitted signal with a frequency separation larger than the coherence bandwidth are then faded independently. [18]

Relative motion between the transmitter and receiver, can cause each multipath wave to undergo a shift in frequency. The frequency shift of the received signal caused by the relative motion is called the *Doppler frequency*. The rate of fading in Rayleigh fading channels is indicated by the *normalized Doppler frequency*, denoted by  $f_D T$ , where  $f_D$  represents the maximum value of a continuum of Doppler frequencies Doppler frequency and  $1/T$  is the symbol rate. Values of  $f_D T$  ranging from 0.0001 to 0.1 are understood to mean very slow to very fast fading respectively. Figures 1.2 and 1.3, show simulated Rayleigh fading envelopes,  $h(t)$ , for values of  $f_D T = 0.01$  and 0.1, respectively. The typical behaviour of the amplitude of the Rayleigh fading process is quasi-oscillatory with sudden rapid deep fades occurring at almost regular intervals. The depth of the fades can easily be more than 20 dB and are the cause of most error events in wireless communication systems.

When flat or frequency non-selective fading is present, the received signal in complex baseband form can be expressed as

$$r(t) = h(t)x(t) + n(t) \tag{1.1.2}$$

where  $x(t)$  and  $r(t)$  are the transmitted and received complex baseband signals, respectively, and  $h(t)$  is the complex baseband equivalent of the fading process.  $h(t)$  is modeled as a complex Gaussian random process, the instantaneous value of which, is referred to as the *channel state*.  $h(t)$ , introduces random phase rotations and random amplitude fluctuations to the transmitted signal. In most cases we require this information at the receiver in

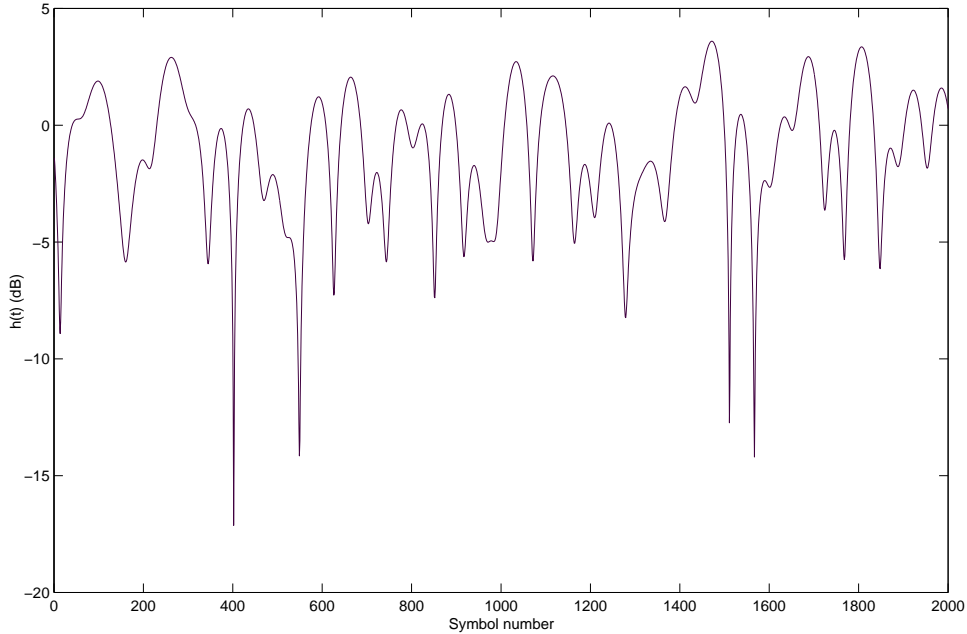


Figure 1.2: Simulated faded carrier amplitude  $h(t)$  for a Rayleigh fading channel with  $f_D T = 0.01$ .

order to successfully detect the received data. Channel state information (CSI)<sup>1</sup> may be estimated through pilot tones, pilot symbols or the need to obtain them can be avoided through differential detection [9]. Often for the purpose of analysis, perfect CSI is assumed to be available at the receiver.

Throughout this work, we shall assume a quasi-static Rayleigh flat fading channel, where the channel coefficients are constant during each transmission frame and vary from one frame to another, resulting in the received signal model of (1.1.2). We assume perfect CSI is available at the receiver throughout the design stage, however the effects of imperfect channel estimation are investigated later via simulation.

---

<sup>1</sup>Here CSI is merely the complex gain factor for the channel or a Matrix of gain factors for the multi-antenna case.

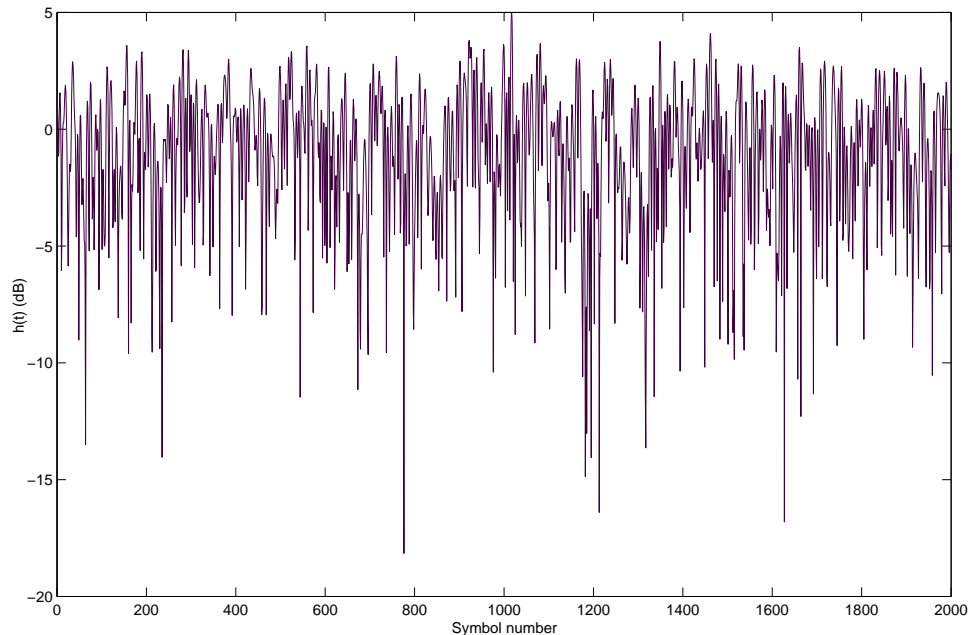


Figure 1.3: Simulated faded carrier amplitude  $h(t)$  for a Rayleigh fading channel with  $f_D T = 0.1$ .

## 1.2 Capacity

The system *capacity* for a given channel is defined as the maximum achievable data rate for which an arbitrarily low probability of error can be achieved, provided the signal can be encoded over an arbitrarily long code word. For digital transmission on a continuous AWGN channel, the capacity is given by the celebrated Shannon formula [52]

$$C = B \log_2(1 + \rho) \quad (1.2.1)$$

where  $C$  represents the *Shannon capacity* (measured in units of bits/sec),  $B$  represents the channel bandwidth and  $\rho$  is the signal-to-noise ratio (SNR). Shannon's coding theorem proves that codes exist, which achieve data rates arbitrarily close to capacity with arbitrarily

small probability of error.  $C$  in the above equation is a form of the so-called *ergodic capacity*, which is one of the parameters often used to provide basis for the comparison of different transmission schemes.

Demand for capacity in wireless communication systems has been rapidly growing worldwide. This is being driven by the demand for enhanced cellular mobile, Internet and multimedia services. As the available radio spectrum is limited, higher data rates can only be achieved by designing more efficient signaling techniques.

Advances in error control coding, such as the invention of turbo codes [44] and low density parity check codes [45, 51] have made it feasible to approach the Shannon limit in systems with a single antenna link on AWGN channels. Turbo codes and low density parity check codes (LDPCs), for example, have come within a fraction of a decibel of the Shannon capacity on AWGN radio channels [25, 22].

The Shannon capacity of fading channels, with receiver CSI only, can be shown to be less than that of an AWGN channel with the same average SNR [20, 21]. In other words, fading reduces the Shannon capacity when CSI is only available at the receiver. It has also been noted in the literature [2] that capacity-achieving codes for fading channels must be sufficiently long so that a received codeword is affected by all possible fading states. This can result in very long codewords and consequently long delays.

Recent research in information theory has shown that large gains in available channel capacity are possible for wireless channels by using multiple-input multiple-output (MIMO) systems [103, 105]. MIMO channels result when multiple antennas are employed at both ends of the wireless link. In [102, 103], theoretical and experimental evidence demonstrates that the available channel capacity grows linearly when the number of transmit and receive antennas grow simultaneously. This provides added capacity with no increase in bandwidth. MIMO systems are often regarded as one of the most significant technical breakthrough in



modern communication [17].

### 1.3 MIMO Systems

MIMO wireless communication systems are important due to their potential to achieve very high spectral efficiency. The idea behind these systems is to exploit the de-correlation of multiple received signals in the presence of multi-path propagation. This allows the separation of data streams occupying the same bandwidth. Unlike traditional radio systems that try to directly combat the effects of multi-path propagation, MIMO systems exploit it thus providing an increase in throughput and reliability with reduced error rates. Since training sequences are typically available in a practical system, MIMO schemes that assume the channel knowledge is only available at the receiver, have in particular attracted a lot of research attention [102].

Practical MIMO modulation schemes with receive-only channel knowledge are principally of two types, diversity systems and spatial multiplexing systems [108]. Diversity modulation, or space-time coding [16, 109, 18], uses codewords designed to maximize the diversity advantage of the transmitted information. Such codes tend to maximize diversity gain at the expense of some loss in available capacity. Spatial multiplexing [48] or Bell Labs Layered Space Time (BLAST) type systems [102], on the other hand, transmit independent data streams from each transmitting antenna, allowing spectral efficiency to be achieved at the expense of a loss in diversity advantage for a fixed number of receive antennas.

The space-time coding work, can be dated back to a 1994 paper by Wittenben [28], which proposes a system using transmit diversity and coding techniques. This paper sparked a lot of research in this area, most significantly that of Tarkoh, Seshadri and Calderbank in 1998 [16]. In their landmark paper, they state the fundamental theory of space-time coding and introduce the first true space-time codes, namely space-time trellis codes (STTCs). This paper was followed by Alamouti's paper [109], which led to the development of what are

now known as space-time block codes (STBCs) [27, 91, 114, 24]. STTCs and STBCs are the two main classes of space-time codes (STCs). STCs are the main focus of this research project and are introduced in more detail in Section 1.4.

The original BLAST structure was developed by Foschini, at Bell labs, in the mid 1990's [102]. It uses a multi-element antenna array at both the transmitter and receiver, where every antenna transmits an independent substream of data. Advanced signal processing at the receiver is used to estimate and decode the received signal blocks. A BLAST system requires more receive than transmit antennas and a rich scattering environment, which often occurs indoors. Vertical-BLAST(V-BLAST) and Diagonal-BLAST (D-BLAST) [111, 110, 30, 29] are the two major classes of BLAST transmission formats.

In V-BLAST [29], the data stream is multiplexed into  $N_t$  independent substreams. Each is passed through an optional temporal encoder, interleaved, mapped to a signal constellation point and transmitted over its corresponding transmit antenna. This process can be considered to be the encoding of the serial data into a vertical vector and is thus referred to as *vertical coding* or V-BLAST. D-BLAST [102] is somewhat more complex and uses a *diagonal coding* structure. The data stream is first parallel encoded but then, rather than transmitting each codeword from one antenna, the codeword symbols are staggered across antennas. As such, a codeword is transmitted by all  $N_t$  transmit antennas. If the frame sizes are not chosen properly, a D-BLAST based system may suffer a significant efficiency loss due to the *wasted* space-time dimension introduced by the staggering effect [2].

At rates of tens of bits/sec/Hz, V-BLAST has been shown [29] to have good performance and relatively simple encoding and decoding. Due to the (successive) interference cancellation techniques employed in the decoding process of V-BLASTs, their decoding complexity increases linearly with the number of transmit antennas. However, BLAST schemes

are unable to work with fewer receive antennas than transmit antennas. This deficiency is especially important for modern cellular systems where a base-station typically has more antennas than the mobile handsets. Furthermore, because BLAST transmits independent data streams from each antenna there is no built-in spatial coding to guard against deep fades suffered by a given transmitted signal.

The initial application of MIMO was proposed for indoor WLANs and fixed wireless access networks. However, it has since found wider applications and some practical MIMO systems have been built and experimentally tested in industry [98, 99]. There is an ongoing effort to standardize a MIMO approach under the name IEEE 802.11n [11]. It will offer up to eight times coverage and about six times the data rates, of current 802.11g [11] networks.

## 1.4 Space-Time Coding

Space-time coding (STC) [18, 24, 16] is a set of practical signal design techniques that offers an efficient means for providing diversity over fading channels with multiple transmit antennas. STC is performed in both the spatial and temporal domains to introduce correlation between signals transmitted from various antennas in different time periods. The spatial-temporal correlation is then used to exploit the scattering environment and minimize transmission errors at the receiver. STC can achieve transmit diversity and coding gain compared to spatially uncoded systems without sacrificing bandwidth [18]. Since their introduction in 1998 [16], STC and the corresponding MIMO signal processing have engendered one of the most vibrant research areas in wireless communications. Many variants of these coding structures have been developed [18, 24, 43].

STBCs and STTCs can be considered to be the two main classes of space-time codes. In this thesis we focus on STTCs, which have been developed to simultaneously provide coding gain and diversity in MIMO systems [16]. Similar to convolutional codes, STTCs use a trellis encoder to introduce redundancy into the transmitted symbol stream, and to

achieve coding gain. The coding gain is dependent on the construction criteria of the code, and on the length of the memory in the encoder. A number of different structures have been proposed for STTCs [112, 118, 119, 120]. In this thesis, we focus on the STTCs originally proposed by Tarokh et. al. [16] and later improved by others, most notably Baro et. al. [117] and Vucetic et. al. [54, 55, 18]. We refer to these STTCs as conventional STTCs (CSTTCs), though the names are sometimes used interchangeably throughout. These codes are discussed in more detail in Chapter 2.

## 1.5 Thesis Focus

The focus of this thesis is on the development of new STTC structures. As discussed in previous sections, STTCs are an important class of space-time codes which can simultaneously offer coding gain, spectral efficiency, and transmit diversity on fading channels.

To improve the spectral efficiency of communication systems for high data rate transmission, it is desirable to construct STTCs using high order signal constellations. However, the design of CSTTCs normally involves the use of a computer search, with the search space increasing exponentially with constellation size, the number of transmit antennas and the number of states in the code trellis. Similarly the number of states, and thus the decoding complexity of the CSTTCs grows exponentially with rate and consequently with the constellation size. Therefore, despite their many benefits, the development of systems based on CSTTCs is still faced with reluctance from system designers when it comes to implementation, especially for systems employing large signal constellations or numbers of transmit antennas.

### 1.5.1 Proposed System Structure

In this thesis, we design and develop a new transmission scheme, which benefits from the advantages of STTCs, but does not have some of the disadvantages, especially for larger

signal constellations. Specifically, we make use of multilevel coding (MLC) [67, 68, 87] concepts in our proposed design to obtain new codes known as multilevel space-time trellis codes (MLSTTCs).

MLC techniques have recently been used in MIMO systems, however most work so far has focused on combinations of STBCs, BLAST and MLC [69, 77, 86]. In this work the focus is placed on STTCs. Our proposed design offers the system designer with flexibility, scalability, versatility and reasonable complexity. More details of this are described in Chapters 3 and 4.

### 1.5.2 Research Objectives

The objective of this research is to investigate combining MLC and STTCs. In addition, appropriate decoding algorithms are proposed and investigated. Ultimately, the goal is to develop a transmission scheme that benefits from the performance of STTCs, but is not as computationally expensive, especially when used with larger signal constellations.

## 1.6 Structure of the Thesis

Chapter 2 provides background information on CSTTCs and their corresponding design criteria. The complexity problems of these codes, as well as an example space-time trellis coded system are also highlighted. MLC techniques are described in Chapter 3, along with an overview of some of existing MIMO-MLC designs. The proposed MLSTTC scheme and its corresponding decoding algorithms are discussed in Chapter 4. Simulation results for the proposed system are presented in Chapter 5 and some of the design tradeoffs are explored. The thesis is concluded in Chapter 6, with a summary of the main results and a list of suggestions for further research.

## Chapter 2

# Space-Time Trellis Codes

This chapter presents an overview of some of the most commonly used design criteria for STCs. In particular the focus is on the original criteria proposed by Tarokh et. al. in 1998 [16] and those later proposed by Vucetic et. al. [18]. A brief outline of the derivations is included to provide an insight into these design criteria. A number of performance bounds involved in designing STCs are also highlighted in this chapter followed by a discussion of the design of CSTTCs, and their corresponding encoding and decoding algorithms. The space-time system model used throughout the work as well as an example CSTTC system (which will be used in later chapters as a component code of the proposed scheme) are presented in this chapter and some of the problems of CSTTCs are discussed. The analysis provided in this chapter is primarily based on the materials presented in [16, 18, 54].

### 2.1 Introduction

Many different STC schemes have been proposed in the literature [18, 24, 43]. Space time block codes and STTCs are two of the major classes of STCs. So-called orthogonal STBCs (OSTBCs) [109, 114] can achieve a maximum possible diversity advantage with a simple decoding algorithm. This simplicity has made them very attractive to researchers and system developers in recent years [101, 27, 24, 98]. However, in general, they cannot provide

coding gain. In addition, for more than two transmit antennas, these codes cannot achieve full rate and thus suffer a throughput penalty. STTCs provide an effective alternative signalling technique. By having a convolutional or trellis code embedded into their design (as opposed to being merely a constellation design), they can simultaneously offer coding gain, spectral efficiency, and diversity improvement on flat Rayleigh fading channels.

## 2.2 System Model

Throughout this work, we consider a base-band, flat-fading, multi-antenna communication system model, where the channel is assumed to be constant for at least  $L(> 1)$  channel uses. Assuming  $N_t$  transmit and  $N_r$  receive antennas, the relationship between the transmitted and received signals, for each channel instant  $H_k$ , can be represented in MIMO vector form as

$$\mathbf{r}_k = \sqrt{\frac{\rho}{N_t}} \mathbf{X}_k \mathbf{H}_k + \mathbf{n}_k \quad (2.2.1)$$

where  $\mathbf{r}_k \in \mathcal{C}(L \times N_r)$  and  $\mathbf{X}_k \in \mathcal{C}(L \times N_t)$  are the received and transmitted matrices of complex values, and  $\mathbf{n}_k \in \mathcal{C}(T \times N_r)$  and  $\mathbf{H}_k \in \mathcal{C}(N_t \times N_r)$  with independent  $\mathcal{CN}(0,1)$  are the additive noise and the channel matrix respectively. In  $\mathbf{X}_k$ ,  $\mathbf{r}_k$  and  $\mathbf{n}_k$ , time runs horizontally and space runs vertically.  $\mathbf{H}_k$  is assumed to be known to the receiver but not to the transmitter. Since  $\mathbf{H}$ ,  $\mathbf{X}$  and  $\mathbf{n}$  are assumed to be independent, the normalization  $\sqrt{\frac{\rho}{N_t}}$ , in (2.2.1), ensures that  $\rho$  is the average SNR at each receive antenna, regardless of  $N_t$ . A typical system of this kind, with  $N_t$  transmit and  $N_r$  receive antennas, where the transmitted data is encoded by a space-time encoder, is depicted in Figure 2.1. At each time instant  $t$ , a block of  $B$  binary information symbols, denoted  $\mathbf{b}_t = (b_t^1, b_t^2, \dots, b_t^B)$ , is fed into the space-time encoder. The encoder maps the block of  $B$  binary input data into  $N_t$  modulation symbols from a signal set of  $M = 2^m$  points, for an  $M$ -ary signal

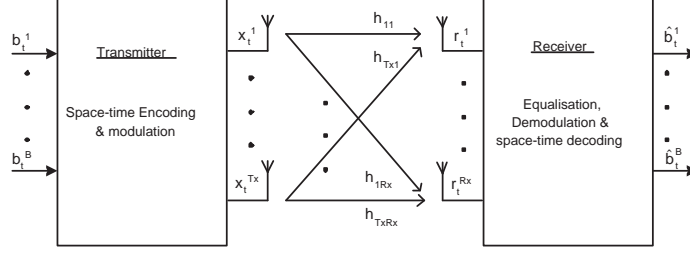


Figure 2.1: MIMO system model.

constellation. The coded data, called the *space-time symbol*, can then be represented by the column vector  $\mathbf{x}_t = (x_t^1, x_t^2, \dots, x_t^{N_t})^T$ , where  $T$  denotes the transpose of the matrix. The  $N_t$  parallel outputs are simultaneously transmitted by  $N_t$  transmit antennas, whereby symbol  $x_t^j$ ,  $1 \leq j \leq N_t$ , is transmitted by antenna  $j$ , with all transmitted symbols having the same duration. Assuming the transmitted data frame length is  $L$  symbols for each antenna, the *space-time codeword matrix*, can be defined as  $\mathbf{X} = [\mathbf{x}_1, \mathbf{x}_2, \dots, \mathbf{x}_L]$ .

The signal is received after being distorted by the channel fading and AWGN. Similarly, the received space-time symbol can be represented as  $\mathbf{r}_t = (r_t^1, r_t^2, \dots, r_t^{N_r})^T$  or in matrix form as  $\mathbf{r} = [\mathbf{r}_1, \mathbf{r}_2, \dots, \mathbf{r}_L]$ , where  $r_t^j$  is the received signal at receive antenna  $j \in \{1, 2, \dots, N_r\}$  at time  $t$

We define the spectral efficiency, to be the number of information bits transmitted per time slot, in this case  $B$  bits/sec/Hz. This is equivalent to the spectral efficiency of a reference uncoded system with one transmit antenna. The rate of the code is defined as the number of information bits over the total number of bits transmitted per interval. In this case, assuming a  $M$ -ary signal constellation, for each  $B$  information bits,  $N_t \times m$  bits are transmitted. The rate of the code is then defined as  $\frac{B}{N_t \times m}$ .



## 2.3 STC Design Criteria and Performance Bounds

A number of design criteria have been proposed for STCs, since their introduction in 1998. The most commonly used techniques are the *rank and determinant* criteria originally proposed by Tarokh et. al. [16] and the *trace criterion* proposed by Vucetic et. al. [54, 18]. Here we provide a summary of these methods, and discuss the conditions under which each criteria is deemed suitable. Throughout, we consider a baseband MIMO communication system with  $N_t$  transmit and  $N_r$  receive antennas, as described in Section 2.2.

### 2.3.1 Pairwise Probability of Error (PEP)

Assuming the transmitted data frame length is  $L$  symbols for each antenna, the  $L \times N_t$  space-time code word matrix can be represented as

$$\mathbf{X} = [\mathbf{x}_1, \mathbf{x}_2, \dots, \mathbf{x}_L] = \begin{bmatrix} x_1^1 & x_1^2 & \cdots & x_1^{N_t} \\ x_2^1 & x_2^2 & \cdots & x_2^{N_t} \\ \vdots & \vdots & \ddots & \vdots \\ x_L^1 & x_L^2 & \cdots & x_L^{N_t} \end{bmatrix} \quad (2.3.1)$$

The PEP is defined as the probability that a maximum likelihood decoder erroneously selects a sequence  $\mathbf{e}_t = (e_1^1, e_1^2, \dots, e_1^{N_t}, e_2^1, \dots, e_2^{N_t}, e_L^1, \dots, e_L^{N_t})$  as its estimate, when the signal transmitted was in fact  $\mathbf{x}_t = (x_1^1, x_1^2, \dots, x_1^{N_t}, x_2^1, \dots, x_2^{N_t}, x_L^1, \dots, x_L^{N_t})$ . Considering the received signal of (2.2.1), and ML concepts, this can happen if and only if,

$$\sum_{t=1}^L \sum_{i=1}^{N_r} \left| r_t^i - \sum_{j=1}^{N_t} h_{j,i}^t x_t^j \right|^2 \geq \sum_{t=1}^L \sum_{i=1}^{N_r} \left| r_t^i - \sum_{j=1}^{N_t} h_{j,i}^t e_t^j \right|^2 \quad (2.3.2)$$

This inequality is equivalent to

$$\sum_{t=1}^L \sum_{i=1}^{N_r} 2\text{Re} \left\{ (n_t^i) * \sum_{j=1}^{N_t} h_{j,i}^t (e_t^j - x_t^j) \right\} \geq \sum_{t=1}^L \sum_{i=1}^{N_r} \left| \sum_{j=1}^{N_t} h_{j,i}^t (e_t^j - x_t^j) \right|^2 \quad (2.3.3)$$

where  $\text{Re}\{\cdot\}$  takes the real part of the argument.

Assuming that ideal CSI is available at the receiver, for a given realization of the fading channel matrix  $\mathbf{H}$ , the term on the right hand side of (2.3.3) becomes a constant that represents a modified Euclidean distance between the two space-time code word matrices  $\mathbf{x}$  and  $\mathbf{e}$ . Denoting this constant by  $d^2(\mathbf{x}, \mathbf{e})$ , the conditional pairwise error probability (PEP) can be represented by

$$P(\mathbf{x}, \mathbf{e} | \mathbf{H}) = Q \left( \sqrt{\frac{E_s}{2N_0} d^2(\mathbf{x}, \mathbf{e})} \right) \quad (2.3.4)$$

where  $N_0/2$  is the noise variance per dimension and  $Q(x)$  is the *Gaussian Q-function* defined by

$$Q(x) = \frac{1}{\sqrt{2\pi}} \int_x^\infty e^{-t^2/2} dt \quad (2.3.5)$$

By using the inequality

$$Q(x) \leq \frac{1}{2} e^{-x^2/2} \quad (2.3.6)$$

the conditional PEP shown in (2.3.3) can be upper bounded by

$$P(\mathbf{x}, \mathbf{e} | \mathbf{H}) \leq \frac{1}{2} \exp\left(-d^2(\mathbf{x}, \mathbf{e}) \frac{E_s}{4N_0}\right) \quad (2.3.7)$$

### 2.3.2 Rank and Determinant Criterion

This criterion was the first criterion used for designing STCs, introduced by Tarokh et. al. [16] in 1998. As the name suggests the criterion is based on the rank and determinant of the *codeword difference matrix*. Consider a codeword difference matrix defined as

$$\mathbf{B}(\mathbf{x}, \mathbf{e}) = \begin{bmatrix} e_1^1 - x_1^1 & \cdots & e_1^{N_t} - x_1^{N_t} \\ e_2^1 - x_2^1 & \cdots & e_2^{N_t} - x_2^{N_t} \\ \vdots & \ddots & \vdots \\ e_L^1 - x_L^1 & \cdots & e_L^{N_t} - x_L^{N_t} \end{bmatrix} \quad (2.3.8)$$

and a *distance matrix* defined as

$$\mathbf{A}(\mathbf{x}, \mathbf{e}) = \mathbf{B}(\mathbf{x}, \mathbf{e})\mathbf{B}^H(\mathbf{x}, \mathbf{e}) \quad (2.3.9)$$

where  $(\cdot)^H$  denotes the Hermitian transpose.

Assuming the number of independent subchannels  $rN_r$  is *small*, then for high SNR, the upper bound on the pairwise error probability of (2.3.3) can be simplified to [16]

$$P(\mathbf{x}, \mathbf{e}) \leq \left( \prod_{i=1}^r \lambda_i \right)^{-N_r} \left( \frac{E_s}{4N_0} \right)^{-rN_r} \quad (2.3.10)$$

where  $r$  is the rank of matrix  $\mathbf{A}(\mathbf{x}, \mathbf{e})$ , and  $\lambda_1, \lambda_2, \dots, \lambda_r$  denote its non-zero eigenvalues.

Using a union bound technique [16], an upper bound for the code frame error probability can be derived which sums the contributions of the PEPs over all error events. As can be seen, the PEP decreases exponentially as we increase the SNR. Thus, at high SNRs, the frame error probability is dominated by the PEP with the minimum product  $rN_r$  over all possible codeword pairs. In order to achieve good performing codes, it is therefore desirable to maximize the minimum rank,  $r$ . The product of the minimum rank and the number of receive antennas,  $rN_r$ , is called the minimum diversity. The maximum possible value of  $rN_r$  is  $N_tN_r$ , however this is often not achievable due to restrictions on code structure [18].

Looking at the (2.3.10), in order to minimize the error probability, one also needs to maximize the non-zero eigenvalues,  $\prod_{i=1}^r \lambda_i$ , of matrix  $\mathbf{A}(\mathbf{x}, \mathbf{e})$  along the pairs of codewords with the minimum rank. Note that,  $\prod_{i=1}^r \lambda_i$ , is the absolute value of the sum of determinants of all the principal  $r \times r$  cofactors of matrix  $\mathbf{A}(\mathbf{x}, \mathbf{e})$  [16].

Thus for small  $rN_r (< 4)$  the design criteria for STCs over quasi-static Rayleigh fading channel can be summarized as:

- Maximize the minimum rank  $r$  of matrix  $\mathbf{A}(\mathbf{x}, \mathbf{e})$  over all pairs of distinct codewords
- Maximize the minimum product,  $\prod_{i=1}^r \lambda_i$ , of matrix  $\mathbf{A}(\mathbf{x}, \mathbf{e})$  among the pairs of distinct codewords with the minimum rank.

These criteria are known as *rank and determinant* criteria [16].

It is worthy to note that the exponent ( $rN_r$ ) of the SNR term in (??), known as *diversity gain*, determines the slope of the error rate curve plotted as a function of the SNR and that the *coding gain* is directly related to  $(\lambda_1 \lambda_2 \dots \lambda_r)^{1/r}$ . Coding gain is what determines the horizontal shift of the uncoded system error rate to the STC error rate curve obtained for any given diversity order. Thus by using the criteria above, we are in effect maximizing both the diversity and the coding gain of the system. Notice also that since the diversity gain is an exponent in the error probability upper bound, achieving a large diversity gain is more important than achieving a high coding gain for systems with small  $rN_r$ .

Tarkoh et. al. [116], developed a number of codes by hand based on this criteria and presented the corresponding performance curves for the flat Rayleigh fading channel. The codes developed by Tarokh were improved by Baro et. al. [117], using the rank and determinant criteria but performing a computer search over all possible codes. They consider a two Transmit antenna model and choose the code which has the maximum rank ( $= 2$ ) and highest determinant. They obtain codes with better performance in comparison.

### 2.3.3 Trace Criterion

For *large* diversity values, corresponding to a large number of independent subchannels, the PEP for high SNR's can be approximated by [18]

$$P(\mathbf{x}, \mathbf{e}) \leq \frac{1}{4} \exp\left(-N_r \frac{E_s}{N_0} \sum_{i=1}^r \lambda_i\right) \quad (2.3.11)$$

Thus, to minimize the error probability, one should maximize the minimum sum of all eigenvalues of matrix  $\mathbf{A}(\mathbf{x}, \mathbf{e})$  among all pairs of distinct codewords. Since  $\mathbf{A}(\mathbf{x}, \mathbf{e})$  is a square matrix, this can be referred to as maximizing the minimum *trace* of the matrix among all pairs of distinct codewords. This can be expressed as

$$\text{tr}(A(\mathbf{x}, \mathbf{e})) = \sum_{i=1}^r \lambda_i = \sum_{i=1}^{N_t} A^{i,i} \quad (2.3.12)$$

where  $A^{i,i}$  are the elements on the main diagonal of matrix  $A(\mathbf{x}, \mathbf{e})$ .  $A^{i,i}$  can be expressed as

$$A^{i,i} = \sum_{t=1}^L (x_t^i - e_t^i)(x_t^i - e_t^i)^* \quad (2.3.13)$$

where  $(.)^*$  represents the complex conjugate operation. Based on (2.3.12) and (2.3.13), we can write

$$\text{tr}(A(\mathbf{x}, \mathbf{e})) = \sum_{i=1}^{N_t} \sum_{t=1}^L |x_t^i - e_t^i|^2 \quad (2.3.14)$$

Thus, it can be seen that the trace of matrix  $\mathbf{A}(\mathbf{x}, \mathbf{e})$  is equivalent to the squared minimum Euclidean distance between the codewords  $\mathbf{x}$  and  $\mathbf{e}$ . As such, maximizing the minimum sum of all eigenvalues of the difference matrix among the pairs of distinct codewords, or maximizing the minimum trace of that matrix, is equivalent to maximizing the minimum Euclidean distance between all pairs of distinct codewords. Therefore, this design criterion is referred to as the *trace criterion*.

The Trace criterion was introduced by Vucetic et. al. [54, 18]. As the authors explain in their work, it is suitable for cases where  $rN_r \geq 4$ , which is consistent with what had

been proposed earlier for trellis codes over fading channels with a large number of diversity branches [56]. The large number of diversity branches reduces the effect of fading and consequently, the channel approaches an AWGN model. In AWGN models, maximizing the minimum Euclidean distance had been proposed [34] in 1982 and been in wide use ever since. Similarly for space-time codes, when the number of independent co-channels is sufficiently large,  $rN_r \geq 4$ , the channel converges to an AWGN model, making the trace criterion more suitable.

Therefore, designing STCs in quasi-static fading channels, either the rank and determinant or the trace criterion can be used depending on the boundary value of  $rN_r$ . The boundary value is chosen to be 4 in the literature and the reasoning is provided both analytically and based on simulation results. It has been shown that so long as  $rN_r \geq 4$ , the best codes based on trace criterion outperform those based on the rank and determinant criteria [54, 55]. The trace criterion is considered in this work.

## 2.4 CSTTC Encoder Structure

In CSTTCs, the encoder maps binary data to modulation symbols, where the mapping function is described by a trellis diagram. Consider a CSTTC system with  $M$ -PSK modulation,  $N_t$  transmit antennas and  $N_r$  receive antennas. At time  $t$ , the encoded  $M$ -PSK symbols  $x_t^1, x_t^2, \dots, x_t^{N_t}$  are simultaneously transmitted over  $N_t$  antennas.

The signal is received after being distorted by the channel fading and AWGN. From (2.2.1), at time  $t$ , the received signal  $r_t^j$  at receive antenna  $j \in \{1, 2, \dots, N_r\}$ , is given by

$$r_t^j = \sqrt{\frac{\rho}{N_t}} \sum_{i=1}^{N_t} h_{i,j}^t x_t^i + n_t^i \quad (2.4.1)$$

where  $h_{i,j}^t$  is the fading coefficient between transmit antenna  $i$  and receive antenna  $j$  at time

$t$ , and  $n_t^j$  denotes the noise component at receive antenna  $j$  at time  $t$ .

An  $M$ -PSK STTC encoder with memory order  $v$  and  $N_t$  transmit antennas is presented in Figure 2.2. This encoder can achieve a bandwidth efficiency of  $m = \log_2 M$  b/s/Hz and consists of  $m$  branches of shift registers with total memory order  $v$ . At time  $t$ ,  $m$  binary inputs  $c_t^k$ ,  $k \in \{1, 2, \dots, m\}$ , are fed into the  $m$  branches. The memory order of the  $k$ -th branch is given by

$$v_k = \lfloor \frac{v + k - 1}{\log_2 M} \rfloor \quad (2.4.2)$$

where  $\lfloor X \rfloor$  denotes the maximum integer not larger than  $X$ .

The  $m$  streams of input bits are simultaneously passed through their corresponding shift

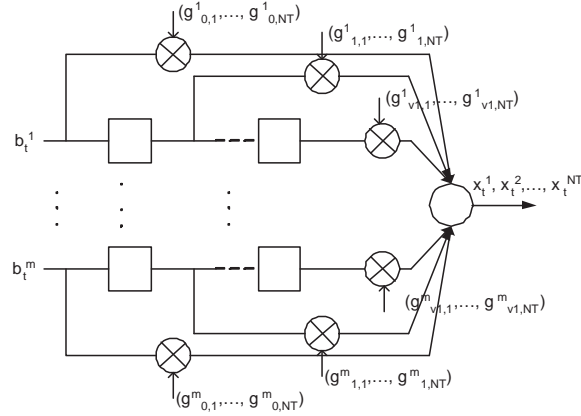


Figure 2.2: General STTC encoder structure for  $N_t$  transmit antennas [18].

register branches and multiplied by the coefficient vectors

$$\begin{aligned} \mathbf{g}^1 &= [(g_{0,1}^1, g_{0,2}^1, \dots, g_{0,N_t}^1), (g_{1,1}^1, g_{1,2}^1, \dots, g_{1,N_t}^1), \dots, (g_{v_1,1}^1, g_{v_1,2}^1, \dots, g_{v_1,N_t}^1)] \\ \mathbf{g}^2 &= [(g_{0,1}^2, g_{0,2}^2, \dots, g_{0,N_t}^2), (g_{1,1}^2, g_{1,2}^2, \dots, g_{1,N_t}^2), \dots, (g_{v_2,1}^2, g_{v_2,2}^2, \dots, g_{v_2,N_t}^2)] \\ &\vdots \\ \mathbf{g}^m &= [(g_{0,1}^m, g_{0,2}^m, \dots, g_{0,N_t}^m), (g_{1,1}^m, g_{1,2}^m, \dots, g_{1,N_t}^m), \dots, (g_{v_m,1}^m, g_{v_m,2}^m, \dots, g_{v_m,N_t}^m)], \end{aligned} \quad (2.4.3)$$

where  $g_{j_k,i}^k$  is an  $M$ -PSK symbol, for  $k \in [1, m]$ ,  $j_k \in [0, v_k]$  and  $i \in [1, N_t]$ .

The encoder output at time  $t$  for transmit antenna  $i$ , can be computed as

$$x_t^i = \sum_{k=1}^m \sum_{j_k=0}^{v_k} g_{j_k,i}^k b_{t-j_k}^k \pmod{M} \quad (2.4.4)$$

These outputs are elements of an  $M$ -ary signal set.

This encoder can also be described in generator polynomial format. The  $k$ th binary input stream  $\mathbf{b}^k$  can be represented as

$$\mathbf{b}^k(D) = b_0^k + b_1^k D + b_2^k D^2 + \dots, \quad k = 1, \dots, m \quad (2.4.5)$$

where  $b_t^k \in [0, 1]$  and  $D$  represents a unit delay operator. The generator polynomial for the  $i$ th transmit antenna can be represented as

$$\mathbf{G}_i^k(D) = g_{0,i}^k + g_{1,i}^k D + \dots + g_{v_k,i}^k D^{v_k}, \quad \begin{array}{l} i = 1, 2, \dots, N_t \\ k = 1, 2, \dots, m \end{array} \quad (2.4.6)$$

The coded symbol sequence transmitted from antenna  $i$  is given by

$$\mathbf{x}^i(D) = \sum_{k=1}^m \mathbf{b}^k(D) \mathbf{G}_i^k(D) \pmod{M} \quad (2.4.7)$$

This can also be written as

$$\mathbf{x}^i(D) = [\mathbf{b}^1(D) \dots \mathbf{b}^m(D)] \begin{bmatrix} \mathbf{G}_i^1(D) \\ \mathbf{G}_i^2(D) \\ \vdots \\ \mathbf{G}_i^m(D) \end{bmatrix} \pmod{M} \quad (2.4.8)$$



where

$$\mathbf{G}_i(D) = \begin{bmatrix} \mathbf{G}_i^1(D) \\ \mathbf{G}_i^2(D) \\ \vdots \\ \mathbf{G}_i^m(D) \end{bmatrix} \quad (2.4.9)$$

is the generator matrix for antenna  $i$ . The generator matrices are designed based on the criteria discussed in Section 2.3.

## 2.5 CSTTC Decoder Structure

For STTCs, the decoder normally employs the Viterbi algorithm to perform maximum likelihood decoding. It is assumed that perfect channel state information (CSI) is available at the receiver. For a branch labelled by the symbol  $\mathbf{x}_t$ , the branch metric is computed as the squared Euclidean distance between the hypothesized received symbols and the actual received signals as

$$\sum_{j=1}^{N_r} \left| r_t^j - \sum_{i=1}^{N_t} h_{i,j}^t x_t^i \right|^2 \quad (2.5.1)$$

The Viterbi algorithm selects the path with the minimum path metric as the decoded sequence [121].

## 2.6 An Example

In this example [54], we consider a 4-state STTC with an underlying constellation of 4 QAM with two transmit antennas. The generator matrix, for the chosen code, designed using the trace criterion is given by

$$G^T = \begin{pmatrix} 0 & 2 & 1 & 2 \\ 2 & 3 & 2 & 0 \end{pmatrix} \quad (2.6.1)$$

The trellis structure for the code is depicted in Figure 2.3. The trellis consists of  $2^v = 4$  states represented by the nodes in this Figure. The encoder takes  $m = 2$  input bits at each time. There are  $2^m = 4$  branches, corresponding to four different input patterns, leaving each state. The branches are labelled by  $b_t^1 b_t^2 / x_t^1 x_t^2$ , where  $b_t^1$  and  $b_t^2$  are a pair of encoder input bits, and  $x_t^1$  and  $x_t^2$  represent two coded QPSK symbols transmitted through antennas 1 and 2, respectively.

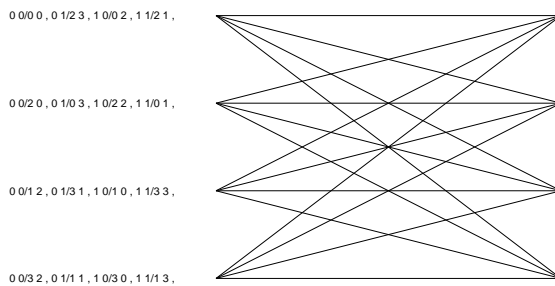


Figure 2.3: An example trellis structure, 2 transmit antennas, QPSK.

The performance of this code is shown in Figure 2.4<sup>1</sup>. This code is used in Chapter 4 as one of the component codes of the proposed scheme. The published results on STTCs,

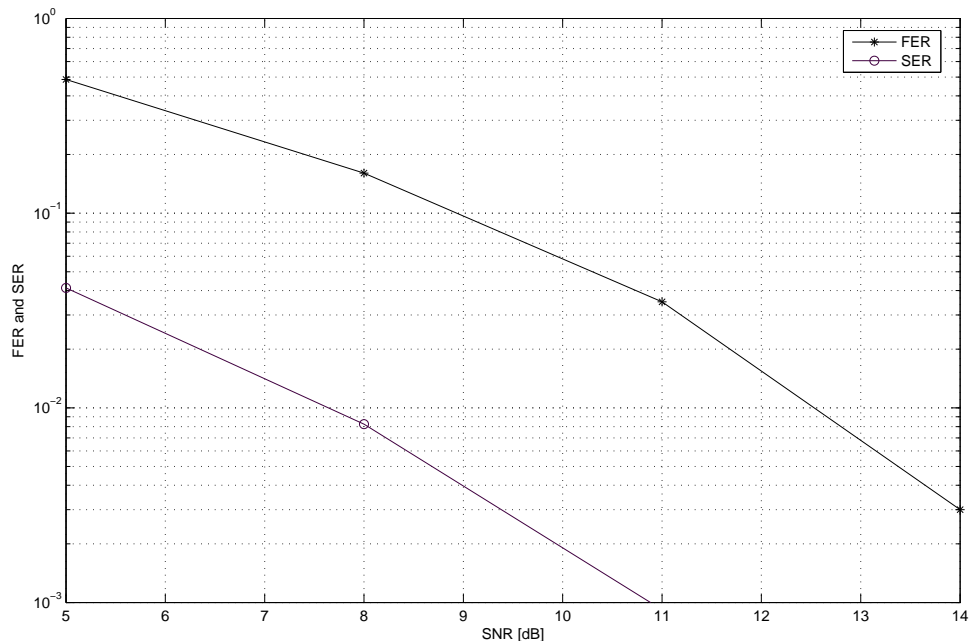


Figure 2.4: Simulated performance of CSTTCs, 4 state, QPSK, 2 transmit antennas.

suggest that as the number of states available in the trellis is increased, the coding gain of the system also increases. This is expected as, in general, longer trellis codes have a larger determinant. Furthermore, it has been shown that the constraint length of the code does not affect the diversity.

The minimum number of states in a given CSTTC, can be shown to be equal to  $M = 2^m$ . We represent the complexity of a CSTTC, designed for an  $M$ -ary constellation by being in the order of *number of states*  $\times$  *number of branches per state*, which in this case is equal to  $4 \times 4$ . This measure is directly related to the size of the trellis code, which in turn affects the code search complexity, the encoding and the decoding complexity. The larger this

<sup>1</sup>Notice that the system parameters (e.g. SNR) are set up as described in Section 2.2.

measure, the more complex the system will be.

In order to design high data rate systems, it is highly desirable to design CSTTCs with high spectral efficiency. However, the exponential growth in the complexity has so far been a major obstacle to the use of CSTTCs, for systems with high spectral efficiency or a larger number of antennas.

## 2.7 Summary

In this Chapter different design criteria for STCs were reviewed. As suggested, the design criteria for quasi-static Rayleigh flat fading channels depends on the code parameter, the rank of the codeword difference matrix  $r$ , and the number of receive antennas in the system,  $N_r$ . If  $rN_r < 4$ , the rank & determinant criterion are applicable, while the trace criterion is more appropriate when  $rN_r \geq 4$ .

CSTTCs and their corresponding encoding and decoding algorithms were discussed. In the next chapter we shall discuss multi-level codes (MLCs). These will be used in Chapter 4 to design a new system. The example CSTTC code presented in this chapter, will be used in Chapter 4 as a component code of the proposed scheme.

## Chapter 3

# Multilevel Coded Modulation

Multilevel coding [67, 68, 87] is a powerful coded modulation technique that provides means of constructing a high complexity code structure using simple component codes. The technique works by partitioning the signal constellation into a multilevel hierarchy and defining a code over each level. These codes are generally decoded in a sequential manner using a multistage decoder (MSD), since decoding the overall multilevel code is usually prohibitively complex. Multilevel codes were originally designed for the AWGN channel. Multilevel codes developed for multiple antenna systems have primarily used block component codes [70, 71, 77, 78].

In this chapter, we provide a brief introduction to multilevel codes and their encoding and decoding. In addition, some of the most commonly used multilevel code structures used for MIMO systems are outlined. The techniques highlighted in this chapter, are later used in Chapter 4 to propose a new scheme which makes use of the multilevel coded modulation concepts and STTCs.

### 3.1 Introduction

During the first few decades after the publication of Shannon's paper on capacity [52], research in coding theory concentrated almost exclusively on designing good codes and

efficient algebraic decoding algorithms for *binary input channels*, where the encoded bits were mapped to one-dimensional BPSK or QPSK signals. Up until the late 1970s, it was widely believed that coding gain could only be achieved through bandwidth expansion and that coding could serve no useful purpose at high spectral efficiencies. Therefore, in applications such as data transmission over dial-up telephone networks, where bandwidth was limited and large modulation alphabets were needed to achieve high spectral efficiencies, coding was thought to be a non-viable option. As a result, the modulation system design was almost entirely focused on constructing large signal sets with the largest possible minimum Euclidean distance between signal points, given constraints on average/peak signal energy [26].

*Coded modulation* refers to a class of techniques in which coding and modulation are combined and jointly optimized in order to improve the performance of a given digital transmission scheme, usually without incurring bandwidth expansion. Thus, coded modulation is referred to as a *bandwidth efficient* signaling technique. In the late 1970s, Ungerboeck [33] and Imai and Hirakawa [67] independently presented two of the most powerful applicable coded modulation techniques to date, namely *trellis coded modulation (TCM)* and *multilevel coded modulation (MLC)*, respectively. The common core in these two techniques is that, unlike classical coding schemes that dealt with Hamming distances, these schemes optimize the code and hence the coded modulation in Euclidean space.

The concept of TCM was originally introduced by Ungerboeck and Csaajka [33] in June 1976 and was later developed in more detail by Ungerboeck in [34, 35, 36]. Other early contributions to the development of TCM include papers by Anderson and Taylor [39], Forney et. al. [40] and Calderbank et. al. [79, 80]. Ungerboeck's TCM is based on mapping by binary set partitioning, whereby the signal set, with an underlying signal constellation of  $M = 2^m$  points, is successively binary partitioned in  $m$  or fewer steps to define a mapping of binary addresses to signal points. Most coded modulation schemes use Ungerboeck's set

partitioning. It maximizes the minimum intra-subset Euclidean distance. In the encoder, the binary addresses are *usually* divided into *least significant* binary symbols, which are convolutionally encoded, and *most significant* binary symbols, which -if present- are left uncoded. An exhaustive computer search is usually used to find the corresponding code parameters, in order to maximize the minimum distance between coded sequences in Euclidean space. A lot of work has been done on TCM designs since this early work. For a summary of some of the more recent work refer to [38, 37, 26, 87] and the references therein. It is worth noting that the STTCs, described in Chapter 2, can in fact be thought of as an extension of TCM to MIMO channels.

MLC [67, 68, 42, 87] efficiently splits the transmission channel into several logical subchannels, with the number of such subchannels depending on the size of the signal constellation of the underlying modulation scheme. Due to the separated subchannels, a MSD can be used. It decodes the component codes sequentially. Generally the MSD starts by decoding the most powerful component code. As each component code is decoded, its output decisions are assumed to be correct and are employed in the decoding of the subsequent and weaker code sequences. A MSD can potentially achieve the performance of a very large and complex code, but requires considerably lower decoding complexity [87]. The idea behind MLC, as originally described by Imai and Hirakawa [67], was to protect each bit in the label of a signal point with an independent binary code. This sort of protection implicitly assumes that some form of partitioning is being employed. Originally these codes were proposed for one-dimensional signaling combined with labeling by binary counting of the signal levels. The partitioning strategy was to maximize the minimum intra-subset Euclidean distance, in a similar manner to the TCM schemes developed by Ungerboeck. Pottie and Taylor later generalized this idea in [68], by using  $q$ -ary,  $q \geq 2$ , component codes based on a binary or nonbinary partitioning of a two-dimensional signal set. In this context, TCM can be thought of as a special case of MLC using a single convolutional code with a nonbinary

output alphabet while higher levels may remain uncoded. Unlike TCM, however, the MLC approach provides flexible transmission rates, through the use of multiple component codes that may have different rates. Furthermore, *any* code, can be used as a component code.

### 3.2 Multilevel Encoder

In a generalised multilevel construction [68, 42, 26, 59, 82], a signal constellation  $S_L$  is partitioned into a partition chain written as  $S_L/S_{L-1}/\dots/S_0$ . Each set or sub-constellation  $S_{i-1}$  is a subset of the set directly above it,  $S_i$ , whereby it divides  $S_i$  exactly into  $S_{i-1}$  and its cosubsets. The elements of the set formed by the partitioning of  $S_i$  into  $S_{i-1}$  and its cosubsets may be labelled by a set of labels  $x_i$ , whereby  $S_{i-1}$  and its cosubsets map onto the elements of  $x_i$  and we can write  $S_i/S_{i-1} \leftrightarrow x_i$ . The labels  $x_i$ , are elements of a discrete alphabet over which a component code  $C_i$  can be defined. The combination consisting of the partition chain  $S_L/S_{L-1}/\dots/S_0$ , the label sets  $x_1, x_2, \dots, x_L$  and the set of codes  $C_1, C_2, \dots, C_L$  form a multilevel code. The general structure of a multilevel encoder is shown in Figure 3.1.

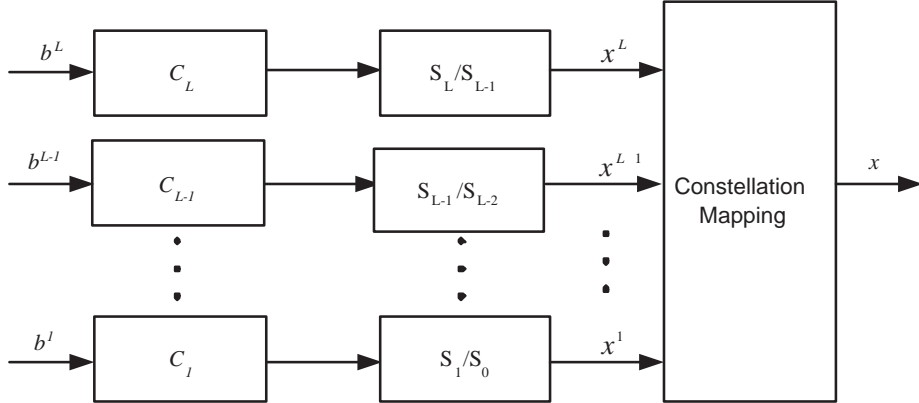


Figure 3.1: General encoder structure for a multilevel code.

Each code,  $C_i$ , accepts  $b_i$  input bits and outputs  $|S_i|/|S_{i-1}|$  bits for each time slot. The output of the encoder for  $C_L$  selects a cosubset of  $S_L/S_{L-1}$ . The next encoder for  $C_{L-1}$



selects a cosubset of  $S_{L-1}/S_{L-2}$ , and so forth, until finally the code  $C_1$  narrows down the selection to a single point on the underlying constellation,  $x$ , which will be transmitted. An overall code  $C$ , may be associated with the  $L$ -level multilevel code. This code is referred to as the *multilevel* code associated with the partition chain  $S_L/S_{L-1}/\dots/S_0$  and the  $L$  independent component codes  $C_1, C_2, \dots, C_L$ .

Several different criteria have been proposed for designing multilevel codes, in particular with respect to selecting the component codes. These include distance based criteria [67, 68, 42], capacity based designs [87, 122, 123], those based on the cutoff rate [87] and the coding exponent [87]. The first two have been the most popular, and have been shown to have good performance in a variety of different scenarios.

The capacity based design rule, proposed by Huber et. al. in the late 1990s [122, 123, 87], chooses the rates of the component codes to be equal to the equivalent capacity of the corresponding equivalent subchannels at that partitioning level for the desired SNR. Although this method has been shown to have good performance, calculating the capacities of equivalent channels, in practical scenarios, can be cumbersome. Furthermore, this design rule was derived assuming infinite length codes, which is impractical.

In this thesis, we use the *balanced distance* design rule, which was the original design rule proposed by Imai et. al. [67] and has been used in the majority of the multilevel designs [68, 42, 82, 71]. This criterion is based on the minimum Euclidean distance. More specifically it aims to maximize the minimum distance of the Euclidean space code by choosing component codes that result in equal minimum squared Euclidean distances on all levels. This then provides equal protection for all bits in each sequence of constellation points.

A variety of different partitioning strategies have been suggested [87, 106, 124, 59, 81]. In this work, we consider a partitioning scheme based on multi-resolution modulation (MRM),

originally introduced in the context of broadcast channels by Cover [88]. In our proposed scheme, we consider MRM in a multi-antenna scenario and propose a method for distributing the data over transmit antennas, space, and time. This is described in detail in Chapter 4.

In contrast to TCM, the design of good multilevel codes is not a straight-forward exhaustive code search. Multilevel codes offer the designer more degrees of freedom. There are a number of potential design tradeoffs involving the underlying signal constellation with respect to the number of points in it and their spacing, the partitioning strategy for the signal constellation, the number of levels in the partition chain, and the codes and code rates at each level. The main tradeoff of interest when designing multilevel codes, is often that of the error performance versus decoding complexity.

### 3.3 Multistage Decoder

Multilevel codes are usually decoded by a staged decoder as shown in Figure 3.2. The decoder, on level  $i$  in the figure decodes the component code  $C_i$ . The staged decoder operates in a sequential manner. First the decoder at level  $L$  makes a decision on the code  $C_L$  and outputs the corresponding data bits,  $b_L$ . This decision information is then passed on from stage  $L$  to stage  $L - 1$  and the decoder at level  $L - 1$  operates in a similar way, outputting  $b_{L-1}$  and the corresponding cosubset information. The process continues down the partition chain until the received sequence is completely decoded.

The fact that the decision at each level assumes a correct decision from the previous level, means there can be error propagation through a MSD. Techniques such as interleaving and iterative multi-stage decoding have been used in the literature to combat these effects [63, 82, 64, 89]. Addressing these issues is beyond the scope of this thesis.

Although interleaving and iterative decoding can potentially improve the performance,

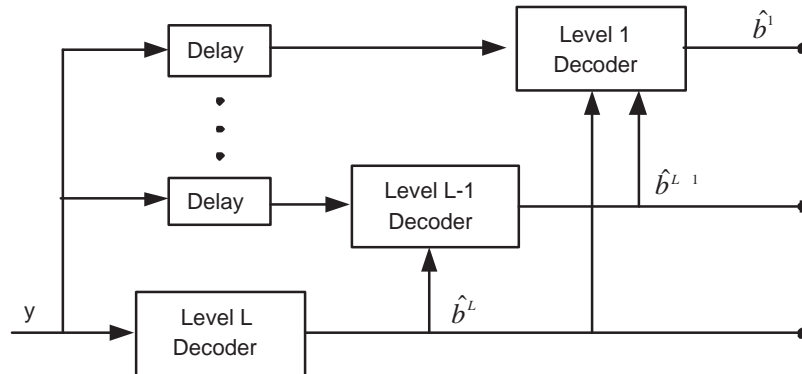


Figure 3.2: General multi-stage decoder for a multilevel code.

there are also drawbacks that need to be considered. In the case of interleavers, for example, the main penalty is the additional delay and in the case of iterative decoding, it is also the added complexity. Consequently, the tradeoffs must be considered carefully, to make sure the additional gain is *worth* the penalty.

### 3.4 MIMO Multilevel Codes

Tarokh et. al. briefly mentioned the idea of using multilevel concepts within space-time codes in their 1998 paper [16], where they introduced STCs. They suggested that multilevel coding would be a good way of producing powerful space-time codes for various high-bit-rate applications. They also presented a simple example for an 8 PSK system using set partitioning and short (length =  $N_t$ ) block codes on each level. Since then, there have been many publications on space-time codes, but very few have considered using multilevel codes in a space-time environment. The few papers which have discussed this topic, have mainly focused on a combination of STBCs, BLAST and MLC [69, 71, 75, 78]. In this section we briefly highlight some of these structures.

In Lampe et al's papers [69, 70], the authors discuss several multilevel code structures for

multi-antenna systems in fast<sup>1</sup> Rayleigh fading channels. They follow the capacity design rules of [87] and argue that any mapping function is optimum in terms of capacity. Under the heading of *multilevel coding*, they make use of a pragmatic mapping approach and map blocks of  $\log_2(M)$  bits to one constituent  $M$ -PSK/ $M$ -QAM symbol transmitted from each antenna, as shown in Figure 3.3. They consider using Ungerboeck and Gray labelling for their MLC structure and use binary block codes as component codes.

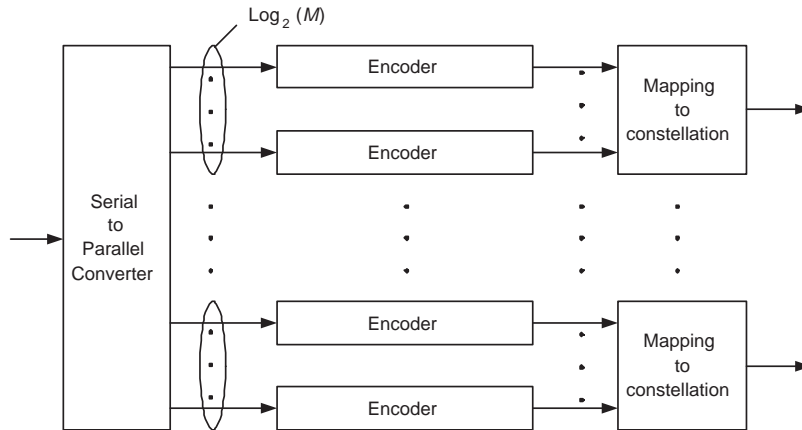


Figure 3.3: A MIMO MLC structure from [69].

The advantage of this method is that it is relatively simple to implement and is somewhat intuitive. It is also optimum in terms of capacity. However, the design leads to a relatively large number of levels ( $= N_t \log_2(M)$ ), where each component code in the MLC spans only a single transmit antenna. The design approach results in independent signaling on each transmit antenna.

Another approach discussed in [69, 70] is *hybrid coded modulation* (HCM), see Figure 3.4. In this approach, each group of  $\log_2(M)$  levels corresponding to one constituent  $M$ -ary symbol are merged leading to only  $N_t$  levels. MLC and multi-stage decoding are applied with respect to these  $N_t$  levels, but within each level bit-interleaved coded modulation (BICM) is performed. HCM is similar to V-BLAST, in that it entails separate coding for each stream

<sup>1</sup>with respect to one coding frame.

(layer) associated with each transmit antenna. Levels of HCM thus correspond to layers in V-BLAST and MSD effectively corresponds to successive interference cancellation. The major difference is that HCM is designed based on MLC capacity design rules.

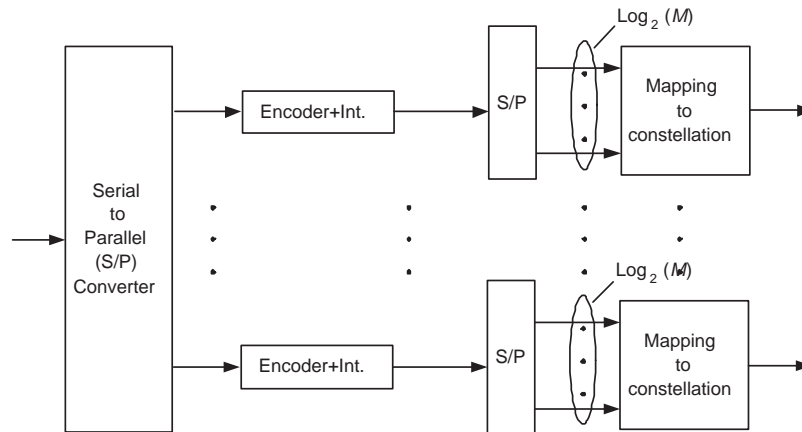


Figure 3.4: Hybrid coded modulation scheme of [69].

HCM is not optimum in terms of capacity. For it to be efficient in terms of capacity, the user is restricted to applying Gray labelling with respect to the constituent signal constellation. On the other hand, HCM has lower implementation complexity than the MLC approach proposed by [69, 70] and has reduced transmission delay. Although not as computationally simple as BICM, it provides better performance. The authors compare the performance of this scheme to that of STBCs, and conclude that independent signalling over two transmit antennas and MLC (HCM) is inferior to STBC transmission. This is explained to be due to the different constituent signal constellations applied, but is considered to be a fair comparison as the number of transmit symbols per modulation interval is equal in all cases.

Another capacity approaching scheme is proposed in [77] and [78], where the authors use a multi-dimensional partitioning scheme based on [106] and make use of binary irregular LDPC component codes on each level. They also propose the corresponding MSD that

makes use of a bank of *sphere decoders* [179] for detection on each level, with a separate sphere decoder for each coset. After detection, the component decoder (an iterative decoder in this case) is used to make a decision on the transmitted coset. This decision is then passed on to the next level and the decoding proceeds in a multi-stage fashion. In [78], an alternative partitioning strategy based on [83, 84] is also discussed.

Yuan et. al. consider the subject of MLC for multi-antenna systems in a number of papers including [71, 75, 76]. They consider different partitioning schemes, primarily the Ungerboeck partitioning [34] and block partitioning [87], and consider QAM and PSK as the underlying constellations. In different papers they consider both distance-based [75] and capacity-based [76] approaches for choosing their component codes. In order to achieve space-diversity, the authors concatenate their MLC system (which is designed for a single antenna system) with an orthogonal STBC, as shown in Figure 3.5.

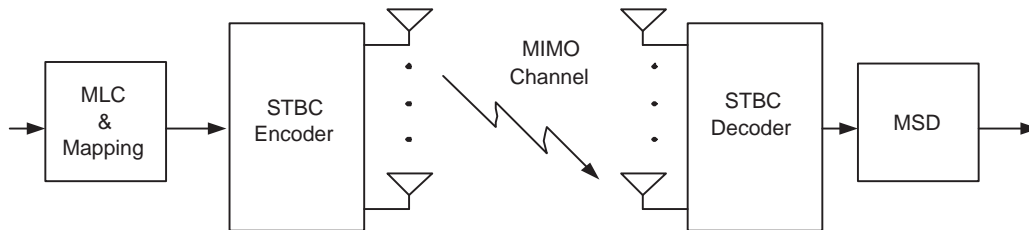


Figure 3.5: The concatenated STBC-MLC system of [75].

At the receiver [75], the STBC is decoded and then the results are passed to a MSD to decode the multilevel codes. The addition of the STBC block in this structure, although providing diversity, can be seen to limit the rate of the overall system.

As can be seen, these works have mostly focused on block codes in their designs and the combination of STBCs, BLAST and MLC. In Chapter 4, we propose a new transmission scheme which makes use of concepts from MLC and STTCs.

### 3.5 Summary

This chapter has presented background on MLC and highlighted the encoding and decoding structure of a multilevel coded system. Some of the MLC structures most commonly used with MIMO systems were also outlined. It was noted that despite their many advantages, to date, there has been little work done on multilevel codes in a space-time environment and the majority of the work done has focused on a combination of block codes, BLAST and STBCs in conjunction with MLC.

In the next chapter, we make use of the techniques highlighted in Chapter 2 and 3 to propose a new transmission scheme which makes use of multilevel coding concepts and STTCs in order to achieve good performance, high throughput and low complexity. Our system offers a more integrated design, which spans both space and time.

## Chapter 4

# Multilevel Space-Time Trellis Codes

In Chapter 2 we studied *conventional space-time trellis codes (CSTTCs)* [91, 54, 55], which can simultaneously provide substantial coding gain, spectral efficiency and diversity improvement. However, as discussed, the exponential increase in decoding complexity with the number of antennas and the size of the modulation set is a major hurdle to them being widely adopted in practice, for larger constellations and higher throughputs. In Chapter 3, we discussed *multilevel coded (MLC) modulation* [67, 68, 87], where a higher complexity coded signal constellation can be constructed using simple component codes.

In this chapter we combine the techniques of Chapter 2 and 3 to develop multilevel space-time trellis codes (MLSTTC's), capable of simultaneously providing bandwidth efficiency, diversity improvement and coding gain with significantly reduced decoding complexity, especially for larger constellations and higher throughputs. The general structure of MLSTTC's is flexible and can easily be tuned to achieve the required balance between spectral efficiency, error performance and decoding complexity. We describe the overall structure and analytical model in this chapter. Performance evaluations and trade-offs are studied in Chapter 5.



## 4.1 Introduction

To enable high spectral efficiency for future high data rate transmissions, it is desirable to construct CSTTC's using high order signal constellations. However, the design of CSTTC's normally involves a computer search, with the size of the search space increasing exponentially with constellation size, number of transmit antennas and number of states in the code trellis. The decoding complexity of the CSTTC's also increases exponentially with the size of the underlying constellation. To the best of the author's knowledge, there are currently no CSTTC's designed for 64 QAM, which would allow 6 bits/sec/Hz. Due to these complexity problems, and despite their many benefits, CSTTC's are still viewed with reluctance from system designers when it comes to implementation.

In this chapter we propose a new class of codes that benefit from many of the advantages of CSTTC's without some of the disadvantages. MLSTTC's present a promising alternative to currently available CSTTC's, by simultaneously offering diversity improvement, coding gain and bandwidth efficiency at significantly lower decoding complexity than CSTTC's. Furthermore, the proposed MLSTTC's provide flexible transmission rates by partially decoupling the dimensionality of the signal constellation from the code rate. Examples of higher rate MLSTTC's are presented in Chapter 5.

In designing MLSTTC's, we make use of the multilevel coding techniques, described in Chapter 3. To date, little work has been done on multilevel ST coded MIMO systems and most of that has been focused on *block codes* [71, 75, 76, 77, 78]. In the proposed MLSTTC's, the focus is placed on using CSTTC's [54, 55] as component codes. Unlike some of the multilevel MIMO structures in the literature [71, 75, 76], the MLSTTC structure is more integrated as it does not require having a separate ST encoder. Furthermore, we depart from the BLAST-based multilevel [70, 69] and multi-layered systems [85, 73, 199] by making better use of both spatial and temporal dimensions. In this chapter, we describe

the overall design strategy. System performance and some of the trade-offs are considered in the next chapter.

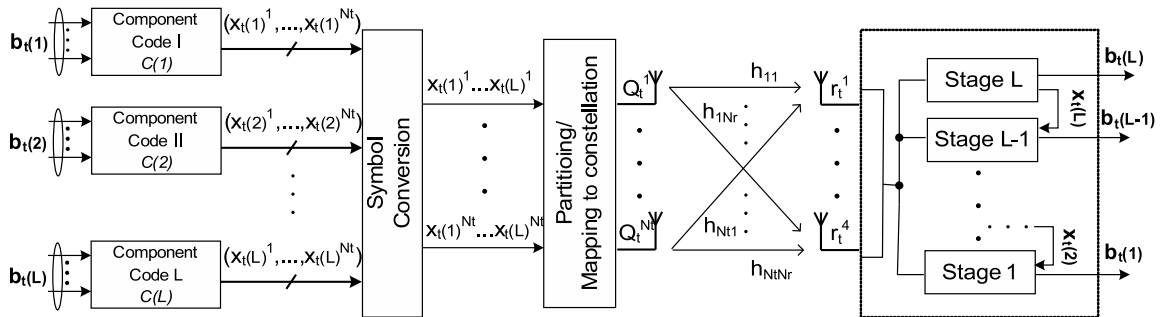
## 4.2 System Model

We consider a MIMO wireless link, with  $N_t$  transmit antennas and  $N_r$  receive antennas. The symbol transmitted at time  $t$  by the  $j$ th transmit antenna is denoted by  $Q_t^j$ , for  $1 \leq j \leq N_t$ . We follow [16, 54, 55, 73], in assuming that the channel exhibits quasi-static frequency flat Rayleigh fading over a frame duration. Thus, it is constant over one frame and varies independently between frames. We assume that perfect CSI is available at the receiver, but that no knowledge of the channel is available at the transmitter.

The received signal at time  $t$ , at the  $i$ th receive antenna is a noisy superposition of independently Rayleigh faded versions of the  $N_t$  transmitted signals and is denoted  $r_t^i$  for  $1 \leq i \leq N_r$ . The discrete complex baseband output of the  $i$ th receive antenna at time  $t$  is given by

$$r_t^i = \sum_{j=1}^{N_t} h_{ij} Q_t^j + n_t^i \quad (4.2.1)$$

where  $h_{ij}$  is the path gain between the  $j$ th transmit and  $i$ th receive antennas and  $n_t^i$  is the noise associated with the  $i$ th receive antenna at time  $t$ . The path gains,  $h_{ij}$ , are modeled as samples of independent complex Gaussian random variables with zero mean and variance of  $1/2$  per dimension, implicitly assuming that the signals transmitted from different antennas undergo independent fading. The noise quantities are samples of independent complex Gaussian random variables with zero mean and variance of  $N_0/2$  per dimension.

Figure 4.1: General structure of an MLSTTC system.<sup>1</sup>

In matrix form, (4.2.1) can be represented as

$$\begin{bmatrix} r_t^1 \\ r_t^2 \\ \vdots \\ r_t^{N_r} \end{bmatrix} = \begin{bmatrix} h_{11} & h_{12} & \dots & h_{1N_t} \\ h_{21} & h_{22} & \dots & h_{2N_t} \\ \vdots & \vdots & \ddots & \vdots \\ h_{N_r1} & h_{N_r2} & \dots & h_{N_rN_t} \end{bmatrix} \begin{bmatrix} Q_t^1 \\ Q_t^2 \\ \vdots \\ Q_t^{N_t} \end{bmatrix} + \begin{bmatrix} n_t^1 \\ n_t^2 \\ \vdots \\ n_t^{N_r} \end{bmatrix} \quad (4.2.2)$$

or in compact form as

$$\mathbf{r}_t = \mathbf{H}_t \mathbf{Q}_t + \mathbf{n}_t \quad (4.2.3)$$

where,  $\mathbf{Q}_t = (Q_t^1, Q_t^2, \dots, Q_t^{N_t})^T$ ,  $\mathbf{r}_t = (r_t^1, r_t^2, \dots, r_t^{N_r})^T$ ,  $\mathbf{n}_t = (n_t^1, n_t^2, \dots, n_t^{N_r})^T$  and  $\mathbf{H}_t$  is the  $N_r \times N_t$  channel matrix whose  $(i,j)$ th entry is represented by  $h_{ij}$  and  $(\cdot)^T$  denotes the transpose operation.

As will be described in detail in Section 4.3.1, the MLSTTC system works by partitioning the underlying signal constellation into a hierarchy of subsets or clusters using the *multi-resolution modulation* (MRM) approach, originally introduced by Cover in 1972 [88] and later used by others including [200]. Each cluster may itself have sub-clusters and so on. The incoming bits are encoded and mapped to the  $2^m$  point MRM constellation; with the most significant coded bits being mapped to the clusters and the least significant bits to the subclusters and so forth. Ultimately, the last bits choose a signal point within the underlying constellation.

This clusterization provides up to  $L$  resolutions for an underlying  $M$ -QAM constellation, with  $M = 4^L$ , where each resolution can be considered as a 4-QAM constellation<sup>2</sup>. Up to  $L$  component codes can be used to encode the incoming bits. A simplified block diagram of a MLSTTC system is presented in Figure 4.1. The component codes are denoted as  $\mathcal{C}(1), \mathcal{C}(2), \dots, \mathcal{C}(L)$  in this figure. Each of these component codes is designed for their corresponding cluster size. The output of each encoder is mapped to its corresponding cluster.

In the designs presented in this thesis, CSTTC's [54, 55] are used as component codes in the MLSTTC's. Potentially, *any* code (including block codes) can be used as a component code. The encoding is over both space and time. Throughout we assume  $rN_r \geq 4$ , where  $r$  is the rank of the code difference matrix. As discussed in Chapter 2, this results in the minimum Euclidean distance dominating performance and thus we design codes for large Euclidean distances, following the trace criterion [54].

The receiver applies a modified version of a CSTTC decoder in each stage. This is discussed in Section 4.4, where we derive branch metrics for the detection and decoding process to take the effect of the MRM partitioning and multi-stage decoding into account. In the remainder of this chapter we will review each block in the system and investigate their designs.

### 4.3 Encoder Design

We now discuss the encoder design. In particular, we highlight the partitioning strategy and constellation design, and provide an overview of the component codes used. The design is carried out in general terms with specific examples provided in Chapter 5.

---

<sup>2</sup>The hierarchy of clusters is analogous to partitioning levels in standard multilevel codes. In the present work, we use 4-point or 4-QAM clusters as the lowest level or base cluster. This is discussed in detail in Section 4.3

### 4.3.1 Partitioning and constellation mapping

The partitioning scheme we use on each of the  $N_t$  transmit antennas is based on MRM, which was originally introduced in the context of broadcast channels [88]. The idea is to divide the underlying signal constellation into a hierarchy of clusters, where each cluster can have its own subclusters. The distance between clusters is greater than the distance between subclusters.

Figure 4.2 shows the application of MRM to a 64-QAM constellation. As can be seen, the 64 points in the underlying constellation are divided into 4 clusters, and each cluster into 4 subclusters and so forth. Thus, we use a 4-cluster as the basic unit of resolution. We partition [68] the multi-resolution constellation by treating each cluster as a 4-QAM constellation. This enables us to directly use CSTTCs designed for 4-QAM in our mapping process. The labelling of the signal constellation points based on the partitioning is also shown in Figure 4.2, where we have 3 clusters, each having 4 subclusters. The circles in the figure denote one subcluster of each cluster.

This clusterization allows us to have  $L$  resolutions for a  $M$ -QAM constellation, with  $M = 4^L$ . We then map the output of the first component code,  $\mathcal{C}(1)$ , to the clusters and the output of the next component code  $\mathcal{C}(2)$  to the subclusters and so forth with the output of  $\mathcal{C}(L)$  selecting the actual constellation points to be transmitted. For the 64-QAM constellation of Figure 4.2, this results in  $L = 3$  levels.

The output of  $\mathcal{C}(L)$ , denoted as  $x_t(L)$ , gets mapped to the actual constellation points, while the outputs generated by  $\mathcal{C}(1)$  to  $\mathcal{C}(L - 1)$ , denoted  $x_t(1), \dots, x_t(L - 1)$  respectively, get mapped to the virtual cluster centre points (centroids) as shown in Figure 4.2, and thus label the corresponding clusters. These component codes are all designed for a 4-QAM constellation and their coded output symbols,  $x_t(1)$  to  $x_t(L)$ , are all drawn from 4-QAM constellations and can be represented either in complex form as  $x_t(l) = a + jb$  —

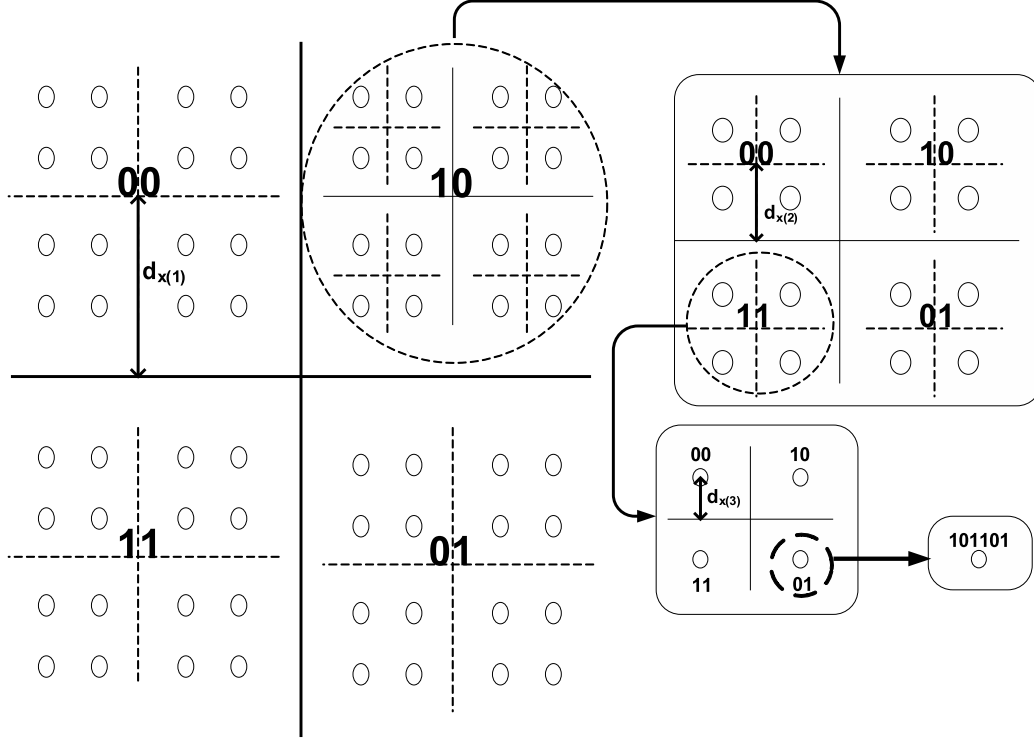


Figure 4.2: Partitioning and labelling of the underlying constellation for 64-QAM.

$a, b \in \{1, -1\}$  or mapped to a ring of integers  $s_t(l) = \mu(x_t(l)) | s_t(l) \in \{0, 1, 2, 3\}$ . Each point in the underlying  $M$ -QAM constellation can be represented in complex form as

$$Q = d_{x(1)}x(1) + d_{x(2)}x(2) + \dots + d_{x(L)}x(L) \quad (4.3.1)$$

where  $d_{x(1)}, \dots, d_{x(L)}$  are the cluster distances corresponding to  $x_t(1), \dots, x_t(L)$ , as shown in Figure 4.2. Note that if the free distances,  $d_{free}$ , of the codes on different levels are not equal but the designer wishes to have equal error protection, or alternatively if the  $d_{free}$  values of all codes are equal but the designer prefers unequal error protection, the distances  $d_{x(1)}$  to  $d_{x(L)}$  can be adjusted to achieve the desired performance. For equal error protection we want  $d_{x(1)}^2 d_{free}^{\mathcal{C}(1)} = d_{x(2)}^2 d_{free}^{\mathcal{C}(2)} = \dots = d_{x(L)}^2 d_{free}^{\mathcal{C}(L)}$ , where  $d_{free}^{\mathcal{C}(l)}$  is the free distance of the  $l$ th component code. An example will be presented in Chapter 5.

### 4.3.2 Component Codes

For the MLSTTC systems discussed in this thesis, we focus primarily on CSTTC's as component codes. However, any codes (including block codes) can potentially be used as component codes.

We consider here the generic case, where an  $M$ -QAM constellation has been partitioned into  $L$  levels of nested clusters, each being representable as a 4-QAM constellation<sup>3</sup>. We initially use  $L$  identical CSTTC's as component codes. These are denoted by  $\mathcal{C}(1), \dots, \mathcal{C}(L)$ , as shown in Figure 4.1.

As explained in Chapter 2, the output of a CSTTC encoder for an  $M$ -ary signal constellation can, in general, be represented as

$$\mathbf{s}^j(D) = \sum_{k=1}^m \mathbf{b}^k(D) \mathbf{G}_j^k(D) \pmod{M} \quad (4.3.2)$$

where  $\mathbf{s}^j(D)$  denotes the  $M$ -ary coded symbol sequence transmitted from antenna  $j$  and  $D$  represents a unit delay operator. The  $k$ th binary input sequence is represented by

$$\mathbf{b}^k(D) = b_0^k + b_1^k D + b_2^k D^2 + \dots, \quad k = 1, \dots, m \quad (4.3.3)$$

where  $b_t^k \in [0, 1]$ ,  $m = \log_2 M$ . The generator polynomial for the  $j$ th transmit antenna is represented by [18]

$$\mathbf{G}_j^k(D) = g_{0,j}^k + g_{1,j}^k D + \dots + g_{v_k,j}^k D^{v_k}, \quad \begin{array}{l} j = 1, 2, \dots, N_t \\ k = 1, 2, \dots, m \end{array} \quad (4.3.4)$$

where  $v_k$  is the memory order of the  $k$ -th branch as defined in Chapter 2. The generator polynomials are designed based on the criteria discussed in Section 2.3. We assume that design of the component codes is based on the trace criterion [54] for quasi-static Rayleigh fading channels.

---

<sup>3</sup>This case is generic in terms of 4-clusters. In principle, one could use 16-clusters, etc.

The CSTTC used has been designed for  $N_t$  antennas and a 4-QAM constellation. It is *not* necessary to use identical component codes in an MLSTTC system. Other variations are possible as will be presented in Chapter 5.

Using 4-QAM clusters, we input two bits into the encoder of each component code at each time  $t$ . These generate  $N_t$  4-QAM symbols per time slot per component code. Hence, the *rate of each component code* is  $\frac{2}{2N_t}$ . In a general CSTTC structure [16, 54, 55], or in multi-layered systems<sup>4</sup> [73, 199, 72], these  $N_t$  4-QAM symbols are transmitted from  $N_t$  separate antennas in each time slot. In a MLSTTC system, the  $LN_t$  4-QAM symbols generated by the  $L$  component codes over  $N_t$  symbol periods jointly define  $N_t$  new QAM symbols from an enlarged constellation. More specifically, the blocks of  $N_t$  symbols generated by  $\mathcal{C}(1)$ , namely,  $x_t(1)^1, x_t(1)^2, \dots, x_t(1)^{N_t}$ , would be used to determine the most significant bits of the new QAM symbols. Similarly the  $N_t$  symbols generated by  $\mathcal{C}(L)$ , namely,  $x_t(L)^1, x_t(L)^2, \dots, x_t(L)^{N_t}$ , determine the least significant bits. Collectively, the outputs from all  $L$  encoders,  $\mathcal{C}(1), \dots, \mathcal{C}(L)$ , generate  $N_t$  new symbols from the enlarged constellation. These  $N_t$  new QAM symbols are denoted by  $(x_t(1)^1 x_t(2)^1 \dots x_t(L)^1), (x_t(1)^2 x_t(2)^2 \dots x_t(L)^2), \dots, (x_t(1)^{N_t} x_t(2)^{N_t} \dots x_t(L)^{N_t})$ . They are mapped to the underlying  $M$ -QAM constellation through the partitioning process. For ease of presentation, this multiplexing process is shown as a separate block called “symbol multiplexing” in Figure 4.1.

Note that due to the multilevel nature of the overall code, using identical codes on all levels, will result in a different level of error protection at each level. This, *unequal error protection*, can be useful in some applications. To obtain *equal error protection* on each level, we have three degrees of freedom to exploit:

1. The number of states used by each component code can be varied; using more states will result in a stronger code.

---

<sup>4</sup>These systems are discussed in more detail in Chapter 5.



2. The constellation distance can be varied as described in Section 4.3.1.
3. The rate of each component code can be varied to change its equivalent minimum distance.

We can use these three degrees of freedom to balance the codes at each level, using the balanced distance design rule [87]. Examples will be discussed in Chapter 5.

### 4.3.3 Mapping Symbols to Antennas

Considering the constellation shown Figure 4.2. At time  $t$ , the symbol transmitted from the  $j$ th transmit antenna can be represented by

$$Q_t^j = d_{x(1)}x_t(1)^j + d_{x(2)}x_t(2)^j + \dots + d_{x(L)}x_t(L)^j \quad j = 1, \dots, N_t \quad (4.3.5)$$

where  $x_t(l)^j$  is the 4-QAM symbol generated by the  $l$ th component code.

A CSTTC designed for an  $M$ -ary constellation, where  $M = 2^m$ , has a throughput of  $m$  bits/sec/Hz [16]. If  $N_t$  transmit antennas are used, then the overall rate is  $\frac{m}{mN_t}$ . In MLSTTC, if we use  $L$  identical  $M$ -QAM CSTTC's designed for  $N_t$  transmit antennas as our component codes, and use  $N_t$  transmit antennas to transmit the information, then we will end up with an overall rate of  $\frac{Lm}{N_t(Lm)}$ . However, it is possible to increase the throughput by changing the rate of the component codes. An example is provided in chapter 5, where we consider subgroups of the antennas and use higher rate CSTTC's to encode some of the clusters.

## 4.4 Detection/Decoding

We use a multi-stage decoder with  $L$  stages to decode the received data, encoded by an  $L$ -level MLSTTC, as shown in Figure 4.1. In the following, we describe the decoding process

where the decoder starts by decoding the output of the  $L$ th component code. The estimated values of  $\mathbf{x}(L)$ ,  $\hat{\mathbf{x}}(L)$ , are then passed to the next decoding stage and are used to decode the values of  $\mathbf{x}(L-1)$  and so forth. The final stage of the decoder uses the estimates obtained from levels  $L$  to 2, namely  $\hat{\mathbf{x}}(L), \hat{\mathbf{x}}(L-1), \dots, \hat{\mathbf{x}}(2)$  to obtain  $\hat{\mathbf{x}}(1)$ .

In this section, we derive decoding metrics for the proposed multi-stage decoder. The derivation is carried out for an arbitrary number of transmit and receive antennas. We start by looking at the form of the received signal. Based on (4.2.1) and (4.3.5), the received signal at the  $i$ th receive antenna at time  $t$  is given by

$$r_t^i = \sum_{l=1}^L \sum_{j=1}^{N_t} h_{i,j} d_{x(l)} x_t(l)^j + n_t^i \quad (4.4.1)$$

The conditional probability density function (pdf), of  $\mathbf{r}_t$  conditioned on the channel matrix and all  $L$  encoder outputs, may then be written as

$$f(\mathbf{r}_t | \mathbf{x}_t(1), \mathbf{x}_t(2), \dots, \mathbf{x}_t(L), \mathbf{H}_t) \quad (4.4.2)$$

where  $\mathbf{x}_t(l) = (x_t(l)^1, x_t(l)^2, \dots, x_t(l)^{N_t})$ , for  $l \in \{1, 2, \dots, L\}$ . As will be described later, this in fact turns out to be a Gaussian pdf.

Assuming that the component codes are independent of the AWGN and of each other, we apply a multi-stage decoder, where  $\mathbf{x}_t(L)$  is decoded first and is passed to the next stage, where  $\mathbf{x}_t(L-1)$  is decoded and so forth (as described above).

#### 4.4.1 Stage L

In the  $L$ th stage, the aim is to decode  $\mathbf{x}_t(L)$ . We make use of the Viterbi algorithm, and thus hypothesize the value of vector  $\mathbf{x}_t(L)$ . The decoder in Stage  $L$ , performs a search to maximize the likelihood function over the hypothesized values of  $\mathbf{x}_t(L)$ . The values of  $\mathbf{x}_t(1)$  to  $\mathbf{x}_t(L-1)$  are unknown at this stage and thus we treat them as “nuisance” variables and

average them out.

Based on (4.4.2), we can then write the conditional pdf as

$$f(\mathbf{r}_t | \mathbf{x}_t(L), \mathbf{H}_t) = \sum_{\substack{\mathbf{x}_t(l), \\ l=1, \dots, L-1}} Pr(\mathbf{x}_t(1), \dots, \mathbf{x}_t(L-1) | \mathbf{x}_t(L), \mathbf{H}_t) f(\mathbf{r}_t | \mathbf{x}_t(1), \dots, \mathbf{x}_t(L-1), \mathbf{H}_t) \quad (4.4.3)$$

Since the component encoders are assumed to be independent of each other, we consider  $\mathbf{x}_t(1), \dots, \mathbf{x}_t(L-1), \mathbf{x}_t(L)$  to be mutually independent. Considering that the channel is also assumed to be independent of the component codes, and that different values of  $\mathbf{x}_t(l)$  have the same probability of being transmitted, the probability  $Pr(\mathbf{x}_t(1), \dots, \mathbf{x}_t(L-1) | \mathbf{x}_t(L), \mathbf{H}_t)$  in the expression on the right hand side of (4.4.3) reduces to a constant and can be ignored when maximizing the likelihood function. Now focusing on the second term, on the right hand side of (4.4.3) and using (4.4.1), we can write

$$\begin{aligned} f(\mathbf{r}_t | \mathbf{x}_t(1), \dots, \mathbf{x}_t(L-1), \mathbf{x}_t(L), \mathbf{H}_t) &= \prod_{i=1}^{N_r} \frac{1}{(\sqrt{2\pi}\sigma_n)^2} \exp \left[ \frac{\left| r_t^i - \sum_{l=1}^L \sum_{j=1}^{N_t} h_{i,j}^t d_{x(l)} x_t(l)^j \right|^2}{2\sigma_n^2} \right] \\ &= \frac{1}{(\sqrt{2\pi}\sigma_n)^{2N_r}} \exp \left[ \sum_{i=1}^{N_r} \frac{\left| r_t^i - \sum_{l=1}^L \sum_{j=1}^{N_t} h_{i,j}^t d_{x(l)} x_t(l)^j \right|^2}{2\sigma_n^2} \right] \end{aligned} \quad (4.4.4)$$

Substituting (4.4.4) into (4.4.3) and ignoring the constant term, we obtain the likelihood function in the form

$$L(\mathbf{x}_t(L)) = f(\mathbf{r}_t | \mathbf{x}_t(L), \mathbf{H}_t) \propto \sum_{\substack{\mathbf{x}_t(l), \\ l=1, \dots, L-1}} \exp \left[ \sum_{i=1}^{N_r} \frac{\left| r_t^i - \sum_{l=1}^L \sum_{j=1}^{N_t} h_{i,j}^t d_{x(l)} x_t(l)^j \right|^2}{2\sigma_n^2} \right] \quad (4.4.5)$$

Taking the logarithm of (4.4.5) and ignoring the terms that are not dependent on  $\mathbf{x}_t(l)$ , we obtain

$$\log \left( \sum_{\substack{\mathbf{x}_t(l), \\ l=1, \dots, L-1}} \exp \left[ \sum_{i=1}^{N_r} \frac{\left| r_t^i - \sum_{l=1}^L \sum_{j=1}^{N_t} h_{i,j}^t d_{x(l)} x_t(l)^j \right|^2}{2\sigma_n^2} \right] \right) \quad (4.4.6)$$

as the corresponding branch metric. As mentioned previously, Stage  $L$  decodes the subset labels  $\mathbf{x}(L)$  using the Viterbi algorithm. More specifically, assuming that  $r_t^i$  is the received signal at the  $i$ th receive antenna at time  $t$ , the branch metric for a transition labelled  $x_t(L)^1, x_t(L)^2, \dots, x_t(L)^j$  is given by (4.4.6). The Viterbi algorithm is used to compute the path with the largest accumulated metric over the duration of a data frame.

Notice that while taking the logarithm is not strictly necessary in calculating the branch metric, we perform it to obtain path metrics as the sum of branch metrics. In Section 4.6 and in Chapter 6, we discuss ways to reduce its complexity.

The decoded values of  $\mathbf{x}(L)$ , denoted  $\widehat{\mathbf{x}}(L)$ , are assumed to be correct and are passed on to the decoder of Stage  $L-1$  and used in decoding  $\mathbf{x}(L-1)$  and so forth. In the next section we will look at stage  $k$  of decoding for  $1 < k < L$ .

#### 4.4.2 Stage $k$

The decoding of the  $k$ th stage is similar to the decoding of stage  $L$ . Now the aim is to decode  $\mathbf{x}_t(k)$ . We make use of the Viterbi algorithm and hypothesize the value of vector  $\mathbf{x}_t(k)$ . Similar to what we had before, the decoder performs a search to maximize the

likelihood function over the hypothesized values of  $\mathbf{x}_t(k)$ . This time however, assuming the decoding starts from stage  $L$ , and  $1 < k < L$ , the outputs of the stage  $L$  to  $k + 1$  decoders (i.e.  $\hat{\mathbf{x}}(L), \dots, \hat{\mathbf{x}}(k + 1)$ ) are available. Therefore, we can take these decisions into account. The values of  $\mathbf{x}_t(1), \dots, \mathbf{x}_t(k - 1)$  are still unknown at this stage and thus are treated as “nuisance” variables and averaged out.

The branch metric is derived using the same procedure as before. For a transition labelled  $x_t(k)^1, x_t(k)^2, \dots, x_t(k)^j$  the branch metric at stage  $k$ , where  $1 < k < L$ , can be calculated as

$$\log \left( \sum_{\substack{\mathbf{x}_t(1), \\ 1: 1, \dots, k-1}} \exp \left[ \sum_{i=1}^{N_r} \frac{\left| r_t^i - \sum_{l=1}^k \sum_{j=1}^{N_t} h^{t,i,j} d_{x(l)} x_t(l)^j - \sum_{p=k+1}^L \sum_{j=1}^{N_t} h^{t,i,j} d_{x(p)} \hat{x}_t(p)^j \right|^2}{2\sigma_n^2} \right] \right) \quad (4.4.7)$$

Note the appearance of the decisions  $\hat{x}_t(p)$ ;  $p = k + 1, \dots, L$  in the third term of the exponent. We next look at the final stage of decoding where the estimated values of  $\mathbf{x}(L), \dots, \mathbf{x}(2)$  are available to the decoder.

### 4.4.3 Stage 1

Stage 1 is the final stage of decoding, where we use the Viterbi algorithm to decode the component code generated by the  $\mathbf{x}(1)$  encoder. Following the same procedure as in Section 4.4.1, for a transition labelled  $x_t(1)^1, x_t(1)^2, \dots, x_t(1)^j$ , we obtain the branch metric

$$\log \left( \sum_{\substack{\mathbf{x}_t(l), \\ l=2, \dots, L}} \exp \left[ \sum_{i=1}^{N_r} \frac{\left| r_t^i - \sum_{l=1}^L \sum_{j=1}^{N_t} h^{t,i,j} d_{x(l)} x_t(l)^j \right|^2}{2\sigma_n^2} \right] \right) \quad (4.4.8)$$

The decoded (estimated) values of  $\mathbf{x}(L), \dots, \mathbf{x}(2)$ , denoted by  $\hat{\mathbf{x}}(L), \dots, \hat{\mathbf{x}}(2)$ , are now available and are passed to the Stage 1 decoder, as shown in Figure 4.1. Therefore, we no longer

average over  $\mathbf{x}(L), \dots, \mathbf{x}(2)$  but instead insert the corresponding decisions  $\hat{\mathbf{x}}(L), \dots, \hat{\mathbf{x}}(2)$ , denoted by  $\hat{x}_t(l)^j$ , directly into the above expression. Doing so eliminates the summation over  $\hat{\mathbf{x}}_t(l)$  and allows (4.4.6) to be reduced to

$$\sum_{i=1}^{N_r} \left| r_t^i - \sum_{j=1}^{N_t} h_{i,j}^t \left( d_{x(1)} x_t(1)^j - \sum_{l=2}^L d_{x(l)} \hat{x}_t(l)^j \right) \right|^2 \quad (4.4.9)$$

This expression is used as the branch metric in Stage 1. Notice that there are no longer any nuisance variables. As can be seen, the metric used in the final stage of decoding is almost identical to the branch metric used in a CSTTC (2.5.1), reproduced here for the reader's convenience:

$$\sum_{i=1}^{N_r} \left| r_t^i - \sum_{j=1}^{N_t} h_{i,j}^t x_t^i \right|^2 \quad (4.4.10)$$

However, the branch metrics used in previous stages are more complex. In the next section, we consider the complexity implications of MLSTTC's and propose a method for reducing the branch complexity for MLSTTC decoding.

## 4.5 Complexity Considerations

An attractive property of the MLSTTC scheme is its low overall complexity compared to CSTTCs, [16, 54, 55], with the same signalling parameters. The scheme makes use of a multilevel structure. The underlying constellation is partitioned and the encoding is done in stages using simpler component codes. A multi-stage decoder is then used to decode the succession of component codes. The overall structure results in reduced complexity, especially for larger signal constellations and larger numbers of states. In general, complexity of the MLSTTC system increases linearly with the size of the underlying constellation, while that of a CSTTC grows exponentially.

Consider a CSTTC transmitting  $b$  bits/sec/Hz with diversity  $rN_r$ . It has been shown [16], that the constraint length of such a code must be at least  $r - 1$ . Since the transmission

rate is  $b$  bits/sec/Hz, the number of branches leaving each state of the trellis diagram is  $2^b$ . For CSTTCs, this is also the modulation set size. At time instance  $r - 1$ , there are  $2^{b(r-1)}$  branches that have diverged from the zero state of the trellis at time zero. Since the constraint length is  $r - 1$ , none of these paths can merge at the same time. Therefore, there are at least  $2^{b(r-1)}$  states in the trellis, and the complexity of the trellis grows exponentially with throughput.

To study the complexity of the decoder, assume a CSTTC with  $N_s$  states, and  $N_b$  branches per state. Each state stores information on hypothesized previously transmitted data (history). Each branch corresponds to  $N_t$  symbols, which are calculated from both the history, and the current received symbol. Assuming perfect channel knowledge, the complexity for a single trellis step is calculated by looking at the number of complex Multiply and Accumulate (MAC) instructions required. Looking at the metric of equation (4.4.10), it can be seen that calculating the metric per branch requires approximately  $(N_t + 1) \times N_r$  complex MAC instructions. Therefore, the total complexity is approximately  $N_s \times N_b \times (N_t + 1) \times N_r$  per time step. For the purpose of comparisons in this thesis, we shall use  $N_s \times N_b$ , which appear for both code types in an identical manner, as a measure of complexity.

For 16 QAM, the upperbound on transmission rate for a CSTTC is 4 bits/sec/Hz and the lower bound on trellis complexity is 16 states with 16 branches leaving each state ( $= 16 \times 16$ ) [16]. As can be seen the complexity grows prohibitively large with throughput. For a throughput of 6 bits/sec/Hz for example, the minimum value of the complexity measure would be  $64 \times 64$ .

A MLSTTC tackles the problem of complexity by making use of the MLC concept to break the complexity into parts. The system thus has the potential to reduce decoding complexity, especially for higher order constellations and larger numbers of states. As an example, for a constellation size of  $2^b$ , where  $b \geq 4$ , the MLSTTC can partition the

underlying QAM constellation into  $L$  4-QAM subsets, with  $2^b = 4^L$ . Multilevel encoding will then result in an overall minimum number of states equal to  $4L$  where 4 branches leave each state due to the 4-QAM subsets. Therefore, the complexity grows linearly with the size of constellation, giving a minimum complexity of  $L \times 4 \times 4 = \frac{2^b}{4} \times 4 \times 4$  as opposed to  $2^b \times 2^b$ .

Thus, the complexity of MLSTTC is manageable and can easily be extended to higher order constellations and higher throughputs. Using a smaller number of states than the equivalent CSTTC, would result in a coding gain loss. However, two points must be noted: First, if we use the same number of states, we can achieve comparable performance to a CSTTC but at a reduced complexity of  $L \times 2^b \times 4$  as opposed to  $2^b \times 2^b$  due to the reduced number of branches. Second, since the MLSTTC decouples the dimensionality of the underlying constellation from the code rate, we can achieve the same throughput as a CSTTC, using a smaller constellation<sup>5</sup>. Therefore, we will have better distance properties than the equivalent CSTTC (which will be using a larger constellation) and can potentially achieve the same performance as a CSTTC using fewer states.

Considering the example constellation of 16-QAM partitioned into  $L = 2$  levels, a MLSTTC can transmit 4 bits/sec/Hz with a minimum complexity of  $2 \times 4 \times 4$ , thereby offering the same throughput with a complexity saving of about 8 times, compared to the equivalent minimum complexity CSTTC with the same throughput. Furthermore, MLSTTC's can offer higher throughput for the same constellation. If we transmit 6 bits/sec/Hz for example<sup>6</sup>, the minimum trellis complexity of a MLSTTC would be a mere 48 versus 4096 for the comparable CSTTC, a complexity saving of over 85 times. In Chapter 5, we provide an example of a MLSTTC system transmitting 6 bits/sec/Hz using a 16-QAM constellation. As can be seen the complexity reduction of MLSTTC compared to a CSTTC becomes more

---

<sup>5</sup>An example of this is presented in Chapter 5, where we achieve a throughput of 6 bits/sec/Hz using a MLSTTC design for a 16-QAM constellation, as opposed to a 64 QAM.

<sup>6</sup>An example is shown in Chapter 5.



pronounced for higher throughputs and larger constellation sizes. Since we are transmitting at the same throughput using a smaller constellation, the MLSTTC is not only less complex in terms of receiver structure, but it has better distance properties than the comparable CSTTC. Therefore, we can achieve the same performance as a 64-QAM CSTTC using a smaller number of states.

As discussed, the trellis complexity of the MLSTTC is smaller than that of a CSTTC. Let us now look at the branch metric complexity for the proposed MLSTTC decoder. In the final stage of decoding (Stage 1), the complexity of the branch metric (4.4.8) is almost equivalent to that of (4.4.10), except for some extra additions and multiplications that are relatively insignificant. The branch metrics used in earlier stages of decoding (e.g. (4.4.6)) are, however, more complex than those of a CSTTC. This extra complexity does not grow exponentially with an increase in the constellation size or the number of states; and as discussed we are using fewer branches than in an equivalent CSTTC. Nonetheless, it is still desirable to reduce this complexity. In the remainder of this section, we discuss a method for reducing the complexity of the branch metric.

#### 4.5.1 Branch Metric Complexity Reduction

One method to reduce the complexity of the branch metric is to use a Max-log approximation. Simulation results in Chapter 5 will show that this method suffers almost no penalty in terms of error performance across the range of SNRs considered.

For the reader's convenience, here we repeat the general form of the metric equation derived in Section 4.4. For an  $L$  level MLSTTC system, if the decoding starts from stage  $L$ , the branch metric at stage  $k$ , where  $1 < k \leq L$ , for a transition labelled  $x_t(k)^1, x_t(k)^2, \dots, x_t(k)^j$  can be calculated as

$$\log \left( \sum_{\substack{\mathbf{x}_t(l), \\ l: 1, \dots, k-1}} \exp \left[ \sum_{i=1}^{N_r} \frac{\left| r_t^i - \sum_{l=1}^k \sum_{j=1}^{N_t} h_{i,j}^t d_{x(l)} x_t(l)^j - \sum_{p=k+1}^L \sum_{j=1}^{N_t} h_{i,j}^t d_{x(p)} \hat{x}_t(p)^j \right|^2}{2\sigma_n^2} \right] \right) \quad (4.5.1)$$

Note that the  $\hat{x}_t(p)^j$  term in (4.5.1) disappears when  $k = L$ . Because of the exponential operation in the branch metric equation (4.5.1), the difference between individual terms tends to be enhanced, and one term normally dominates the metric [197]. Mathematically, we can then use the following approximation to reduce complexity

$$\log \sum_j \exp a_j \simeq \max_j a_j \quad (4.5.2)$$

Applying this approximation to the branch metric of (4.5.1), and ignoring the constant term in the denominator, for a received signal  $r_t^i$ , and a transition labelled  $x_t(k)^1, x_t(k)^2, \dots, x_t(k)^j$ , the approximate branch metric is then given by

$$\max_{\substack{\mathbf{x}_t(l), \\ l: 1, \dots, k-1}} \sum_{i=1}^{N_r} \left| r_t^i - \sum_{l=1}^k \sum_{j=1}^{N_t} h_{i,j}^t d_{x(l)} x_t(l)^j - \sum_{p=k+1}^L \sum_{j=1}^{N_t} h_{i,j}^t d_{x(p)} \hat{x}_t(p)^j \right|^2 \quad (4.5.3)$$

The Viterbi algorithm is then used to decode the path with the lowest accumulated metric.

The complexity of level  $k$  of the MLSTTC, using (4.5.3) as branch metric, can be written as  $N_b \times N_s \times N_r \times [1 + N_t(L - k + 1 + 2^{k-1}(k - 1))]$ . Throughout we have used the trellis complexity (i.e. number of states and branches  $N_s \times N_b$ ) as our measure of complexity comparison, however it must be noted that the branch metric in (4.5.3), as it stands, requires more calculations per branch than a CSTTC owing to the maximization operation. Specific examples are discussed in Chapter 5. In Chapter 6 we discuss other methods to further reduce the branch metric complexity.

## 4.6 Summary

It is desirable to construct STTCs employing high order constellations to meet the ever increasing demand for high data rate transmission. However, to the author's knowledge, there has been no CSTTC published for 64-QAM or larger constellations.

In this Chapter, we have combined the techniques of MLC modulation and STTC to propose a new scheme, MLSTTC, capable of simultaneously providing bandwidth efficiency, diversity improvement and coding gain with reduced decoding complexity, especially for larger constellations and higher throughputs. The exhaustive code search problem is also largely eliminated in designing MLSTTCs in that we can use the existing CSTTC's (designed for smaller constellations) as component codes to construct a code for larger constellations, without having to go through the code search.

The general structure of MLSTTC's is very flexible and can easily be tuned to achieve the required balance between spectral efficiency, error performance and decoding complexity. We have described the overall structure and analytical model in this chapter. Performance evaluations and trade-offs are studied in Chapter 5.

## Chapter 5

# System Performance

In Chapter 4 we proposed a transmission scheme, MLSTTC, capable of simultaneously providing bandwidth efficiency, diversity improvement and coding gain with reduced decoding complexity, especially for larger constellations and higher throughputs. We mentioned that the structure of MLSTTCs is flexible and can easily be tuned to achieve the required balance between spectral efficiency, error performance and decoding complexity. We will explore examples in this chapter. The overall structure and analytical model was described in Chapter 4.

In this chapter we evaluate the system and its performance through simulating examples of the design for an underlying 16-QAM constellation, using up to 4 transmit and 4 receive antennas and achieving a throughput of up to 6 bits/sec/Hz. Concluding remarks and suggestions for future research are presented in Chapter 6.

### 5.1 Introduction

Throughout this chapter, we consider examples of MLSTTC systems designed for an underlying 16-QAM constellation. The model described in Chapter 4 was derived for an arbitrary number of antennas. Here we simulate performance with up to 4 transmit and

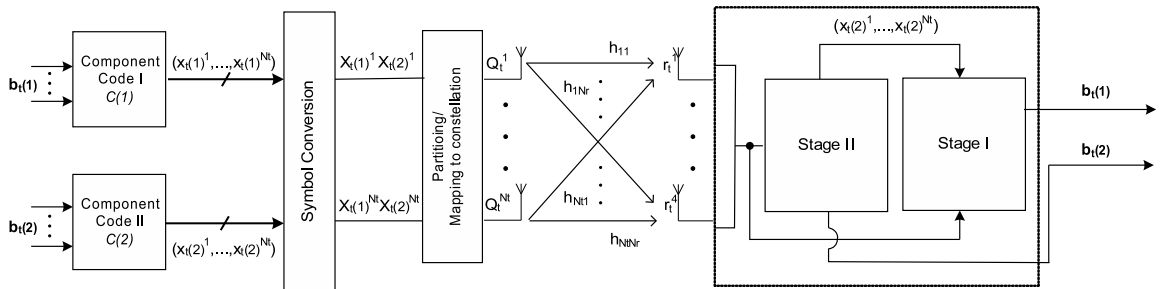


Figure 5.1: An example MLSTTC system.

receive antennas and consider transmitting up to 6 bits/sec/Hz. We use CSTTC's [54] as component codes. We evaluate system performance, discuss the effects of imperfect CSI, correlation, and transmit and receive diversity on this performance and present example systems offering equal and unequal error protection.

For performance comparison, we consider multi-layered schemes, in Section 5.10.4, which have similar complexity to that of a MLSTTC and similar throughput. We show that MLSTTC's offer performance improvement, through being more integrated. Furthermore, we demonstrate that MLSTTC's provide a more economical design, as they can offer a better performance using fewer transmit antennas, when compared with the multi-layered schemes.

## 5.2 An example MLSTTC system

In this section we describe an example MLSTTC system, designed for 16-QAM, using two component codes. A simplified block diagram of the system is shown in Figure 5.1. The setup is based on the model described in Section 4.2.

As described in Chapter 4, the underlying signal constellation is partitioned into a hierarchy of clusters using the MRM approach. This clusterization provides two resolutions for the 16-QAM constellation, where each resolution can be considered as a 4-QAM constellation. This application of MRM to a 16-QAM constellation is shown in Figure 5.2.

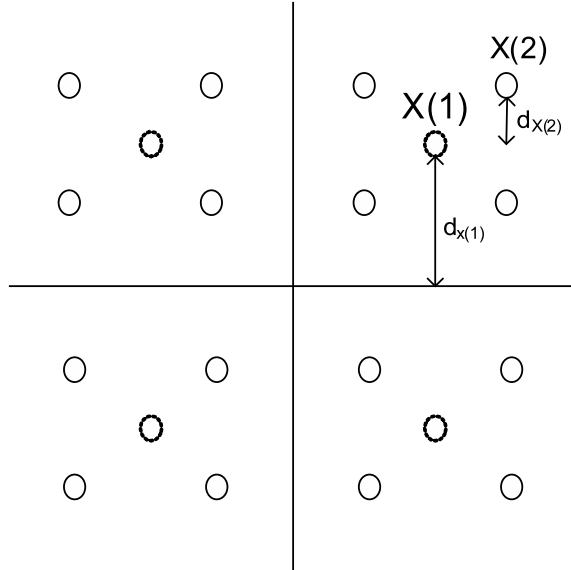


Figure 5.2: Partitioning and labelling of the 16-QAM constellation.

As shown in Figure 5.2, the 16 points of the underlying constellation are divided into four clusters, and each cluster consists of 4 effective points<sup>1</sup>. We thus partition [68] the multi-resolution constellation by treating each cluster as a 4-QAM. This enables us to use CSTTCs designed for QPSK directly in our mapping. Figure 5.3, shows the labelling of the signal constellation points.

Having two cluster levels, we use two component codes to encode the incoming bits. The outputs of the first and second encoder, namely  $\mathcal{C}(1)$  and  $\mathcal{C}(2)$  in Figure 5.1, are mapped to the clusters of the two levels respectively.

In the designs presented in this thesis, CSTTC's [54, 55] are used as component codes in the MLSTTC's. Potentially, *any* code (including a block codes) could be used as a component code. The encoding is over both space and time. Throughout we assume  $rN_r \geq 4$ , where  $r$  is the rank of the codeword difference matrix. As discussed in Chapter 2, this results in the minimum Euclidean distance dominating performance and thus we design

---

<sup>1</sup>Note that  $X(1)$  points are virtual points.

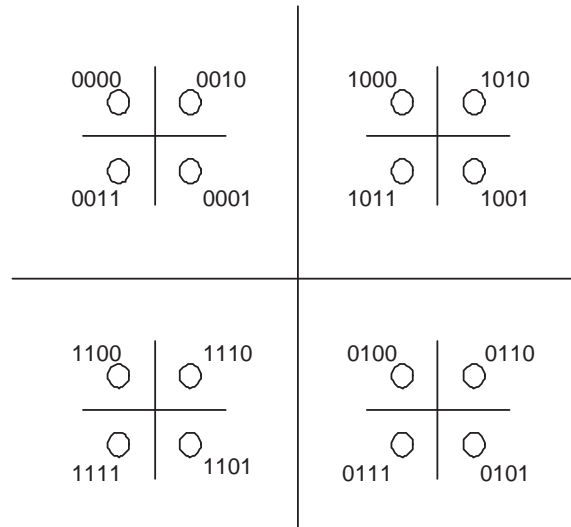


Figure 5.3: The labelling of the 16-QAM MRM constellation.

codes for large Euclidean distances, following the trace criterion [54].

A CSTTC designed for an  $M$ -ary constellation, where  $2^m = M$ , has a throughput of  $m$  bits/sec/Hz [16]. When employing  $N_t$  antennas it results in an overall rate of  $\frac{m}{N_t m}$ . In an MLSTTC, if we use two identical  $M$ -QAM CSTTC's designed for  $N_t$  transmit antennas (with a rate of  $\frac{1}{N_t}$ ) as our component codes, and then use  $N_t$  transmit antennas to transmit information, we obtain an overall rate of  $\frac{m+m}{N_t(m+m)}$ . The MLSTTC employs an overall  $4^L$ -QAM constellation, meaning  $M^2$ -QAM in this case.

For the 16-QAM constellation, we employ two 4-QAM CSTTC's. In each  $T$ -sec time interval, each antenna transmits one 16-QAM symbol resulting in an overall rate of  $4/8$ , for two antennas. This is equivalent to an overall throughput of 4 bits/sec/Hz. Higher throughputs are possible by using larger constellations or component codes with different rates. An example system that transmits 6 bits/sec/Hz is discussed in Section 5.10.

In the simulations of this chapter, unless otherwise stated, we consider a frame size of 130 symbols. We also assume that max-log decoding is used and that the system model follows that described in Chapter 4.

### 5.3 Unequal Error protection

The performance of MLSTTC's, for two transmit and two receive antennas is shown in Figure 5.4. The system model is shown in Figure 5.1, where we have used two identical 4-state CSTTC's as component codes. The spectral efficiency is 4 bits/sec/Hz and the underlying constellation is 16 QAM. The plot shows the frame error rate (FER) and the symbol error rate (SER) for the two levels  $\mathcal{C}(1)$  and  $\mathcal{C}(2)$ . The overall error performance is dominated by  $\mathcal{C}(2)$  and is indeed virtually the same as that of  $\mathcal{C}(2)$  in this case. In the simulations of this section we assume perfect CSI at the receiver and no correlation between subchannels. The component codes used are those described in detail in Chapter 2.

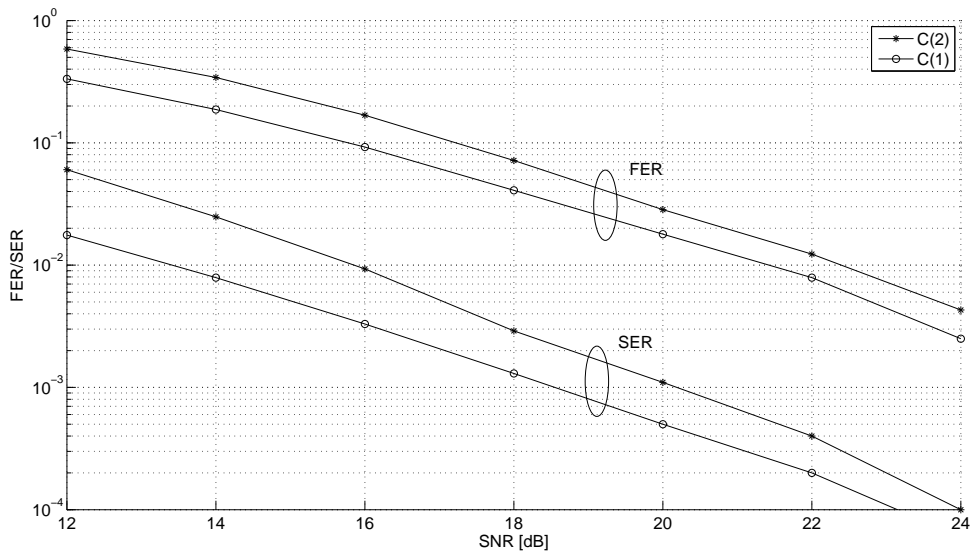


Figure 5.4: Error performance of a MLSTTC, with  $N_t = N_r = 2$ , and  $\mathcal{C}(1) = \mathcal{C}(2)$  with 4 states.

Due to the multilevel nature of MLSTTC, we can achieve different levels of protections at the different levels. This could be an advantage in scenarios where unequal error protection is desired. This might arise; for example, in voice and data systems where voice is typically more tolerant to errors than data (data received in error must generally be



re-transmitted). Another example would be for certain types of compression. For example, in image compression, the bits corresponding to the low-resolution reproduction of the image are required, whereas high-resolution bits simply refine the image. Therefore, with our system when the channel is in deep fades, high-priority bits will be received correctly with a higher probability. It is however also possible to achieve equal error protection using MLSTTC, and an example of how to do so is presented in Section 5.10.

## 5.4 Imperfect Channel State Information

Elsewhere in this thesis we assume that perfect CSI is available at the receiver. In a practical system though, this is normally not the case. In Figure 5.5, we show the performance of the system for an arbitrary 10% error in the channel state estimate in the receiver. This has been simulated by adding random Gaussian noise with variance of 0.1 to the CSI that is passed to the receiver. As can be seen 1 – 2 dB is lost due to imperfect CSI.

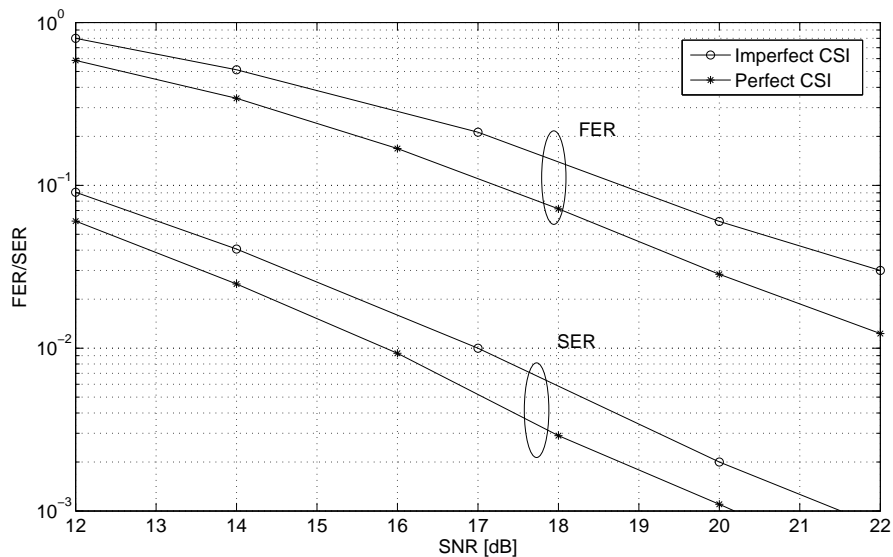


Figure 5.5: Effect of imperfect CSI, with  $N_t = N_r = 2$ , and  $\mathcal{C}(1) = \mathcal{C}(2)$  with 4 states.

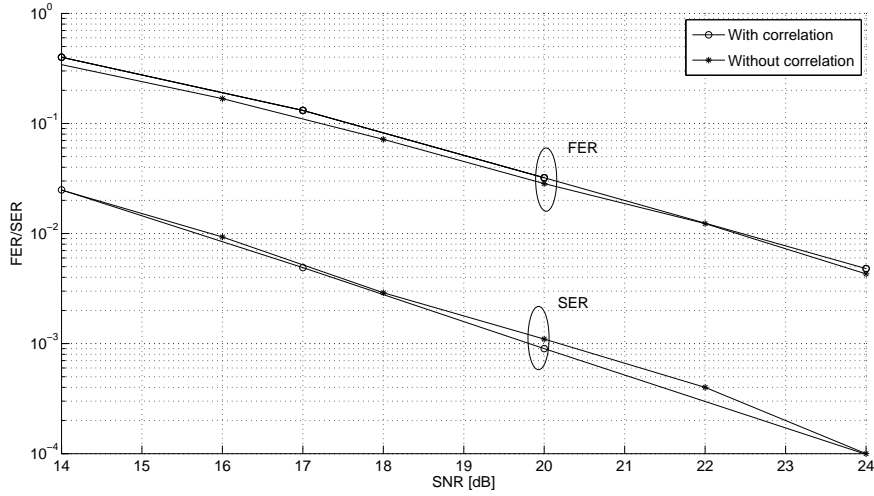


Figure 5.6: Effect of channel correlation, with  $N_t = N_r = 2$ , and  $\mathcal{C}(1) = \mathcal{C}(2)$  with 4 states.

## 5.5 Effect of Channel Correlation

Elsewhere in the thesis we assume the channels are uncorrelated. Figure 5.6 illustrates the effect of channel correlation on code performance for an arbitrary correlation factor of 0.5, where 0.5 is the correlation factor between the receive antennas as defined in [18]. It can be seen that the coder performance is only slightly degraded in the presence of this level of correlation between subchannels.

## 5.6 Receive Diversity

Thus far, we have considered a 2 by 2 system. Here we consider the effect of receive diversity on the error performance of the code. Figure 5.7 shows the error performance of a MLSTTC system, similar to that used in Section 5.3, but using 4 receive antennas. Figures 5.8 and 5.9 present an error performance comparison for the MLSTTC system operating with different numbers of receive antennas. The simulation results show that increasing the number of receive antennas yields a significant performance gain.

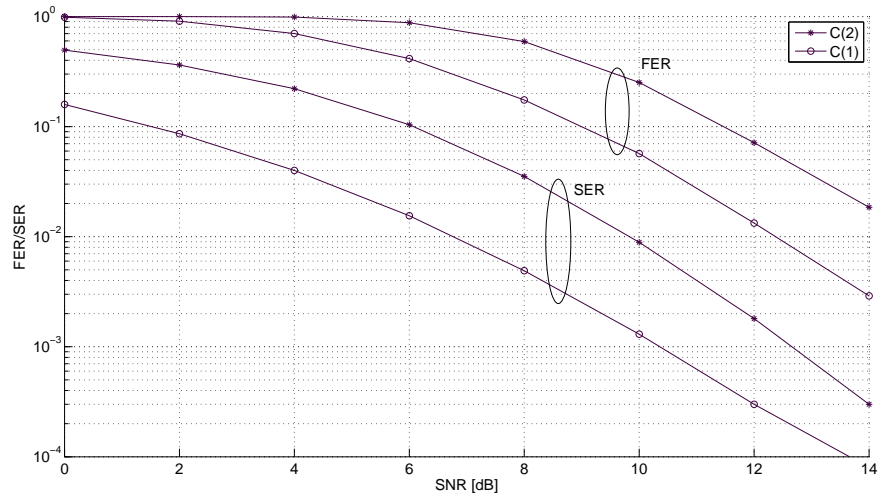


Figure 5.7: Error performance for  $N_t = 2$ ,  $N_r = 4$ , and  $\mathcal{C}(1) = \mathcal{C}(2)$  with 4 states.

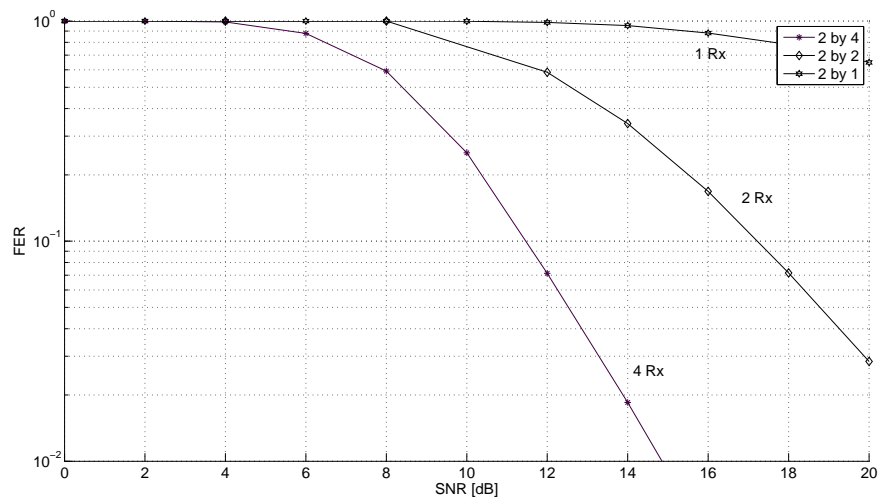


Figure 5.8: FER performance for different number of receive antennas, with  $N_t = 2$ , and  $\mathcal{C}(1) = \mathcal{C}(2)$  with 4 states.

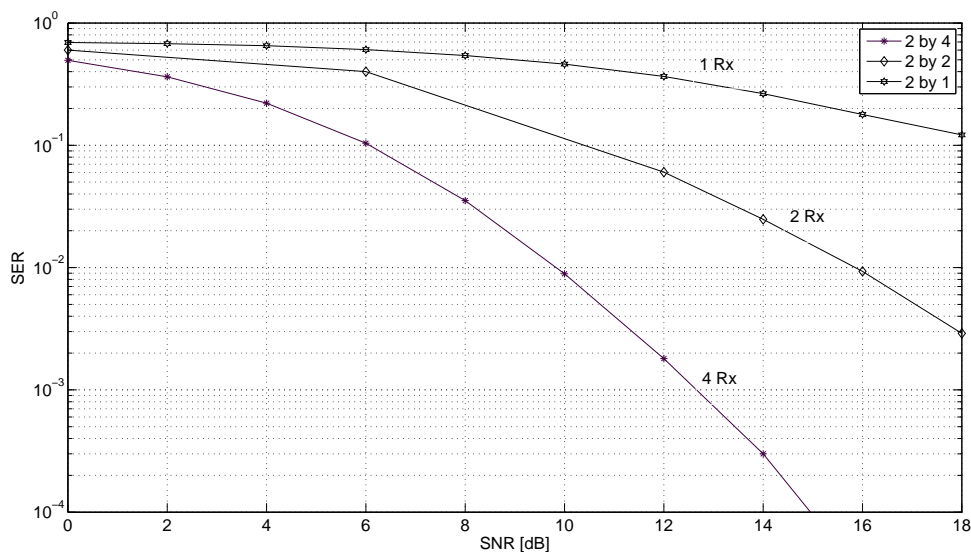


Figure 5.9: SER performance for different number of receive antennas, with  $N_t = 2$ , and  $\mathcal{C}(1) = \mathcal{C}(2)$  with 4 states.

## 5.7 Transmit Diversity

In this section we look at the effects of transmit diversity on error performance. To achieve increased transmit diversity, here we use the same overall design as used in Figure 5.1, but we use component codes designed for 4 transmit antennas [54] in a  $N_t = N_r = 4$  configuration. Figure 5.10 illustrates the error performance of the 4 by 4 system and Figure 5.11 presents an error performance comparison between an MLSTTC system using 2 and 4 transmit antennas. The number of receive antennas has been kept constant at 4 in both cases. As can be seen increasing the number of transmit antennas provides a slight improvement in error performance. The trellis diagram of the component codes is shown in Figure 5.12.

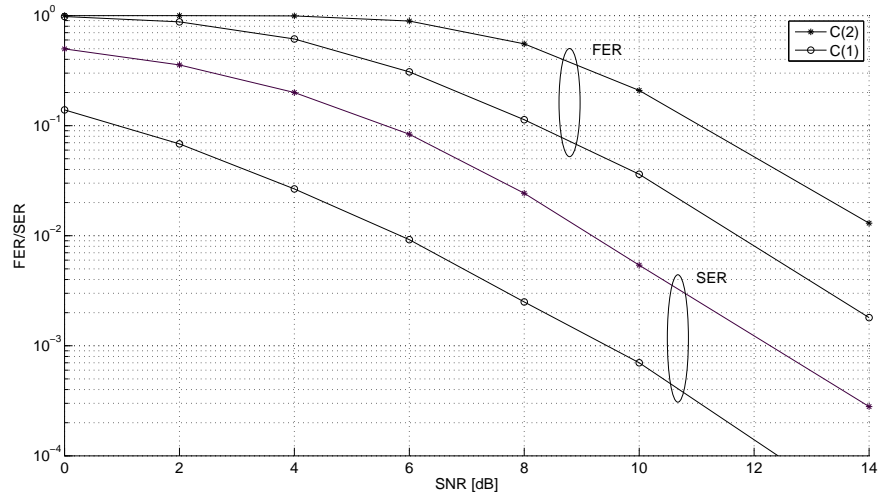


Figure 5.10: MLSTTC performance with  $N_t = N_r = 4$ , and  $\mathcal{C}(1) = \mathcal{C}(2)$  with 4 states.

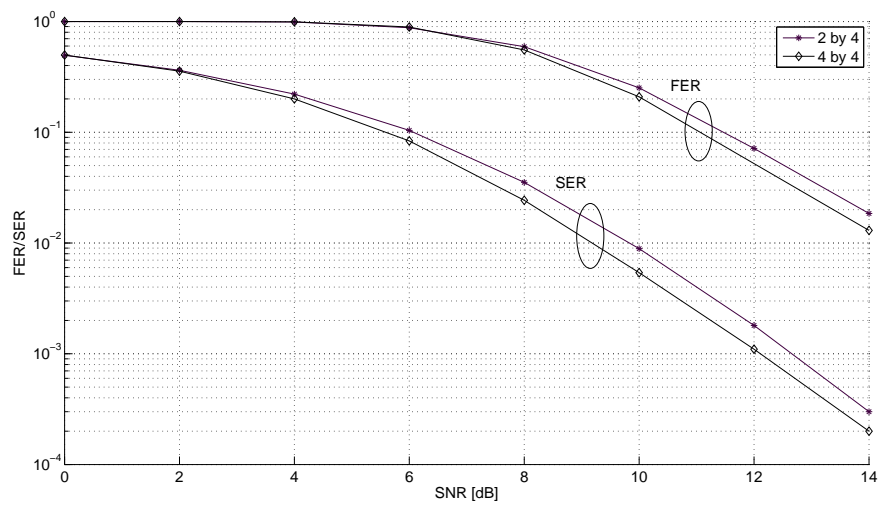


Figure 5.11: Error performance for different number of transmit antennas,  $N_r = 4$ ,  $\mathcal{C}(1) = \mathcal{C}(2)$  with 4 states.

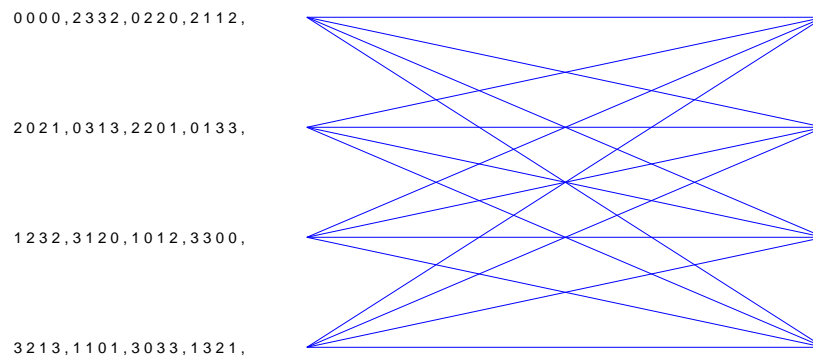


Figure 5.12: Trellis diagram for a CSTTC [54] designed for 4 transmit antennas.

## 5.8 Reduced Complexity Decoding

In Section 4.5.1, we discussed a method for reducing the branch complexity of the proposed MLSTTC decoder by using a max-log approximation. In this section, we compare the error performance of the system using the full complexity metric versus the reduced complexity metric. As we can see, in Figure 5.13 the performance degradation due to the use of the reduced complexity metric is negligible. Therefore, throughout this chapter we use the reduced complexity metric in the simulations.

## 5.9 Comparison with CSTTC's

Figure 5.14 shows the overall FER performance of an MLSTTC system for two transmit and four receive antennas. Two identical 4-state CSTTC's have been used as component codes, resulting in an overall 16-QAM constellation. The performance of this code is shown compared to that of a CSTTC [16] designed for a 16-QAM constellation and two transmit antennas. Clearly, the overall performance of MLSTTC is on average about 1 dB worse

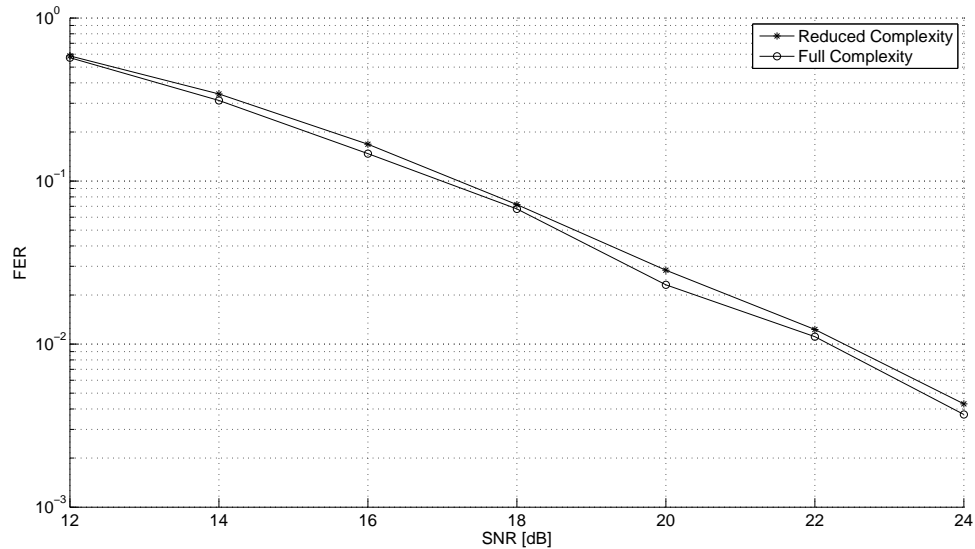


Figure 5.13: System performance under full complexity and reduced complexity metric,  $N_t = N_r = 2$ ,  $\mathcal{C}(1) = \mathcal{C}(2)$  with 4 states.

than that of CSTTC. We are, however, obtaining, similar diversity, suggesting that the loss is in coding gain. Moreover, the MLSTTC presented in this Figure, achieves the same spectral efficiency (4 bits/sec/Hz) as a CSTTC with a factor of 4 reduction in the overall complexity. The trellis complexity of the MLSTTC is about 8 times less complex than that of the CSTTC. In chapter 6 we suggest a possible approach for further reducing the branch metric calculation, which can further reduce the overall complexity.

Comparing a MLSTTC with a CSTTC, another point to consider is that of the code search problem. Specifically, as previously mentioned, the design of CSTTC's normally involves a computer search, with the size of the search space increasing exponentially with constellation size, number of transmit antennas and number of states in the code trellis. In MLSTTCs, however, we can use existing CSTTC's (designed for smaller signal constellations) as component codes to construct codes for larger constellations, without having to conduct the code search. Although, we note that a complete search may result in better

performance.

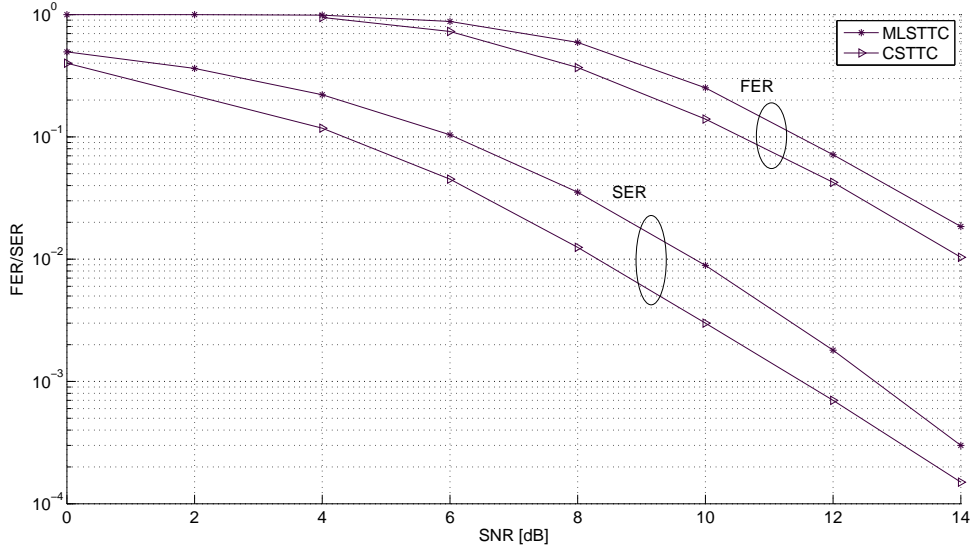


Figure 5.14: Error performance of MLSTTC vs CSTTC,  $N_t = 2$ ,  $N_r = 4$ , MLSTTC:  $\mathcal{C}(1) = \mathcal{C}(2)$  with 4 states, CSTTC: 16 states.

Figures 5.15 and 5.16 show the trellis diagrams of the CSTTC and a component code of the MLSTTC. This provides a visual comparison for the relative complexity of the two codes.

## 5.10 Higher Throughput MLSTTC's

In this section we present a MLSTTC system that achieves a throughput of 6 bits/sec/Hz using an underlying 16-QAM constellation. To the best of the author's knowledge, at the time of writing, no comparable CSTTC has been developed for a 64 QAM constellation (which is required to give a throughput of 6 bits/Sec/Hz). We will, therefore, use layered space-time codes [198, 199] as a basis for performance comparison.

The design is carried out for 4 transmit antennas and follows the procedure explained in Chapter 4. The constellation is partitioned as shown in Figure 5.2. The design has two



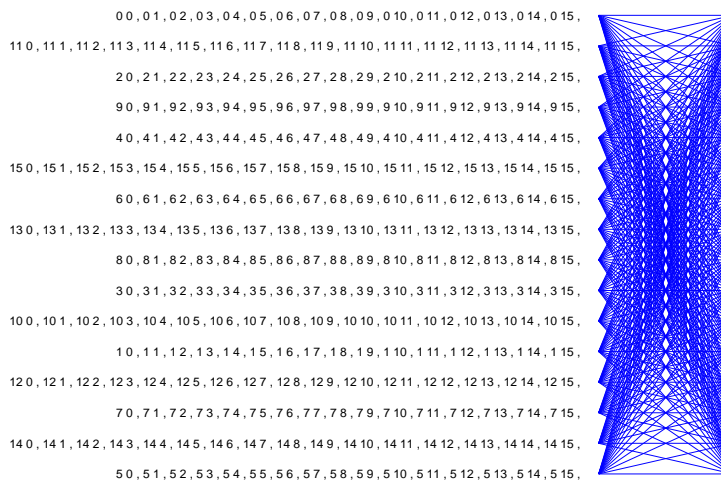


Figure 5.15: The trellis diagram of a 16 state CSTTC [16].

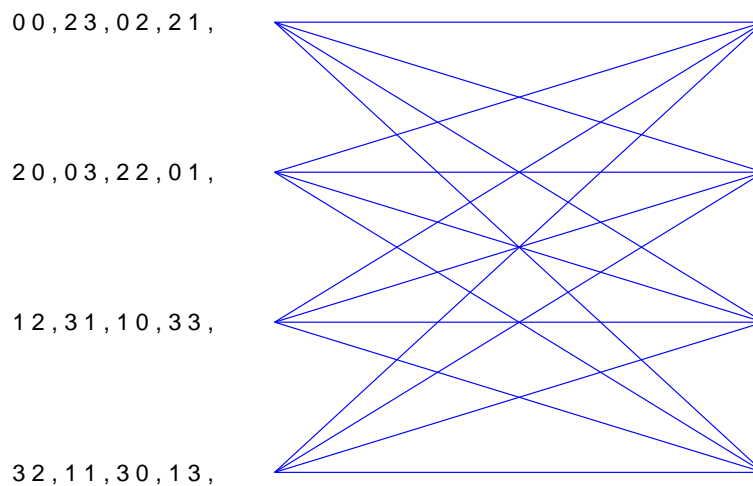


Figure 5.16: Trellis diagram of the MLSTTC component codes.

levels, whereby level 2 employs a CSTTC [54],  $\mathcal{C}(2)$ , designed for four transmit antennas and an underlying constellation of 4-QAM. On level 1 however, we use two component codes,  $\mathcal{C}_a(1)$  and  $\mathcal{C}_b(1)$ , each being a CSTTC designed for two transmit antennas and an underlying constellation of 4-QAM. Therefore, the codewords transmitted from transmit antenna 1 and 2 consist of the encoded output of  $\mathcal{C}_a(1)$  and  $\mathcal{C}(2)$ , arranged as explained in Section 4.3.3. Similarly, the codewords transmitted from transmit antenna 3 and 4 consist of the encoded output of  $\mathcal{C}_b(1)$  and  $\mathcal{C}(2)$ . Notice that a CSTTC designed for an underlying constellation of 4-QAM provides a throughput of 2 bits/sec/Hz. Therefore, this design provides us with an overall throughput of 6 bits/sec/Hz. A block diagram of the system is presented in Figure 5.17.

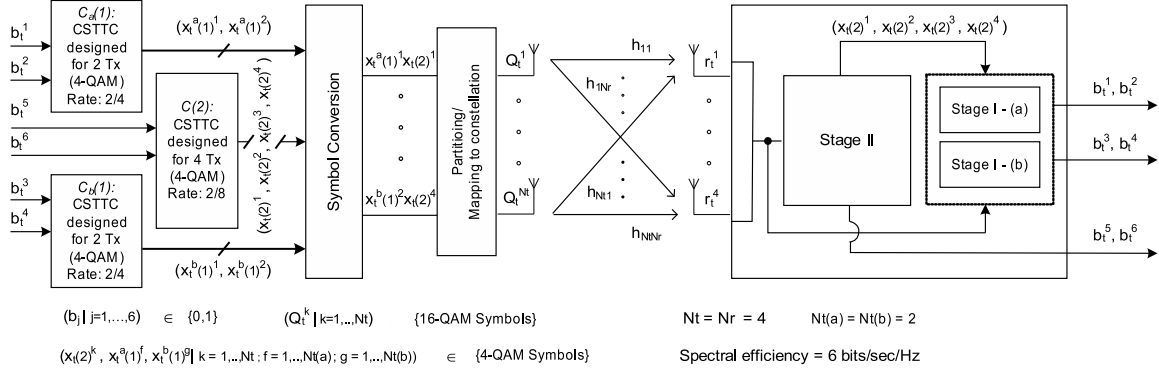


Figure 5.17: MLSTTC system diagram,  $N_t = 4$ , 16-QAM, 6 bits/sec/Hz.

The decoding methodology described in Chapter 4 is employed in the decoder. Let  $r_t^i$  be the received signal at receive antenna  $i$  at time  $t$ , considering the system model (depicted in Figure 5.17), we can write:

$$r_t^i = \sum_{j=1}^{N_t} h_{i,j}^t d_{x(2)} x_t(2)^j + \sum_{j=1}^{N_t(a)} h_{i,j}^t d_{x^a(1)} x_t^a(1)^j + \sum_{j=1+N_t(a)}^{N_t(b)+N_t(a)} h_{i,j}^t d_{x^b(1)} x_t^b(1)^j + n_t^i \quad (5.10.1)$$

where,  $d_{x^a(1)} = d_{x^b(1)} = d_{x(1)}$  (as depicted in Figure 5.2) and  $n_t^i$  is the noise associated with the  $i$ th receive antenna at time  $t$ . For the system presented in Figure 5.17,  $N_t(a) = N_t(b) =$

2, represent the number of transmit antennas over which the sub-component codes (a) and (b) are defined and thus the number of transmit antennas spanned by those codes. Note that  $N_t(a) + N_t(b) = N_t$ . As before, we assume perfect CSI is available at the receiver.

As described in Chapter 4, a MSD is used. We start by decoding  $\mathcal{C}(2)$ . A Viterbi algorithm is used, where the corresponding branch metric, for a received signal  $r_t^i$  and a transition labelled  $x_t(2)^1 x_t(2)^2 \dots x_t(2)^j$  is given by

$$\max_{\mathbf{x}_t(1)} \sum_{i=1}^{N_r} \left| r_t^i - \sum_{j=1}^{N_t} h_{i,j}^t d_{x(2)} x_t(2)^j - \sum_{j=1}^{N_t} h_{i,j}^t d_{x(1)} x_t(1)^j \right|^2 \quad (5.10.2)$$

Similarly, in the next stage, we use two Viterbi decoders in parallel to decode  $\mathcal{C}_a(1)$  and  $\mathcal{C}_b(1)$ . The corresponding branch metrics are :

$$\max_{\mathbf{x}_t^b(1)} \sum_{i=1}^{N_r} \left| r_t^i - \sum_{j=1}^{N_t(a)} h_{i,j}^t d_{x^a(1)} x_t^a(1)^j - \sum_{j=1+N_t(a)}^{N_t(b)+N_t(a)} h_{i,j}^t d_{x^b(1)} x_t^b(1)^j - \sum_{j=1}^{N_t} h_{i,j}^t d_{x(2)} \hat{x}_t(2)^j \right|^2 \quad (5.10.3)$$

$$\max_{\mathbf{x}_t^a(1)} \sum_{i=1}^{N_r} \left| r_t^i - \sum_{j=1+N_t(a)}^{N_t(b)+N_t(a)} h_{i,j}^t d_{x^b(1)} x_t^b(1)^j - \sum_{j=1}^{N_t(a)} h_{i,j}^t d_{x^a(1)} x_t^a(1)^j - \sum_{j=1}^{N_t} h_{i,j}^t d_{x(2)} \hat{x}_t(2)^j \right|^2 \quad (5.10.4)$$

where  $\hat{x}_t(2)$  denotes the decision from the  $\mathcal{C}(2)$  decoder.

### 5.10.1 Error Performance

The overall error performance of the MLSTTC, at a throughput of 6 bits/sec/Hz, is presented in Figure 5.18.

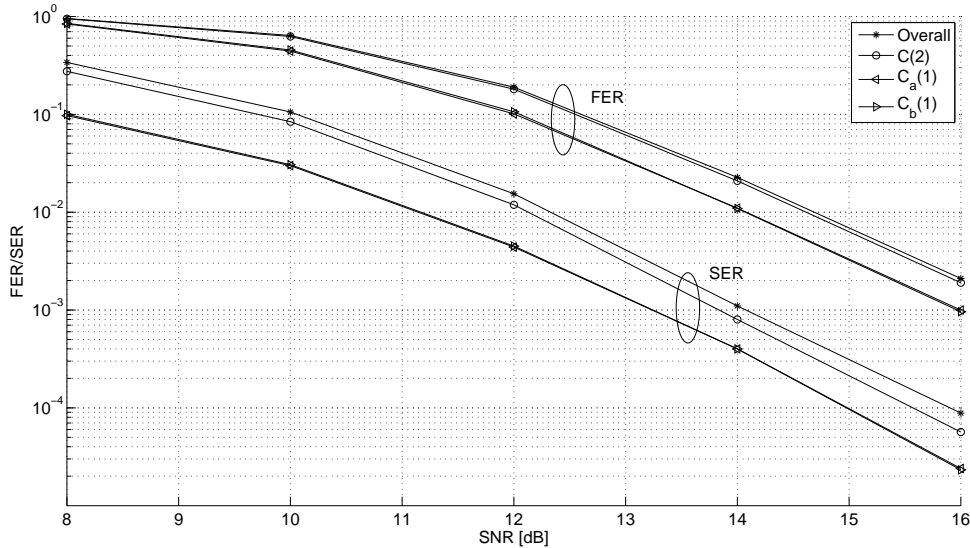


Figure 5.18: MLSTTC error performance,  $N_t = N_r = 4$ ,  $\mathcal{C}^a(1) = \mathcal{C}^b(1)$  with 4 states,  $\mathcal{C}(2)$  with 16 states, 6 bits/sec/Hz.

On level 2, we have used a 16 state CSTTC designed for a 4-QAM constellation and 4 transmit antennas. This code has an equivalent rate of  $2/8$  and will offer a squared Euclidean distance,  $d_E^2$ , of 32. On levels  $1_a$  and  $1_b$ , we have used two identical 4 state CSTTCs, designed for 4-QAM and 2 transmit antennas. These codes have an equivalent rate of  $2/4$  and offer a  $d_E^2$  of 10. This leads to an equivalent distance of 32 on level 2 and 40 on level 1. As expected this leads to unequal error protection on the two levels. In the next section, we use the balanced distance rule [87] to achieve equal error protection on the two levels.

### 5.10.2 Equal Error Performance

As discussed in the previous section, using a 16 state code on level 2 and two 4 state codes on level 1, results in an equivalent distance of 40 on level 1 and 32 on level 2<sup>2</sup>. To achieve equal error protection, using the balanced distance rule, we want these two equivalent distances to be almost equal. We can achieve that by using a code with a larger number of states on level 2. For example, if we use a 64 state code on level 2, the equivalent distance becomes 40 instead of 38, achieving almost equal error protection on the two levels. FER performance for this scenario is shown in Figure 5.19.

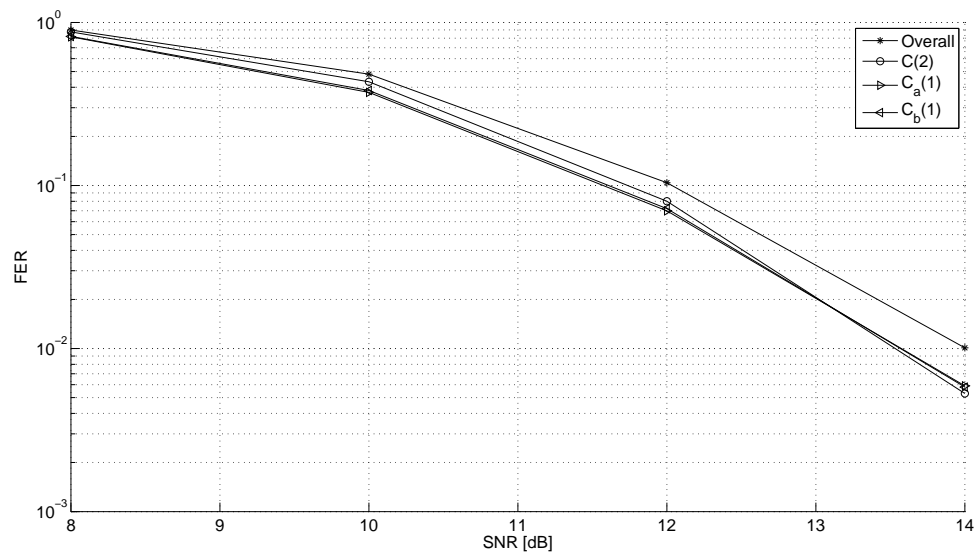


Figure 5.19: Equal error protection on the two levels in MLSTTC, by using a 64 state CSTTC on level 1 and two 4-state codes on level 2.

---

<sup>2</sup>Distances are calculated according to [18].

### 5.10.3 Effect of Number of States

Figure 5.20 shows the effect of increasing the number of states on the error performance of the MLSTTC. One of the curves shows the performance of MLSTTC with two 4 states CSTTC's on level 1 and a 64 state CSTTC on level 2. The other curve shows performance of a MLSTTC with two 4 states CSTTC's on level 1 and a 16 state CSTTC on level 2. Both show the overall performance, use 4 transmit antennas, 4 receive antennas and transmit 6 bits/sec/Hz. As can be seen, increasing the number of states on level 2 improves the performance. This improvement is more pronounced at higher SNRs.

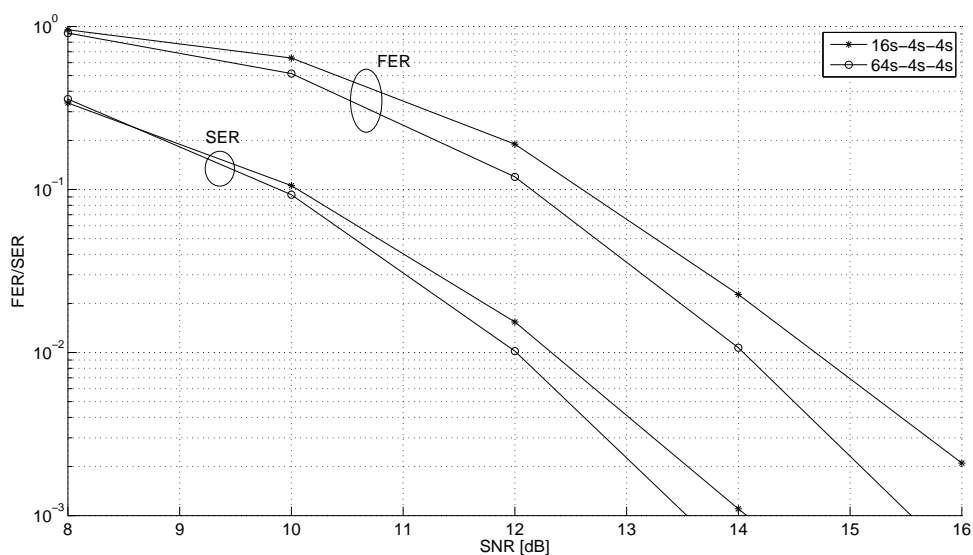


Figure 5.20: Effect of number of states on MLSTTC performance,  $N_t = N_r = 4$ ,  $C_a = C_b$  with 4 states, 6 bits/sec/Hz.

#### 5.10.4 Comparison with Layered STTC's

As discussed, previous work on MIMO-MLC has mostly been focused on block codes and the combination of STBCs, BLAST and MLC [71, 75, 76, 77, 78]. To the author's knowledge, at the time of writing, there have been no CSTTC's proposed for a 64-QAM constellation, which would have the same throughput as the MLSTTC system discussed in the last section.

There have however been multi-layered designs, whereby STTCs have been used in conjunction with a BLAST structure to design high-throughput codes. Here, we compare our system with one such system [199], proposed recently, which uses similar component codes to ours and offers the same throughput. First though, a brief background on these codes is presented for the readers convenience.

In [198], Tarokh et. al. discuss the problems of complexity in STTCs with large number of antennas and/or when a high throughput is required. To address the problem, they propose a system that partitions the antennas at the transmitter into small groups, and uses individual CSTTCs, called component codes, to transmit information from each group of antennas. At the receiver, they use a linear processing technique that suppresses signals transmitted by other groups of antennas by treating them as interference. More recently, in [199], Han et. al. suggest a modified decoder which outperforms that of Tarokh et. al.. Here we provide a brief description of the system. We then compare performance to that of a MLSTTC with the same throughput and spectral efficiency.

The system is designed based on a combination of BLAST and STTCs, as shown in Figure 5.21, where space-time trellis coding is introduced into each layer of a V-BLAST structure. At the receiver, the STTCs are decoded individually using a STTC decoder, along with a group interference suppression method to suppress signals from other component codes. In the examples presented in these papers, CSTTCs with an underlying constellation of 4-QAM designed for two transmit antennas are used as component codes. At each time slot, the encoded symbols of the first CSTTC encoder are transmitted by antennas one and

two, and the encoded symbols of the second STTC are transmitted with antenna three and four and so forth. The group interference suppression is used before decoding the CSTTCs. The decoding algorithm proposed in [198] is based on zero-forcing, and therefore ignores the influence of the additive noise. The authors of [199] derive a decoding algorithm based on MMSE concepts, where they use group interference cancellation combined with interference cancelation and the simulation results show that their system outperforms that of [198].

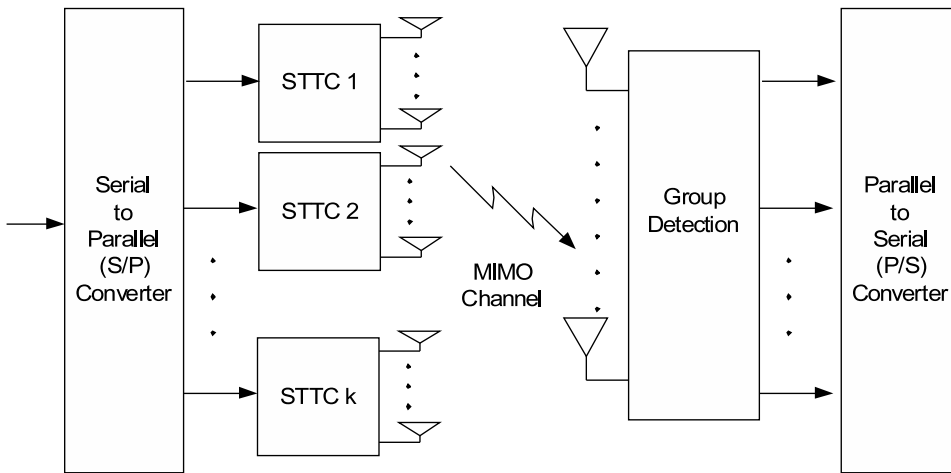


Figure 5.21: The general block diagram of a layered STTC system.

In an example in their paper [199], Hans et. al. transmit 6 bits/sec/Hz using their multi-layered approach. They use 6 transmit and 6 receive antennas. The 6 transmit antennas are divided into three layers, where each layer is composed of two antennas. The transmission power is equally allocated among the three layers. They use 32-state, 8-state and 4-state 4-QAM modulated CSTTCs as their component codes. The decoding starts by decoding the strongest code (32 state) first and then proceeding to the 8-state and 4-state. The performance is shown to be 1 dB better than that of Tarokh et. al's system. Here we compare the performance of the system of [199], with that of the multi-level system, shown in Figure 5.17, which offers the same throughput (6 bits/sec/Hz). We use a 32 state and two 4-state CSTTCs as component codes, with 4 transmit, and 4 receive antennas.



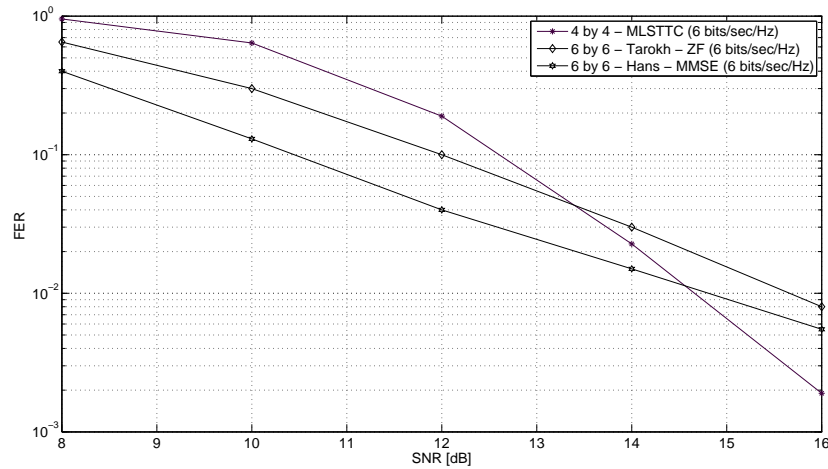


Figure 5.22: Error performance of MLSTTC vs layered STTC's, MLSTTC:  $N_t = N_r = 4$ ,  $\mathcal{C}_a(1) = \mathcal{C}_b(1)$  with 4 states,  $\mathcal{C}(2)$  with 32 states, 6 bits/sec/Hz, layered STTC [198, 199]:  $N_t = N_r = 6$ ,  $\mathcal{C}(1)$  with 4 states,  $\mathcal{C}(2)$  with 8 states,  $\mathcal{C}(3)$  with 32 states, 6 bits/sec/Hz.

As can be seen, although the multi-layered system performs better at low SNR, the MLSTTC is better at high SNR. It is also worth noting that MLSTTC uses fewer antennas than the layered approach, while achieving greater diversity (as evident from the slope of the FER curves presented). The adverse effect of using a larger number of antennas, so far as system complexity and cost is concerned, has been addressed in the literature and different approaches have been suggested to reduce the number of antennas, in particular in the transmitter where costly linearized power amplifiers are required [174]. Therefore, a major advantage of MLSTTC over the layered approach is the fact that it uses fewer antennas to achieve the same throughput.

The other problem faced by the layered system of [199] and [198] is that, as with BLAST systems, it cannot work for one receive antenna. A MLSTTC, however can work with any number of receive antennas, as shown in the next section.

### 5.10.5 Receive Diversity

BLAST systems, although having good performance and simple encoding and decoding, cannot work with fewer receive antennas than transmit antennas [2]. This deficiency is especially important for modern cellular systems where a base-station typically has more antennas than the mobile handsets. Multi-layered systems, based on the BLAST structure, also suffer from this problem. MLSTTC does not have this deficiency. Figure 5.23 illustrates the performance of the MLSTTC system for different number of receive antennas. In this figure, we are using 4 transmit antennas, and are transmitting 6 bits/sec/Hz. As component codes, we are using a 16 state CSTTC on level 2 and two 4 state CSTTCs on level 1. As expected, a good performance improvement is achieved through adding extra receive antennas.

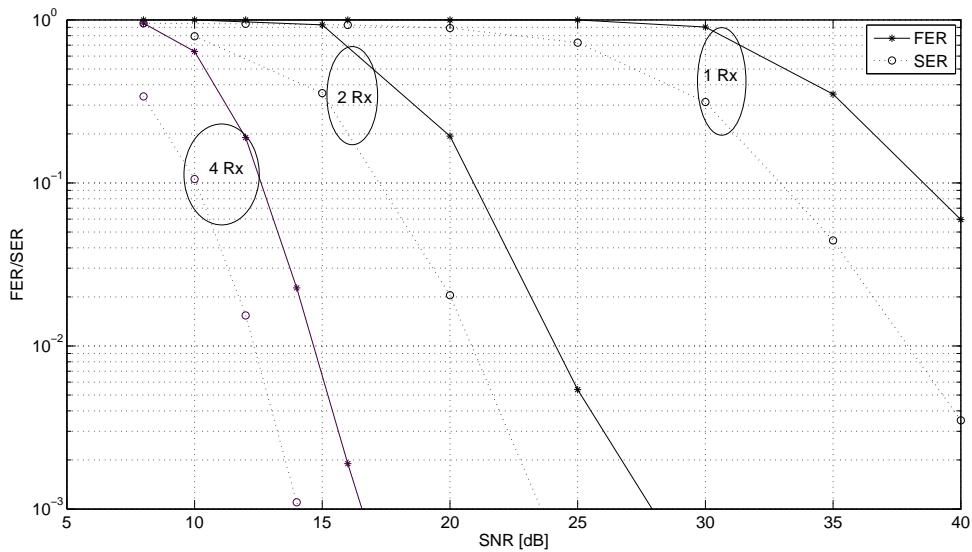


Figure 5.23: Receive diversity effect for a higher throughput MLSTTC, with  $N_t = 4$ ,  $\mathcal{C}_a(1) = \mathcal{C}_b(1)$  with 4 states,  $\mathcal{C}(2)$  with 16 states, 6 bits/sec/Hz.

## 5.11 Summary

In Chapter 4 we proposed a novel transmission scheme, MLSTTC, capable of simultaneously providing bandwidth efficiency, diversity improvement and coding gain with significantly reduced decoding complexity, especially for larger constellations and higher throughputs. The structure of MLSTTC's is flexible and can be tuned to achieve the required balance between spectral efficiency, error performance and decoding complexity. The overall structure and analytical model was described in Chapter 4. In this chapter we have evaluated the system and its performance through simulating examples of the design for an underlying constellation of 16-QAM, with up to 4 transmit and 4 receive antennas and a throughput of up to 6 bits/sec/Hz.

We observed the performance of the system with sub-channel correlation and imperfect channel estimation and have observed the effect of transmit and receive diversity on the performance. The error performance of MLSTTC, transmitting 4 bits/sec/Hz, was compared with that of a CSTTC. For the example investigated, it was shown that MLSTTC experiences about 1 dB degradation in performance for a trellis complexity saving of about 8 times. The MLSTTC structure is more flexible and is particularly attractive for higher order constellations.

An example of a higher throughput MLSTTC system was presented, transmitting 6 bits/sec/Hz. Using a 16 state code at one level and two identical 4 state codes at the other level, the MLSTTC system is more than 40 times less complex than its equivalent CSTTC for the same throughput (which must be designed for an underlying 64 QAM constellation). More specifically the CSTTC complexity, based on the measure introduced, is  $64 \times 64$ , while that of MLSTTC is  $24 \times 4$  and can go as low as  $12 \times 4$  (by using a 4 state code instead of 16), i.e. 85 times less complex. To the authors knowledge, no one has so far implemented an CSTTC on 64 QAM but since we have better distance properties (considering we are

working on 16 QAM), we conjecture that our performance is potentially the same (if not better), depending on the number of states we use.

MLSTTC's offer flexibility: The system designer can choose the balance between complexity, error performance and throughput depending on their particular application. It is also worth mentioning that so far as other parts of the system are concerned, dealing with a 16 QAM constellation is more desirable than a 64 QAM.

The same is true if we go up to higher order constellations. For example, we can use an underlying constellation of 64 QAM to transmit 8 bits/sec/Hz in MLSTTC and if we compare our performance to an equivalent 256 QAM CSTTC, not only can our system be about 1024 times less complex but we also have better distance properties (because of using 64 QAM instead of 256 QAM). Another way to scale the system, in terms of throughput, is to use higher rate codes on the two levels, thus increasing the throughput and perhaps losing some performance. Notice we can also achieve 8 bits/sec/HZ using a 16-QAM constellation with MLSTTC, by using more antennas or higher rate component codes. The system is in general very scalable.

The performance of the high throughput MLSTTC was compared with layered STTC's and it was shown that at higher SNRs, MLSTTC outperforms layered STTC's - while using fewer antennas at both the transmitter and receiver. Furthermore, unlike layered systems, MLSTTC can work with any number of receive antennas.

In summary, MLSTTC can offer equal or unequal error protection and provides a scalable and flexible alternative to the already available codes and provides the system designer with the flexibility of choosing their desired balance between code performance, complexity and throughput.

## Chapter 6

# Conclusion

Demand for capacity in wireless communication systems has been rapidly growing worldwide. This has been driven by the increasing data rate requirements of cellular mobile systems, and increasing demand for wireless Internet and multimedia services. As the available radio spectrum is limited, higher data rates can only be achieved by designing more efficient signaling techniques.

To improve spectral efficiency for future high data rate transmissions, it is desirable to construct STTCs with high order signal constellations. However, the design of a STTC normally involves the use of computer search, with the search space increasing exponentially with constellation size, the number of transmit antennas and the number of states in the code trellis. A similar increase occurs in the decoding complexity of STTCs. Therefore, despite their many benefits, STTCs are still faced with reluctance from system designers when it comes to implementation, especially when for systems which require the use of larger signal constellations or a larger number of antennas.

This project develops a new transmission scheme to benefit from the advantages of STTCs but without the complexity disadvantages, especially for large signal constellations. We achieve this aim by developing a new class of codes, called Multilevel Space-Time Trellis

Codes (IMLSTTC). The new scheme presents a promising alternative to currently available STTCs, by offering the flexibility of having a higher spectral efficiency (if desired) and lower decoding complexity (especially for larger constellations and large number of states).

## 6.1 Design considerations

The proposed system makes use of MLC concepts, which are summarized in Chapter 3. The partitioning scheme used is based on MRM (originally introduced in [10], in the context of broadcast channels). Throughout the present work, we use CSTTCs as component codes, although it is possible to use other component codes (including block codes). We design and develop a MSD that employs a modified version of a CSTTC decoder in each stage. We derive new branch metrics for our detection and decoding process to take the effect of the MRM partitioning and MSD into account. The derivation has been carried out for a general case. To design the codes, we use the trace criterion [18] which aims to maximize the minimum Euclidean distance between distinct codewords. The partitioning scheme is well suited to the overall design structure and fits naturally with the STTC structure, thus preserving the coding advantages of STTCs, when they are used as component codes, and with a MLC structure in that it lends itself neatly to the idea of having different protection levels on each stage.

Furthermore, we have considered the effects of multi-dimensionality introduced by using multiple antennas in the design and detection/decoding stage. Our system performs the encoding over both time and space, thus fully exploiting the dimensions available (as opposed to a BLAST type system, whereby the encoding is done separately for each level). Performance of the system is demonstrated by simulation for up to 4 antennas and up to 6 bits/sec/Hz using an underlying 16 QAM signal constellation.

## 6.2 Coding implications

One of the attractive features of the proposed coding scheme is that it allows the user to implement this coding scheme for large constellations and a larger number of transmit antennas using existing codes designed for smaller constellations and/or fewer antennas, thus eliminating the need to conduct an exhaustive computer search - which can be prohibitively expensive for larger systems (e.g. with search space growing exponentially with the size of the underlying constellation for CSTTCs). The simulation results have suggested that at lower spectral efficiencies, it provides a lower complexity alternative to CSTTCs while suffering a slight performance degradation, but providing the advantage of being scalable as well as having a lower decoding complexity. At higher spectral efficiencies and high SNRs, it is shown to outperform layered systems in both cost (using fewer antennas) and error performance.

## 6.3 Throughput Improvement

MLSTTCs can be designed to achieve higher throughputs for a given constellation, compared to their CSTTCs counterparts. In Chapter 4, we presented an example MLSTTC system that achieved a throughput of 6 bits/sec/Hz using an underlying 16-QAM constellation. To the author's knowledge, at the time of writing, no comparable CSTTC has been developed for a 64 QAM constellation (which is required to give a throughput of 6 bits/Sec/Hz). We, therefore, used layered space-time codes [198, 199] as a basis for comparison and found out that MLSTTC used fewer antennas (4 transmit and 4 receive antennas - as opposed to 6) and achieved the same throughput, while outperforming the layered designs in higher SNR regimes. Another way to achieve a higher throughput, would be to use higher rate codes as component codes.

## 6.4 Complexity Considerations

MLSTTC uses simple component codes and multi-stage decoding. It thereby achieves a lower complexity compared to an equivalent CSTTC, designed for the same throughput. As discussed in Chapter 5, the complexity saving becomes more pronounced for higher throughputs and larger constellations.

## 6.5 Scalability and Flexibility

MLSTTC provide a flexible and scalable design alternative to CSTTC, in that it allows the system designer to choose the balance between complexity, error performance and throughput depending on their particular application. It can provide a higher throughput for a given constellation compared to a CSTTC and, unlike BLAST-based systems, can work with any number of transmit and receive antennas. It was explained in Chapter 4 and 5 that the system can be scaled in terms of size of the constellation, throughput, and number of antennas.

## 6.6 Future Research Direction

There are many possible directions for future research on this topic. Here we highlight a few suggestions.

One area to investigate is the decoding. It appears possible to use an estimation method (e.g. MMSE) to obtain a rough estimate of the cluster centroids and then to use those estimates in decoding of the subsequent level. The advantage of this technique is that it significantly reduces the branch metric complexity, in that we would not need to average over all possible values.

Another possible extension would be to consider having access to channel information



in the transmitter. If that assumption is made, one can use the information to improve the FER performance by setting the signal power on different antennas differently (based on the channel), helping them be easier to detect in the receiver. It has however been shown in the literature that if channel knowledge is not available in the transmitter the best approach is to spread the power equally among all antennas, which is what we are doing at the moment. Notice that space-time coded structures, in general, can benefit from having CSI at the transmitter.

Investigating the performance of the system under alternative channel models, and component codes, extension to frequency selective channels, studying the effect of feedback, interleavers and iterative decoding would be other areas that could be looked into. Additional areas to consider would be using higher level codes (for example to achieve 8 bits/sec/Hz with a 16-QAM signal constellation) or using larger signal constellations (e.g. a 64-QAM signal constellation). CSTTCs are not necessarily a magic bullet for this application. Studying out other code combinations (such as conventional trellis codes) could yield interesting results. Implementing the system on hardware and further investigating the corresponding complexity issues provide another direction for future research.

# Bibliography

- [1] W. C. Y. Lee, *Wireless and cellular telecommunications*, 3rd ed., McGraw-Hill, 2006
- [2] A. Goldsmith, *Wireless communication*, Cambridge University Press, 2005
- [3] D. Tse, and P. Viswanath, *Fundamentals of wireless communication*, Cambridge University Press, 2005
- [4] T. S. Rappaport, *Wireless communications - Principles and practice*, 2nd ed. Prentice-Hall, Englewood Cliffs, N.J., 2001
- [5] A.P. Oodan, *Telecommunications Quality of Service management: From legacy to emerging services*, The IET Telecommunication Series, 2003
- [6] M. Patzold, *Mobile fading channels*, Wiley, New York, 2002
- [7] D. Parsons, *The mobile radio propagation channel*, Wiley, New York, 1994
- [8] T. M. Cover, and J. A. Thomas, *Elements of information theory*, Wiley, New York, 1991
- [9] H. Meyr, M. Moeneclaey, S. Fechtel, *Digital Communication Receivers*, Wiley, New York, 1998
- [10] IEEE Virtual Museum, available online at: <http://www.ieee-virtual-museum.org/>  
(Last visited October 2006)
- [11] IEEE 802 Standards, available online at <http://standards.ieee.org/getieee802/>  
(Last visited January 2007)

- [12] E. Katz, "Heinrich Rudolf Hertz," *Bios of famous electrochemists and physicists who contributed to understanding of Electricity, Biosensors and Bioelectronics*, Dept. of Physical Chemistry, The Hebrew University of Jerusalem, available online at: <http://chem.ch.huji.ac.il/eugeniik/history/hertz.htm> (Last visited October 2006)
- [13] J. D. Jenkins, "The discovery of radio waves", available online at: <http://www.sparkmuseum.com/> (Last visited October 2006)
- [14] Encarta Encyclopedia, Microsoft Corp., CD-ROM 2005 edition
- [15] G. Garratt, *The early history of radio: from Faraday to Marconi*, IEE History of Technology Series, 1994.
- [16] V. Tarokh, N. Seshadri, and A. R. Calderbank, "Space-time codes for high data rate wireless communication: Performance criterion and code construction," *IEEE Trans. Inform. Theory*, vol. 44, pp. 744-765, Mar. 1998
- [17] D. Gesbert, M. Shafi, D. Shiu, P. J. Smith and A. Naguib, "From theory to practice: an overview of MIMO space-time coded wireless systems," *IEEE Journal on Selc. Areas in Commun.*, vol. 21, no. 3, pg. 281-302, Apr. 2003
- [18] B. Vucetic and J. Yuan, *Space-time coding*, John Wiley & Sons Ltd, 2003
- [19] L. Cimini, "Analysis and simulation of a digital mobile channel using orthogonal frequency division multiplexing," *IEEE Trans. Commun.*, vol. 33, pg. 665-675, July 1985
- [20] R. J. McEliece and W. E. Stark, "Channels with block interference," *IEEE Trans. Inform. Theory*, pg. 44-53, Jan. 1984
- [21] I. C. Abou-Faycal, M. D. Trott, and S. Shamai, "The capacity of discrete-time memoryless Rayleigh fading channels," *IEEE Trans. Inform. Theory*, pg. 1290-1301, May 2001

- [22] T. J. Richardson, M. A. Shokrollahi and R. L. Urbanke, "Design of Capacity-Approaching Irregular Low-Density Parity Check Codes," *IEEE Trans. Inform. Theory*, VOL. 47, NO. 2, pp.619-637, Feb 2001
- [23] D. Agrawal, V. Tarokh, A. Naguib, and N. Seshadri, "Space-time coded OFDM for high data-rate wireless communication over wideband channels," in *Proc. IEEE VTC'98*, pg. 2232-2236 - Ottawa, Canada, May 1998
- [24] E. G. Larsson and P. Stoica, *Space-time block coding for wireless communications*, Cambridge University Press, 2003
- [25] C. Heegard and S. B. Wicker, *Turbo Coding*, Kluwer, Boston, 1999
- [26] S. Lin, and D. J. Costello, *Error Control Coding*, 2nd ed., N.J. Prentice Hall, 2004
- [27] V. Tarokh, H. Jafarkhani, and A. Calderbank, "Space-time block codes from orthogonal designs," *IEEE Trans. Inform. Theory*, vol. 48, pp. 1456-1467, July 1999
- [28] A. Wittneben, "The diversity gain of transmit diversity in wireless systems with Rayleigh fading," in *Proc. IEEE ICC'94*, vol. 2, pg. 1121-1125, New Orleans, USA, May 1994
- [29] P. Wolniasky, G. Foschini, G. Golden, and R. Valenzuela, "V-BLAST: An architecture for realizing very high data rates over the rich-scattering wireless channel," in *Proc. ISSSE'98*, pg. 295-300, Sept. 1998
- [30] D. Shiu and M. Kahn, "Layered space-time codes for wireless communications using multiple transmit antennas," in *Proc. IEEE ICC'99*, vol. 1, pg. 436-440, June 1999
- [31] X. Li, N. Seshadri, and S. Ariyavisitakul, "Channel estimation for OFDM systems with transmitter diversity in mobile wireless channels," *IEEE J. Select. Areas Commun.*, vol. 17, pg. 461-471, Mar. 1999
- [32] A. Paulraj, R. Nabar, D. Gore, *Introduction to space-time wireless communications*, Cambridge University Press, 2003

- [33] G. Ungerboeck, and I. Csajka, "On improving data-link performance by increasing channel alphabet and introducing sequence coding," in *Proc. IEEE Int. Symp. Info. Theory (ISIT)*, Sweden, June 1976
- [34] G. Ungerboeck, "Channel coding with multilevel/phase signals," *IEEE Trans. Info. Theory*, Vol. 28, pg. 55-67, Jan. 1982
- [35] G. Ungerboeck, "Trellis-coded modulation with redundant signal sets, Part I: Introduction," *IEEE Commun. Mag.* Vol. 25, pg. 5-11, Feb. 1987
- [36] G. Ungerboeck, "Trellis-coded modulation with redundant signal sets, Part II: State of the art," *IEEE Commun. Mag.* Vol. 25, pg. 12-21, Feb. 1987
- [37] E. Biglieri, D. Divsalar, P. J. McLane, and M. K. Simon, *Introduction to trellis coded modulation*, MacMillan, N.Y., 1991
- [38] G. D. Forney, and G. Ungerboeck, "Modulation and coding for linear Gaussian channels," *IEEE Trans. Inform. theory*, vol. 44, pg. 2384-2415, Oct. 1998
- [39] J. B. Anderson, and D. P. Taylor, "A bandwidth-efficient class of signal space codes," *IEEE Trans. Inform. Theory*, vol. 24, pg. 703-712, Nov. 1978
- [40] G. D. Forney, R. G. Gallager, G. Lang, F. Longstaff, and S. Qureshi, "Efficient modulation for band-limited channels," *IEEE J. Select. Areas Commun. (JSAC)*, vol. 2, pg. 632-647, Sept. 1984
- [41] J. Cheng, H. Wang, and S. Cheng, "Space-time block coded transmit diversity for OFDM systems in mobile channels," in *Proc. IEEE PIMRC'02*, pg. 208-211, Sept. 2002
- [42] A. Calderbank, "Multilevel codes and multistage decoding," *IEEE Trans. Commun.*, vol. 37, pg. 222-229, Mar. 1989
- [43] S. Haykin, M. Moher, *Modern wireless communications*, Pearson Prentice Hall, NJ. 2005

- [44] C. Berrou, A. Glavieux, and P. Thitimajshima, "Near Shannon limit error correcting coding and decoding: turbo codes," *In Proc. ICC*, pg. 1064-1070, June 1993
- [45] R. G. Gallager, *Low density parity check codes*, MIT Press, Cambridge, Massachusetts, 1963
- [46] A. Triolo, J. Liberti, and T. Hoerning, "OFDM space-time trellis coded MIMO systems with experimental results," in *Proc. MILCOM'02*, vol. 1, pg. 577-581, Oct. 2002
- [47] Y. Sasazaki, and T. Ohtsuki, "Improved design criteria and new codes on space-frequency trellis coding over frequency selective fading channels," in *Proc. IEEE VTC'02*, pg. 2187-2191, Sept. 2002
- [48] A. Paulraj, T. Kailath, "*Increasing capacity in wireless broadcast systems using distributed transmission/directional reception (DTDR)*", U.S. Patent 5 345 599, Sept. 1994
- [49] O. Trikkonen, and A. Hottinen, "Improved MIMO performance with non-orthogonal space-time block codes," in *Proc. IEEE GLOBECOMM'01*, vo. 2, pg. 1122-1126, Nov. 2001
- [50] X. li, T. Luo, g. Yue and C. Yin, "A squaring method to simplify the decoding of orthogonal space-time block codes," *IEEE Trans. Commun.*, pg. 1700-1703, Oct. 2001
- [51] D. C. MacKay, "Near Shannon limit performance of low density parity check codes," *Electronic Letters*, Vol. 32, pg. 1645-1646, August 1966
- [52] C. E. Shannon, "A mathematical theory of communication," *Bell Sys. Tech. J.*, vol. 27, pg. 379-423 (part one), pg. 623-656 (part two), 1949
- [53] Y. Hong, J. Yuan, and X. Shao, "Robust space-time trellis codes for OFDM systems over quasi-static frequency selective fading channels," in *Proc. IEEE PIMRC'03*, pg. 434-438, Sept. 2003

- [54] Z. Chen, J. Yuan and B. Vucetic, "An improved space-time trellis coded modulation scheme on slow Rayleigh fading channels," *IEEE ICC'01*, Helsinki, Finland, pp. 1110-1116, Jun. 2001
- [55] Z. Chen, J. Yuan, and B. Vucetic, "Improved space-time trellis coded modulation scheme on slow Rayleigh fading channels," *Electron. Lett.*, vol. 37, No. 7, pg. 440-441, Mar. 2001
- [56] J. Ventura-Traveset, G. Caire, E. Bligieri, and G. Taricco, "Impact of diversity reception on fading channels with coded modulation," *IEEE Trans. Commun.* vol. 45, No. 5, pg. 563-572, May 1997
- [57] S. Muller, and J. Huber, "OFDM with reduced peak-to-average power ratio by optimum combination of partial transmit sequences," *Electron. Lett.*, vol. 33, pg. 368-369, 1997
- [58] A. Jone, T. Wilkinson, and S. Barton, "Block coding scheme for reduction of peak-to-mean envelope power ratio of multicarrier transmission schemes," *Electron. Lett.*, vol. 30, pg. 2098-2099, 1994
- [59] R. Van Nobelen, *Coding for the Rayleigh fading channel*, PhD Thesis, University of Canterbury, New Zealand, Feb. 1996
- [60] J. G. Proakis, *Digital communications*, 4th ed., New York, McGraw-Hill, 2001
- [61] Y. Gong and K. B. Letaief, "Performance evaluation and analysis of space-time coding for high data rate wireless personal communication," *IEEE VTC'99*, 1999, pp. 1331-1335
- [62] Y. Gong and K. B. Letaief, "Performance evaluation and analysis of space-time coding in unequalized multipath fading links," *IEEE Trans. Commun.*, vol. 48, no. 11, Nov. 2000, pp. 1778-1782
- [63] N. Seshadri, and C. W. Sundberg, "Multilevel trellis coded modulations for the Rayleigh fading channels," *IEEE Trans. Commun.*, vol. 41, no. 9, pg. 1300-1310, Sept. 1993

- [64] T. Woerz, and J. Hagenauer, "Iterative decoding for multilevel codes using reliability information," *Globecomm*, pg. 1779-1784, 1992
- [65] W. J. Choi and J. M. Cioffi, "Space-time block codes over frequency selective Rayleigh fading channels," *IEEE VTC' 99*, vol. 5, 1999, pp. 2541-2545.
- [66] X. Ma and G. B. Giannakis, "Space-time-multipath coding using digital phase sweeping," *GLOBECOM*, Taipei, Taiwan, R.O.C, Nov. 17-21, 2002
- [67] H. Imai, and S. Hirakawa, "A new multilevel coding method using error correcting codes," *IEEE Trans. Inform. Theory*, Vol. 23, pg. 371-377, May 1977
- [68] G. J. Pottie, and D. P. Taylor, "Multilevel codes based on partitioning," *IEEE Trans. Inform. Theory*, Vol. 35, pg. 387-98, Jan. 1989
- [69] L. Lampe, R. Schober, and R. F. Fischer, "Multilevel coding for multiple-antenna transmission," *IEEE Trans. Wireless Commun.* vol. 3, no. 1, pp. 203 - 208, Jan. 2004
- [70] L. H. Lampe, R. Schober, and R. F. Fischer, "Multilevel coding for multiple-antenna transmission," in *Proc. ISIT*, pg. 104, Lausanne, Switzerland, July 2002
- [71] D. F. Yuan, F. Zhang, A. F. Sui, and Z. W. Li, "Concatenation of space-time block codes and multilevel codes over Rayleigh fading channels," in *Proc. VTC Fall*, pg. 192-196, Oct. 2001
- [72] Y. Wu, Y. Yang, and X. Luo, "Improving the performance of V-BLAST with STTC," *IEEE ICCS'02*, vol. 1, pg. 174-177, Nov. 2002
- [73] V. Tarokh, A. Naguib, N. Seshadri, and A. R. Calderbank, "Combined Array Processing and Space-time Coding," *IEEE Trans. Inform. Theory*, vol. 45, no. 4, pg. 1121-1128, May 1999
- [74] C. Han, and D. Yuan, "An improved group detection algorithm for ML-STTC in wireless communication systems," *IEEE ICMTAS'05*, vol. 1, pg. 1-4, Nov. 2005
- [75] D. F. Yuan, P. Zhang, and Q. Wang, "Multilevel codes (MLC) with multiple antennas over Rayleigh fading channels," *IEEE 54th VTC Fall*, vol. 3, pg. 1289 - 1293, Oct. 2001



- [76] D. Yuan, Q. Wang, and P. Zhang, "The research for optimal mapping strategies for concatenation scheme (MLC-STBC) in Rayleigh fading channels, " *MILCOM'01*, vol. 2, pg. 1124-1127, Oct. 2001
- [77] P. A. Martin, D. M. Rankin, and D. P. Taylor, "Space-time multilevel codes," *IEEE VTC'05*, Stockholm, Sweden, Mar. 2005
- [78] P. A. Martin, D. M. Rankin, and D. P. Taylor, "Multi-dimensional space-time multilevel codes," *IEEE Trans. Wireless Commun.*, vol. 5, Issue 9, pg. 2569-2577, Sept. 2006
- [79] A. R. Calderbank, and J. E. Mazo, "A new description of trellis codes," *IEEE Trans. Inform. Theory*, vol. 30, pg. 781-791. Nov. 1984
- [80] A. R. Calderbank, and N. Sloane, "New trellis codes based on lattices and cosets," *IEEE Trans. Inform. Theory*, vol. 33, pg. 177-195, March 1988
- [81] A. R. Calderbank, and N. Seshadri, "Multilevel codes for unequal error protection," *IEEE Trans. Inform. Theory*, vol. 39, no. 4, pg. 1234-1248, 1993
- [82] P. A. Martin, *Adaptive iterative decoding*, PhD thesis, University of Canterbury, New Zealand, Feb. 2001
- [83] G. D. Forney Jr., "Coset codes - part 1: Introduction and geometrical classification," *IEEE Trans. Inform. Theory*, vol. 34, no. 5, pg. 1123-1151, Sept. 1988
- [84] G. D. Forney Jr., "Coset codes - part 2: Binary lattices and related codes," *IEEE Trans. Inform. Theory*, vol. 34, no. 5, pg. 1152-1187, Sept. 1988
- [85] G. J. Foschini, "Layered Space-Time Architecture for Wireless Communication in a Fading Environment When Using Multiple Antennas," *Bell Labs Technical Journal*, vol. 1, No. 2, pg. 41-59, Autumn 1996
- [86] D. Yuan, P. Zhang and Q. Wang, "The concentration scheme MLC-STBC combining MLC and STBC over Rayleigh fading channels", *IEEE 2001*

- [87] U. Waschmann, R. F. Fischer, and J. B. Huber, "Multilevel codes: Theoretical concepts and practical design rules," *IEEE Trans. Inform. Theory*, Vol. 45, pg. 1361-1391, July 1999
- [88] T. Cover, "Broadcast channels," *IEEE Trans. Inform. Theory*, vol. 18, pp. 2-14, Jan 1972
- [89] D. Yuan, and X. Zhu "Multiple hierarchical transmission scheme with bit interleaver over Rayleigh fading channel," *IEEE 54th VTC Fall*, vol. 4, pg. 2439-2441, Oct. 2001
- [90] S. Alamouti, "A simple transmit diversity technique for wireless communications," *IEEE J. Select. Areas Commun.*, vol. 16, pp. 1451-1458, Oct. 1998.
- [91] V. Tarokh, H. Jafarkhani, and A. R. Calderbank, "Space-time block codes from orthogonal designs," *IEEE Trans. Inform. Theory*, vol. 45, pp. 1456-1467, July 1999
- [92] O. Tirkkonen and A. Hottinen, "Square-matrix embeddable space-time block codes for complex signal constellations," *IEEE Trans. Inform. Theory*, vol. 48, pp. 384-395, Feb. 2002.
- [93] W. Su and X.-G. Xia, "Two generalized complex orthogonal space-time block codes of rates  $7/11$  and  $3/5$  for 5 and 6 transmit antennas," *IEEE Trans. Inf. Theory*, vol. 49, no. 1, pp. 313-316, Jan. 2003.
- [94] W. Su and X.-G. Xia, "On complex orthogonal space-time block codes from complex orthogonal designs," *Wireless Personal Commun.*, vol. 25, pp. 1-26, Apr. 2003.
- [95] H. Gou, "Space-time block coding", *Technical Report*, University of Maryland, College Park, May 2003
- [96] V. Tarokh, H. Jafarkhani, and Calderbank, "Space-time block coding for wireless communications: Performance results," *IEEE J. Sel. Areas Commun.*, vol. 17, no. 3, pp. 451-460, Mar. 1999
- [97] A. V. Geramita and J. M. Geramita, "Complex orthogonal designs," *J. Comb. Theory, Ser. A*, vol. 25, pp. 211-225, Jan. 1978.

- [98] M. Baghaie A, S. Kuo, and I. V. McLoughlin, "FPGA implementation of space-time block coding systems," *IEEE 6th circuits and systems symp. on frontiers of mobile and wireless commun.*, vol. 2, pp. 591-594, June 2004
- [99] Lyrtech Ltd, <http://www.lyrtech.com/DSP-development/>, (Last visited October 2006)
- [100] B. M. Hochwald and T. L. Marzetta, "Unitary space-time modulation for multiple-antenna communications in Rayleigh flat fading," *IEEE Trans. Inform. Theory*, Mar. 2000.
- [101] H. Jafarkhani, "A quasi-orthogonal space time block code," *IEEE Trans. Commun.*, vol. 49, pp. 1-4, Jan. 2001.
- [102] G. J. Foschini, "Layered space-time architecture for wireless communication in a fading environment when using multiple antennas," *AT&T Bell Labs. Tech. J.*, vol. 1, no. 2, pp. 41-59, 1996.
- [103] E. Telatar, "Capacity of Multi-Antenna Gaussian Channels," *Euro. Trans. on Telecomms.*, Vol. 10, No. 6, pg. 585-589, Nov-Dec. 1999
- [104] S. Sandu and A. J. Paulraj, "Space-time block codes versus space-time trellis codes," *IEEE ICC'01*, 2001
- [105] G. J. Foschini, and Jr., M. J. Gans, "On limits of wireless communication in a Fading Environment When Using Multiple Antennas," *Wireless Pers. Comms.*, vol. 6, no. 2, pp. 311-335, March 1998
- [106] L. F. Wei, "Trellis coded modulation with multidimensional constellations," *IEEE Trans. Inform. Theory*, vol. 33, no.4, pg. 483-501, July 1987
- [107] M. O. Damen, K. Abed-Meraim, and J.-C. Belfiore, "A generalized lattice decoder for asymmetrical space-time communication architecture," in *Proc. ICASSP*, pg. 2581-2584, 2000.

- [108] R. Heath and Jr., A. Paulraj, "Switching between multiplexing and diversity based on constellation distance," in *Proc. Allerton Conf. Communication, Control and Computing*, Oct. 2000.
- [109] S. M. Alamouti, "A simple transmitter diversity scheme for wireless communications," *IEEE J. Select. Areas Commun.*, vol. 16, pp. 1451-1458, Oct. 1998
- [110] G. D. Golden, G. J. Foschini, R. A. Valenzuela, and P. W. Wolniansky, "Detection algorithm and initial laboratory results using V-BLAST spacetime communication architecture," *Electron. Lett.*, vol. 35, pp. 1416, Jan. 1999.
- [111] G. J. Foschini, G. D. Golden, R. A. Valenzuela, and P. W. Wolniansky, "Simplified processing for high spectral efficiency wireless communication employing multi-element arrays," *J. Select. Areas Commun.*, vol. 17, pp. 1841-1852, Nov. 1999.
- [112] W. Firmanto, B. Vucetic, J. Yuan, and Z. Chen, "Space-time turbo trellis coded modulation for wireless data communications," *EUROSIP Journ. on Appld. Sig. Processing*, No. 5, pg. 459-470, May 2002
- [113] X. Ma and G. B. Giannakis, "Space-time coding for doubly-selective channels," in *IEEE International Symposium on Circuits and Systems*, Phoenix, AZ, pp. 647-650, May 2002
- [114] V. Tarokh, H. Jafarkhani, and A. R. Calderbank, "Space-time block coding for wireless communications: performance results," *IEEE J. Select. Areas Commun.*, Vol. 17, Issue 3, pg. 451-460, Mar 1999
- [115] W. Su, and X. Xia, "A design of quasi-orthogonal space-time block codes with full diversity," in *Proc. IEEE CSSC'02*, vl. 2, pg. 1112-1116, Nov. 2002
- [116] V. Tarokh, A. Naguib, N. Seshadri, and A. Calderbank, "Combined array processing and space-time coding," *IEEE Trans. Info. Theory*, vol. 45, Issue 4, pg. 1121-1128, May 1999
- [117] S. Baro, G. Bauch, and A. Hansmann, "Improved codes for space-time trellis-coded modulation," *IEEE Commun. Lett.*, vol. 4, Issue 1, pg. 20-22, Jan. 2000

- [118] W. Firmanto, J. Yuan, B. Vucetic, "Turbo codes with transmit diversity - performance analysis and evaluations," *IEICE Trans. Commun.*, vol. E85-B, No. 5, May 2002
- [119] H. Jafarkhani, and N. Seshadri, "Super-orthogonal space-time trellis codes," *IEEE Trans. on Inform. Theory*, vol. 49, pg. 937-950, April 2003
- [120] D. Ionescu, K. Mukkavilli, Z. Yan, J. Lilleberg, "Improved 8-state and 16-state space time codes for 4-PSK with two transmit antennas," *IEEE Commun. Lett.*, vol. 5, pg. 301-333, , Jul. 2001
- [121] G. David Forney, Jr., "The Viterbi algorithm," *Proc. of the IEEE*, Vol. 61, No. 3, pp. 268-278. March, 1973
- [122] J. Huber, and U. Wachsmann, "Capacities of equivalent channels in multilevel coding schemes," *Electron. Lett.*, vol. 30, pg. 557-558, Mar. 1994
- [123] R. Fischer, J. Huber, and U. Wachsmann, "Multilevel coding: Aspects from information theory," in *Proc IEEE Global Telecommun. Conf. (GLOBEGOM'96)*, pg. 26-30, London, U.K., Nov. 1996
- [124] S. Mallik, *Multilevel coding schemes for underspread fading channels*, Master Thesis, University of Illinois at Urbana-Champaign, U.S.A., 2004
- [125] W. H. Gerstacker, F. Obernosterer, R. Schober, A. T. Lehmann, A. Lampe, P. Gunreben, "Equalization concepts for Alamouti's space-time block code," *IEEE Trans. on Commun.*, vol. 52, Issue 7, pp. 1178 - 1190, Jul. 2004
- [126] W. Choi and J. M. Cioffi, "Multiple input/multiple output (MIMO) equalization for space-time block coding," *IEEE Pacific Rm Conf. on Commun., Comput., and Sig. Proc.*, Victoria, Canada, Aug. 1999, pp. 341-344
- [127] S. L. Ariyavisitakul, J. H. Winters and I. Lee, "Optimum space-time processors with dispersive interference: unified analysis and required filter span," *IEEE Trans. on Commun.*, vol. 47, Jul. 1999, pp. 1073-1083

- [128] C. Miller, D. Taylor, and P. Gough, "Estimation of co-channel signals with linear complexity," *IEEE Trans. Commun.*, vol. 49, pp. 1997-2005, Nov. 2001.
- [129] E. Lindskog and A. Paulraj, "A transmit diversity scheme for channels with inter-symbol interference," in *Proc. of ICC*, 2000, vol. 1, pp. 307-311.
- [130] E. G. Larsson, P. Stoica, E. Lindskog and J. Li, "Space-time block coding for frequency-selective channels," in *IEEE International Conference on Acoustic, Speech, and Signal Processing*, 2002, May 13-17, 2002, pp. 2405-2408.
- [131] S. Zhou and G. B. Giannakis, "Single-carrier space-time block-coded transmissions over frequency-selective fading channels," in *IEEE Trans. Inform. Theory*, vol. 49, Jan 2003, pp. 164 -179.
- [132] S. Zhou and G. B. Giannakis, "Space-time coded transmissions with maximum diversity gains over frequency-selective multipath fading channels," in *Proc. of Global telecommunications conference*, San Antonio, TX, Nov. 25-29, pp. 440-444.
- [133] D. Gore, S. Sandhu and A. Paulraj, "Delay diversity code for frequency selective channels," *Electronics Letters*, vol. 37, No. 20, Sep. 2001, pp. 1230-1231.
- [134] M. Qin and R. S. Blum, "Properties of space-time codes for frequency selective channels and trellis code designs", in *IEEE ICC'03*, vol. 4, May 2003 pp. 2286 - 2290
- [135] Y. Liu, M. P. Fitz and O. Y. Takeshita, "Space-time codes performance criteria and design for frequency selective fading channels ," in *ICC*, 2001, vol. 9, pp. 2800-2804.
- [136] Z. Liu and G. B. Giannakis, "Space-time block-coded multiple access through frequency-selective fading channels," in *IEEE Trans. on Commun.*, vol. 49, No. 6, June 2001, pp. 1033-1044.
- [137] M. Qin and R. S. Blum, "Properties of space-time codes for frequency selective channels," *IEEE Trans. on Sig. Proc.*, vol. 52, pp. 694 - 702, March 2004

- [138] A. V. Geramita and J. Seberry, *Orthogonal Designs: Quadratic Forms and Hadamard Matrices (Lecture Notes in Pure and Applied Mathematics)*, New York: Marcel Dekker, 1979, vol. 43.
- [139] J. Hammer, "Orthogonal designs and generalized Fourier-Walsh transforms," *Utilitas Math.*, vol. 50, pp. 113-125, 1996.
- [140] X.-B. Liang, "Orthogonal designs with maximal rates," *IEEE Trans. Inf. Theory*, vol. 49, no. 10, pp. 2468-2503, Oct. 2003.
- [141] X.-B. Liang and X.-G. Xia, "On the nonexistence of rate-one generalized complex orthogonal designs," *IEEE Trans. Inf. Theory*, vol. 49, no. 11, pp. 2984-2989, Nov. 2003
- [142] X.-B. Liang, "A high-rate orthogonal space-time block code," *IEEE Commun. Lett.*, vol. 7, no. 5, pp. 222-223, May 2003.
- [143] A. Hurwitz, "ber die Komposition der quadratischen Formen von beliebig vielen Variablen," *Nachr. Gesell. d. Wiss. Gttingen*, pp. 309-316, 1898, Reprinted in *Math. Werke. Basel, Switzerland: Birk- huser*, 1963, vol. 2, pp. 565-571.
- [144] A. Hurwitz, "ber die Komposition der quadratischen Formen," *Math. Ann.*, vol. 88, pp. 1-25, 1923, Reprinted in *Math. Werke. Basel, Switzerland: Birkhuser*, 1963, vol. 2, pp. 641-666
- [145] G. Ganesan, and P. Stoica, "Space-time block codes: a maximum SNR approach," *IEE Trans. on Info. Theory*, vol. 14, no. 4, pp. 1650-1656, May 2001
- [146] B. A. Sethuraman and B. S. Rajan, "An algebraic description of orthogonal designs and the uniqueness of the Alamouti code," *GLOBECOME 2002* Taipei, Taiwan, R.O.C., vol. 2, Nov. 2002, pp. 1088-1092.
- [147] N. Al-Dhahir, C. Fragouli, A. Stamoulis, W. Younis, and A. R. Calderbank, "Space-time processing for broadband wireless access," *IEEE Commun. Mag.*, vol. 40, no. 9, pp. 136-142, Sept. 2002.

- [148] H. Wang and X.-G. Xia, "Upper bounds of rates of space-time block codes from complex orthogonal designs," *IEEE Inform. Theory*, vol. 49, pp. 2788-2796, Oct. 2003.
- [149] W. Su, X.-G. Xia, and K. J. R. Liu, "A systematic design of high-rate complex orthogonal space-time block codes," *IEEE Commun. Lett.*, vol. 8, no. 6, pp. 380-382, Jun. 2004.
- [150] T. H. Liew and L. Hanzo, "Space-time codes and concatenated channel codes for wireless communications," *Proc. IEEE*, vol. 90, pp. 187-219, Feb. 2002.
- [151] E. Lindskog and A. Paulraj, "A transmit diversity scheme for channels with inter-symbol interference," in *Proc. IEEE ICC'2000* New Orleans, LA, 2000, pp. 307-311.
- [152] D. Flore, and E. Lindskog, "Time-reversal space-time block coding vs. transmit delay diversity - a comparison based on a GSM-like system," in *Proc. Digital Signal Processing Workshop*, Hunt, Texas, 2000
- [153] P. Stoika, and E. Lindskog, "Space-time block coding for channels with intersymbols interference," *Digital signal processing*, vol. 12, no. 4, pp. 616-627, 2002
- [154] B. Hochwald and W. Sweldens, "Differential unitary space time modulation," *IEEE Trans. Commun.*, vol. 48, pp. 2041-2052, Dec. 2000.
- [155] S. Sandhu and A. Paulraj, "Union bound on error probability of linear space-time block codes," in *Proc. ICASSP* Salt Lake City, UT, vol. 4, 2001, pp. 2473-247
- [156] Y. Xin, Z. Wang, and G. B. Giannakis, "Spacetime diversity systems based on linear constellation precoding," *IEEE Trans. Wireless Commun.*, vol. 2, pp. 294-309, Mar. 2003.
- [157] O. Tirkkonen, "Optimizing spacetime block codes by constellation rotations," in *Proc. Finnish Wireless Communications Workshop*, Oct. 2001.
- [158] M. O. Damen, K. Abed-Meraim, and J.-C. Belfiore, "Diagonal algebraic spacetime block codes," *IEEE Trans. Inform. Theory*, vol. 48, pp. 628-636, Mar. 2002.



- [159] L. Liu, and H. Jafarkhani, "Application of quasi-orthogonal space-time block codes in beamforming," *IEEE Trans. Signal Proc.*, vol. 53, pp. 54-63, Jan. 2005
- [160] O. Tirkkonen, A. Boariu, and A. Hottinen, "Minimal nonorthogonality rate 1 space-time block code for 3+ Tx," in *Proc. IEEE Int. Symp. Spread Spectrum Techniques and Applications Parsippany, NJ*, Sep. 2000, pp. 429-432
- [161] N. Sharma and C. B. Papadias, "Improved quasi-orthogonal codes through constellation rotation," *IEEE Trans. Commun.*, vol. 51, no. 3, pp. 332-335, Mar. 2003.
- [162] L. A. Dalton and C. N. Georghiades, "A four transmit antenna orthogonal space-time code with full diversity and rate," in *Proc. 40th Annu. Allerton Conf. Communications, Control, Computing Monticello, IL*, Oct. 2002.
- [163] L. M. A. Jalloul, K. Rohani, K. Kuchi, and J. Chen, "Performance analysis of CDMA transmit diversity methods," in *Proc. IEEE Vehicular Technology Conf. Amsterdam, The Netherlands*, vol. 3, Oct. 1999, pp. 1326-1330.
- [164] Y. Xin, Z. Wang, and G. B. Giannakis, "Linear unitary precoders for maximum diversity gains with multiple transmit and receive antennas," in *Proc. 34th Asilomar Conf. Signals, Systems, Computers Pacific Grove, CA*, Oct. Nov. 2000, pp. 1553-1557
- [165] Y. Xin, Z. Wang, and G. B. Giannakis, "Space-time diversity systems based on unitary constellation-rotating precoders," in *Proc. IEEE Int. Conf. Acoustics, Speech, Signal Processing Salt Lake City, UT*, May 2001, pp. 2429-2432.
- [166] C. B. Papadias and G. J. Foschini, "A space-time coding approach for systems employing four transmit antennas," in *Proc. IEEE Int. Conf. Acoustics, Speech, Signal Processing Salt Lake City, UT*, May 2001, pp. 2481-2484.
- [167] A. Yongacoglu and M. Siala, "Performance of diversity systems with 2 and 4 transmit antennas," in *Proc. Int. Conf. Communication Technology (WCC-ICCT) Beijing, China*, 2000, pp. 148-150.
- [168] V. M. DaSilva and E. S. Sousa, "Fading-resistant modulation using several transmitter antennas," *IEEE Trans. Commun.*, vol. 45, no. 10, pp. 1236-1244, Oct. 1997

- [169] B. Hassibi and B. M. Hochwald, "High-rate codes that are linear in space and time," *IEEE Trans. Info. Theory*, vol. 48, no. 7, July 2002
- [170] G. Ganesan, and P. Stoica, "Space-time block codes: A maximum SNR approach," *IEEE Trans. Info. Theory*, vol. 47, pp. 1650-1656, May 2001.
- [171] R. Heath, and A. Paulraj, "Linear Dispersion Codes for MIMO systems based on frame theory," *IEEE Trans. Signal Processing*, vol. 50, no. 10, Oct. 2002
- [172] R. Gohary, and T. Davidson, "Design of Linear Dispersion Codes: some asymptotic guidelines and their implementations," *IEEE SP workshop on Signal Processing Advances in Wireless Comms.*, Rome, June 2003.
- [173] A.R. Ghaderipoor, L. Beigy, and S.H. Jamali, "Analytical survey on linear dispersion space-time codes," in *Proc. ICASSP '02*, vol.3, pp. 13-17, May 2002
- [174] M. Baghaie A, I. McLoughlin, P. Martin, K. Mehrotra, D. P. Taylor, "Transmit Antenna Selection in UHF MIMO Linking," *IEEE 63rd VTC, Melbourne, Australia, May 2006*
- [175] L. Liu, and H. Jafarkhani, "Application of quasi-orthogonal space-time block codes in beamforming," *IEEE Trans. Signal Processing*, vol. 53, no. 1, pp. 54-63, Jan. 2005
- [176] H. El Gamal and M. O. Damen, "Universal space-time coding," *IEEE Trans. Inf. Theory*, vol. 49, no. 5, pp. 1097-1119, May 2003.
- [177] M. O. Damen, K. Abed-Meraim, and J.-C. Belfiore, "Diagonal algebraic spacetime block codes," *IEEE Trans. Inform. Theory*, vol. 48, pp. 628-636, Mar. 2002
- [178] M. O. Damen, "Joint coding/decoding in a multiple access system, application to mobile communications," Ph.D. dissertation: ENST, Paris, France. [Online]. Available: <http://www.ee.ualberta.ca/~damen>, Oct. 1999.
- [179] M. O. Damen, A. Chkeif, and J.-C. Belfiore, "Lattice codes decoder for space-time codes," *IEEE Commun. Lett.*, vol. 4, pp. 161-163, May 2000.

- [180] H. El Gamal and A. R. Hammons, Jr, "A new approach to layered spacetime coding and signal processing," *IEEE Trans. Inform. Theory*, vol. 47, pp. 2321-2335, Sept. 2001.
- [181] H. El Gamal and M. Bourles, "On the design of adaptive space-time codes," *presented at the Information Theory Workshop Cairns*, Australia, Sept. 2001.
- [182] G. Gritsch, H. Weinrichter, and M. Rupp, "MIMO paradox of non-orthogonal space-time block codes," *Electronic Letters*, vol. 41, no. 6, pp. 343-344, Mar. 2005
- [183] J. Hou and M. H. Lee, "Universal rotated space time block codes," *IEEE ICPWC'05*, pp. 109-112, Jan. 2005
- [184] L. Zheng and D. N. C. Tse, "Diversity and multiplexing: A fundamental tradeoff in multiple-antenna channels," *IEEE Trans. Inform. Theory*, vol. 49, pp. 1073-1096, May 2003.
- [185] H. El Gamal, G. Caire, and M. O. Damen, "Lattice coding and decoding achieve the optimal diversity-multiplexing tradeoff of MIMO channels," *IEEE Trans. Inf. Theory*, vol. 50, pp. 968-985, Jun. 2004.
- [186] V. Tarokh and H. Jafarkhani, "A differential detection scheme for transmit diversity," *IEEE J. Select. Areas Commun.*, vol. 18, pp. 1169-1174, July 2000.
- [187] G. Ganesan, and P. Stoica, "Differential space-time modulation," *IEEE Trans. Inform. Theory*, vol. 46, pp.2567-2578, Nov. 2000
- [188] G. Bauch, "Concatenation of space-time block codes and "turbo"-TCM," *IEEE ICC'99*, vol. 2, pp. 1202-1206, Jun. 1999
- [189] M. Uysal and C. N. Georghiades, "New space-time block codes for high throughput efficiency," *IEEE GLOBECOM '01.*, vol. 2, pp. 1103 - 1107, Nov. 2001
- [190] Y. E. Liu, M. P. Fitz, and O. Y. Takeshita, "A rank criterion for QAM space-time codes," *IEEE Trans. Info. Theory*, vol. 48, pp. 3062-3079, Dec. 2002.

- [191] P. A. Martin and D. P. Taylor, "High-throughput error correcting space-time block codes," *IEEE Commun. Lett.*, vol. 8, no. 7, pp. 458-460, Jul. 2004
- [192] L. -F. Wei, "Trellis coded modulation with multidimensional constellations," *IEEE Trans. Info. Theory*, vol. 33, pp. 438-501, July 1987
- [193] L. Xian and H. Liu, "Space-time block codes from cyclic design," *IEEE Commun. Lett.*, vol. 9, no. 3, pp. 231 - 233, Mar. 2005
- [194] H. Boleskei and A. J. Paulraj, "Performance of space-time codes in the presence of spatial fading correlation," in *Asilomar Conf. on Signals, Systems, and Computeres*, 2000
- [195] S. Siwamogsatham and M. O. Fitz, "Robust space-time coding for correlated rayleigh fading channels," in *Proc. 38th Annual Allerton Conf. on Communication, Control, and Computing*, 2000
- [196] H. Kan, and H. Shen, "A counterexample for the open problem on the minimal delays of orthogonal designs with maximal rates," *IEEE Trans. Info. Theory*, vol. 51, no. 1, pp. 355- 359, Jan. 2005
- [197] H. Anton, *Calculus*, John Wiley Sons, NY, 1999
- [198] V. Tarokh, A. Naguib, and N. Seshadri, "Combined Array Processing and Space-time Coding," *IEEE Trans. Inform. Theory*, vol. 45, no. 4, pg. 1121-1128, May 1999
- [199] C. Han, and D. Yuan, "An improved group detection algorithm for ML-STTC in wireless communication systems," *IEEE ICMTAS'05*, vol. 1, pg. 1-4, Nov. 2005
- [200] K. Miyauchi, S. Seki, and H. Ishio, "New Technique for Generating and Detecting Multilevel Signal Formats," *IEEE Trans. Commun.* Vol. 24, pg. 263- 267, Feb. 1976